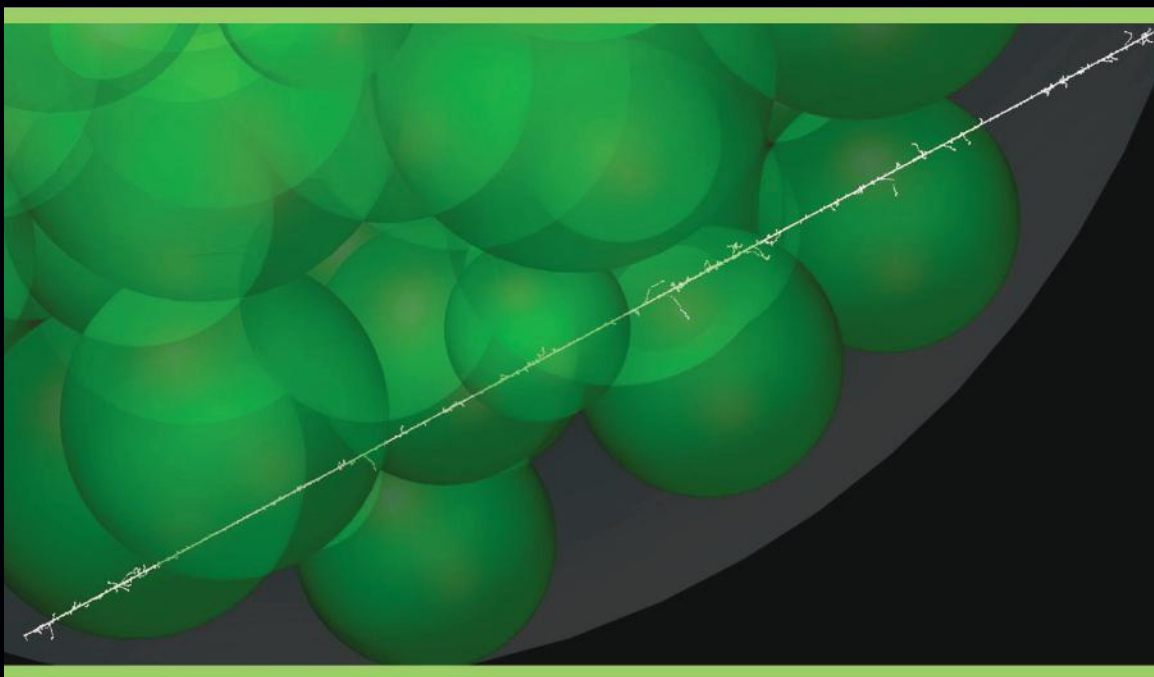


Interaction of Radiation with Matter



Hooshang Nikjoo

Shuzo Uehara

Dimitris Emfietzoglou



CRC Press
Taylor & Francis Group

Interaction of Radiation with Matter

Interaction of Radiation with Matter

Hooshang Nikjoo

Shuzo Uehara

Dimitris Emfietzoglou



CRC Press

Taylor & Francis Group

Boca Raton London New York

CRC Press is an imprint of the
Taylor & Francis Group, an **informa** business

CRC Press
Taylor & Francis Group
6000 Broken Sound Parkway NW, Suite 300
Boca Raton, FL 33487-2742

© 2012 by Taylor & Francis Group, LLC
CRC Press is an imprint of Taylor & Francis Group, an Informa business

No claim to original U.S. Government works
Version Date: 20120412

International Standard Book Number-13: 978-1-4665-0960-3 (eBook - PDF)

This book contains information obtained from authentic and highly regarded sources. Reasonable efforts have been made to publish reliable data and information, but the author and publisher cannot assume responsibility for the validity of all materials or the consequences of their use. The authors and publishers have attempted to trace the copyright holders of all material reproduced in this publication and apologize to copyright holders if permission to publish in this form has not been obtained. If any copyright material has not been acknowledged please write and let us know so we may rectify in any future reprint.

Except as permitted under U.S. Copyright Law, no part of this book may be reprinted, reproduced, transmitted, or utilized in any form by any electronic, mechanical, or other means, now known or hereafter invented, including photocopying, microfilming, and recording, or in any information storage or retrieval system, without written permission from the publishers.

For permission to photocopy or use material electronically from this work, please access www.copyright.com (<http://www.copyright.com/>) or contact the Copyright Clearance Center, Inc. (CCC), 222 Rosewood Drive, Danvers, MA 01923, 978-750-8400. CCC is a not-for-profit organization that provides licenses and registration for a variety of users. For organizations that have been granted a photocopy license by the CCC, a separate system of payment has been arranged.

Trademark Notice: Product or corporate names may be trademarks or registered trademarks, and are used only for identification and explanation without intent to infringe.

Visit the Taylor & Francis Web site at
<http://www.taylorandfrancis.com>

and the CRC Press Web site at
<http://www.crcpress.com>

Contents

Preface	xiii
About the Authors	xv

Section I

1. Introduction	3
1.1 Radiation Transport Codes.....	5
1.1.1 Amorphous Track Codes	8
1.1.2 Condensed History Monte Carlo (CHMC) Codes	8
1.1.3 3D and 4D Monte Carlo Track Structure Codes.....	10
Questions	11
References	11
2. Basic Knowledge of Radiation.....	15
2.1 Definitions of Radiation	15
2.2 Electron Volt.....	16
2.3 Special Theory of Relativity	17
2.4 Electromagnetic Wave and Photon	19
2.5 Interaction Cross Sections.....	21
2.6 Quantities and Units of Radiation.....	24
2.6.1 Relevant to Radiation Fields.....	24
2.6.2 Relevant to Interactions	25
2.6.2.1 Cross Section (σ)	25
2.6.2.2 Mass Attenuation Coefficient (μ/ρ)	25
2.6.2.3 Mass Energy Transfer Coefficient (μ_{tr}/ρ).....	26
2.6.2.4 Mass Energy Absorption Coefficient (μ_{en}/ρ).....	26
2.6.2.5 Total Mass Stopping Power (S/ρ)	26
2.6.2.6 LET (Linear Energy Transfer) or Restricted Linear Collision Stopping Power (L_{Δ})	27
2.6.2.7 Radiation Chemical Yield (G)	27
2.6.2.8 Average Energy per Ion Pair (W)	27
2.6.3 Relevant to Doses.....	27
2.6.3.1 Energy Imparted (ϵ)	27
2.6.3.2 Absorbed Dose (D).....	28
2.6.3.3 Absorbed Dose Rate (\dot{D})	28
2.6.3.4 Kerma (K)	28
2.6.3.5 Kerma Rate (\dot{K})	29
2.6.3.6 Exposure (X)	29
2.6.3.7 Exposure Rate (\dot{X})	29

2.6.4	Relevant to Radioactivities	29
2.6.4.1	Decay Constant (λ)	29
2.6.4.2	Activity (A)	30
2.6.4.3	Air Kerma Rate Constant (Γ_δ)	31
2.6.4.4	Exposure Rate Constant (Γ_δ)	32
2.6.5	Relevant to Radiation Protection	32
2.6.5.1	Dose Equivalent (H)	32
2.7	Summary	33
	Questions	34
	References	34
	For Further Reading	34
3.	Atoms	35
3.1	Atomic Nature of Matter	35
3.2	Rutherford's Atomic Model	36
3.3	Bohr's Quantum Theory	37
3.4	Quantum Mechanics	39
3.4.1	de Broglie Wave of Electrons	39
3.4.2	Uncertainty Principle	40
3.4.3	Schrödinger Equation	41
3.4.4	Wavefunction	43
3.5	Atomic Structure	44
3.5.1	Electron Orbit	44
3.5.2	Pauli's Exclusion Principle	45
3.6	Summary	46
	Questions	47
	For Further Reading	47
4.	Atomic Nucleus	49
4.1	Constituents of Nucleus	49
4.2	Binding Energy of Nucleus	49
4.3	Nuclear Models	51
4.3.1	Liquid Drop Model	51
4.3.2	Shell Model	52
4.3.3	Collective Model	53
4.4	Nuclear Reaction	54
4.4.1	Characteristics	54
4.4.2	Cross Section	55
4.4.3	Threshold Value of Reaction	56
4.5	Nuclear Fission	57
4.6	Nuclear Fusion	58
4.7	Summary	59
	Questions	60
	For Further Reading	60

5. Radioactivity	61
5.1 Types of Radioactivity	61
5.1.1 α -Decay	61
5.1.2 β^- Decay	63
5.1.3 γ -Decay	65
5.1.4 Internal Conversion	65
5.1.5 β^+ Decay	66
5.1.6 Electron Capture	67
5.1.7 Radiative and Nonradiative Transitions	69
5.2 Formulas of Radioactive Decay	71
5.2.1 Attenuation Law	71
5.2.2 Specific Activity	73
5.2.3 Radioactive Equilibrium	73
5.2.3.1 Secular Equilibrium	73
5.2.3.2 General Formula	74
5.2.3.3 Transient Equilibrium	74
5.2.3.4 Nonequilibrium	75
5.3 Summary	75
Questions	75
References	76
For Further Reading	76
6. X-Rays	77
6.1 Generation of X-Rays	77
6.2 Continuous X-Rays	79
6.3 Characteristic X-Rays	80
6.4 Auger Electrons	81
6.5 Synchrotron Radiation	82
6.6 Diffraction by Crystal	84
6.7 Summary	86
Questions	87
For Further Reading	87
7. Interaction of Photons with Matter	89
7.1 Types of Interaction	89
7.1.1 Thomson Scattering	89
7.1.2 Photoelectric Effect	89
7.1.3 Compton Scattering	90
7.1.4 Pair Creation	92
7.1.5 Photonuclear Reaction	93
7.2 Attenuation Coefficients	94
7.3 Half-Value Layer of X-Rays	96
7.4 Mass Energy Absorption Coefficients	98
7.5 Summary	101

Questions	102
For Further Reading	102
8. Interaction of Electrons with Matter	103
8.1 Energy Loss of Charged Particles.....	103
8.2 Collision Stopping Power.....	105
8.3 Radiative Stopping Power.....	108
8.4 Ranges.....	110
8.5 Multiple Scattering.....	112
8.6 Cerenkov Radiation	115
8.7 Summary	117
Questions	117
For Further Reading	118
9. Interaction of Heavy Charged Particles with Matter.....	119
9.1 Collision Stopping Powers.....	119
9.2 Nuclear Stopping Powers.....	123
9.3 Ranges.....	126
9.4 Straggling of Energy Loss and Range.....	128
9.5 Summary	129
Questions	130
References	130
For Further Reading	130
10. δ-Ray, Restricted Stopping Power, and LET	131
10.1 δ -Ray	131
10.2 Restricted Stopping Power.....	132
10.3 LET	135
10.4 Summary	136
Questions	136
References	136
11. Introduction to Monte Carlo Simulation.....	137
11.1 Monte Carlo Method	137
11.2 Sampling of Reaction Point.....	137
11.3 Condensed History Technique	141
11.4 Slowing Down of Electrons	146
11.5 Conversion of Angles	147
11.6 Intersection at Boundary.....	148
11.7 Summary	150
Questions	151
References	151

Section II

12. Cross Sections for Interactions of Photons with Matter 155

12.1 Coherent Scattering 155

12.2 Photoelectric Effect 157

12.3 Incoherent Scattering..... 158

12.4 Pair Creation 162

12.5 Soft X-Rays 166

12.6 Summary 170

Questions 170

References 171

13. Cross Sections for Interactions of Electrons with Water..... 173

13.1 Ionization 173

13.1.1 Secondary Electrons 173

13.1.2 Total Cross Sections..... 179

13.2 Excitation 181

13.3 Elastic Scattering 184

13.4 Stopping Powers..... 186

13.5 Summary 187

Questions 188

References 188

14. Cross Sections for Interactions of Low-Energy Protons
($<1 \text{ MeV}^{-1}$) in Water 191

14.1 Ionization 191

14.1.1 Secondary Electrons 191

14.1.2 Total Cross Sections..... 195

14.2 Excitation 197

14.3 Elastic Scattering 197

14.4 Charge Transfer..... 201

14.5 Stopping Powers..... 202

14.5.1 Electronic Stopping Powers..... 202

14.5.2 Nuclear Stopping Powers 209

14.6 Summary 209

Questions 210

References 210

15. Cross Sections for Interactions of Low Energy α -Particles
($<2 \text{ MeV}^{-1}$) in Water 213

15.1 Ionization 213

15.1.1 Secondary Electrons 213

15.1.2 Total Cross Sections..... 214

15.2	Excitation	217
15.3	Elastic Scattering	218
15.4	Charge Transfer	219
15.5	Stopping Powers	221
15.5.1	Electronic Stopping Powers	221
15.6	Summary	225
	Questions	225
	References	226
16.	Cross Sections for Interactions of High-Energy Protons (>1 MeV⁻¹) in Water	227
16.1	Ionization	227
16.1.1	Secondary Electrons	227
16.1.2	Total Cross Sections	230
16.2	Excitation	231
16.3	Elastic Scattering	231
16.4	Summary	232
	Questions	233
	References	233
17.	Model Calculations Using Track Structure Data of Electrons	235
17.1	Ranges and W Values	235
17.2	Depth-Dose Distributions	235
17.3	Electron Slowing Down Spectra	237
17.4	Summary	241
	References	241
18.	Model Calculations Using Track Structure Data of Ions	243
18.1	KURBUC Code System for Heavy Particles	243
18.2	Ranges and W Values	243
18.3	Depth-Dose Distributions	247
18.4	Radial Dose Distributions	249
18.5	Restricted Stopping Powers	249
18.6	Summary	251
	References	251

Section III

19.	Inelastic Scattering of Charged Particles in Condensed Media: A Dielectric Theory Perspective	255
19.1	Introduction	255
19.2	Formal Scattering Theory: The Problem	258

19.3	Born Approximation.....	260
19.3.1	Validity Range.....	261
19.3.2	Dynamic Structure Factor	261
19.3.3	Oscillator Strength.....	263
19.3.4	Dielectric Response Function.....	266
19.3.5	Kramers-Krönig Relations.....	270
19.3.6	Dielectric Formulation	270
19.4	Bethe Approximation	273
19.5	Electron Gas Theory	275
19.5.1	Plasmons	277
19.5.2	Drude Model	280
19.5.3	Lindhard Model.....	284
19.5.4	Landau Damping.....	290
19.5.5	Mermin Model	292
19.5.6	Plasmon Pole Approximation	295
19.5.7	Many-Body Local Field Correction	298
19.5.8	Static Approximation	301
19.6	Optical Data Models.....	305
19.6.1	Optical Limit.....	305
19.6.2	Models Based on the Drude Dielectric Function	311
19.6.2.1	OREC Version	311
19.6.2.2	Ritchie-Howie Version.....	313
19.6.2.3	Extension to Arbitrary q	315
19.6.3	Models Based on the Lindhard Dielectric Function.....	317
19.6.3.1	Penn Model	317
19.6.3.2	Ashley Model.....	321
19.6.4	Models Based on the Mermin Dielectric Function.....	322
19.6.5	Hybrid Models	323
19.6.5.1	Liljequist Model.....	323
19.6.5.2	Two-Mode Model	325
	References	327

Section IV

20. Questions and Problems	333
----------------------------------	-----

Preface

The subject of this book is primarily the physics of the interactions of ionizing radiation in water and the Monte Carlo simulation of radiation tracks. The book explores the subject from an elementary level and progresses to the state of the art in our physical understanding of radiation track structure in living matter. Section I of the book deals with the elementary knowledge of the radiation field. In Section II we explore the cross sections for electrons and heavy ions—the most important information in need for the simulation of radiation track at the molecular level. And in Section III we discuss in some detail the inelastic scattering and energy loss of charged particles in condensed media with emphasis on liquid water. Section IV provides a large number of questions and problems to explore the subject of this book.

The book was partly designed to be used as a textbook in radiation interaction courses. More generally, we hope the book becomes a platform for education in this topic at the master and PhD levels for medical physics, health physics, and nuclear engineering students.

We express our gratitude to all those who have given us help with the preparation of the book. In particular, we like to thank colleagues at the Radiation Biophysics Group of the Karolinska Institute, Peter Girard, Thiansin Liamsuwan, Reza Taleei, Tommy Sundstrom, Lennart Lindborg, and Krishnaswami Sankaranarayanan for their help.

About the Authors

Hooshang Nikjoo is professor of radiation biophysics at the Department of Oncology-Pathology, Karolinska Institutet. He obtained his BSc (hon) in physics and PhD in radiation physics at the Polytechnique of South Bank London. Previously, he worked for many years at the MRC Radiobiology Unit, later renamed the Genome Stability Unit, Harwell, Oxfordshire, UK. His scientific research interests encompass computational approaches in molecular radiation biology, including Monte Carlo track structure methods, modeling DNA damage and repair, and estimation of radiation risk in humans from exposures to low levels of ionizing radiations using a genome-based framework.



Shuzo Uehara is an emeritus professor of physics at the School of Health Sciences, Kyushu University. He graduated from the Department of Physics of Kyushu University and received his MSc and PhD in experimental nuclear physics from Kyushu University. His research interests include Monte Carlo simulation of ionizing radiation and its application to medicine and biology.



Dimitris Emfietzoglou is an assistant professor in the Medical Physics Laboratory of the University of Ioannina Medical School. He graduated from the Department of Physics of the University of Athens and received his MSc and PhD in radiation science from Georgetown University in Washington, DC. His research interests include theoretical and computational aspects of the interaction of ionizing radiation with biomaterials and nanostructures, and Monte Carlo particle transport simulation.



Section I

1

Introduction

Figure 1.1 is simulated for the passage of a radiation track through the human cell nucleus using Monte Carlo track structure technology. The track is crossing some of the 23 pairs of simulated chromosome volumes. It is a simple picture but tells a thousand-word story. In this book we tell you about the interaction of radiation tracks in the biological medium.

Interaction of radiation with biological matter in the human cell nucleus induces genomic instability, DNA damage, mutation, or cell death. What are the consequences to the cell and the organism in which it resides when perceived as irreducible systems?

Radiation is a double-edged sword. It is a harmful agent to organic and inanimate matter; on the other hand, it is a tool vastly used as a drug to eradicate cancerous cells. Radiation interacts with matter by depositing energy in the form of ionizations and excitations. These physical events leave a history behind that is known as track. Tracks come in many forms—long and short, thin and fat, sparse and dense. All these attributes describe the nature of the particle (or the radiation), whether it is a photon, electron, or heavy ion. Figure 1.1 shows a track segment of 1 MeV/u α -particles crossing a human cell nucleus. It shows interactions of the particle with the atoms in the medium. These interactions, shown as dots, seem to be very close to each other. Intuitions and perception could be very misleading in this case. The diameter of this particular cell is about 10 μm . How close are these interactions? Does it matter to the cell if these interactions are densely close or sparsely spaced? Why are they closely or sparsely spaced? The track shows branches coming off the center line. Some particles produce short but some very long branches. Is there significance to these? Some particles stop in matter completely, leaving behind a short track; some travel through a thick tissue before coming to rest. What is significant of such radiations and how useful are they in industrial use or in medical applications?

This book is about radiation tracks. We explore the physics of radiation tracks, share with you our knowledge gained over the past 30 years in this topic, and show you how radiation tracks can be simulated in a computer experiment. Interaction of radiation with matter is a beautiful subject, and radiation track is the story of a history to tell. This book takes you from the classical physics of track description to the modern aspects of condensed physics in matter. We start the learning with the essential preliminary knowledge and progress from there. There are many questions, exercises, and problems to reinforce the learning and the experience. The authors of

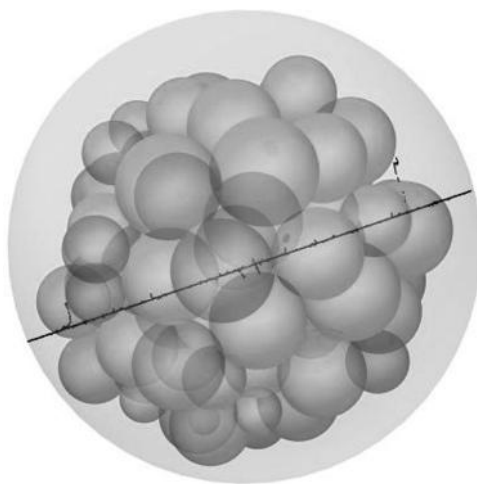


FIGURE 1.1 (SEE COLOR INSERT)

A 1 MeV/u α -particle crossing a cell nucleus.

this book are passionate about their science, and they want to share the knowledge with the young scientists and the students.

Discovery of radiation started with the work of scientific world luminaries Michael Faraday, James Clark Maxwell, Einstein, J.J. Thompson, Madame Curie, and others who established the nature of light and electromagnetic radiation. Since then much progress and insight have been gained in our scientific knowledge. Today, biology presents us as the most complex scientific discipline with many unsolved fundamental questions. A typical human cell nucleus, nearly $10\ \mu\text{m}$ in diameter, contains over a billion DNA molecules. The compact DNA when unwound will stretch to about 180 cm. By current estimates, the human genome contains nearly 100,000 proteins and some 20,000 genes. This is the most complex system in the living environment. What type of physics and mathematics do we need to describe such a complex system that is neither linear nor thermodynamically a closed system? The subject of this book is far from the discussion of biological complexities, but we hope through the discussion of interaction of radiation with matter we open that frontier to greater scrutiny. This book describes interactions of ionizing radiation with matter in its biologically simplest form—water—and develops descriptive models for such a system.

We now scrutinize Figure 1.1 in more detail at the microscopic level. Figure 1.2 brings the view closer to examine the track for a 200 nm length. In this segment of the track there are 507 primary ion (red dots) and 2,073 secondary electron interactions (black dots). As this track was generated in track segment mode, elastic interactions were not considered. Figure 1.3 demonstrates a number of tracks generated in “track segment” and “full slowing down” modes. These include electron, proton, and carbon ions.

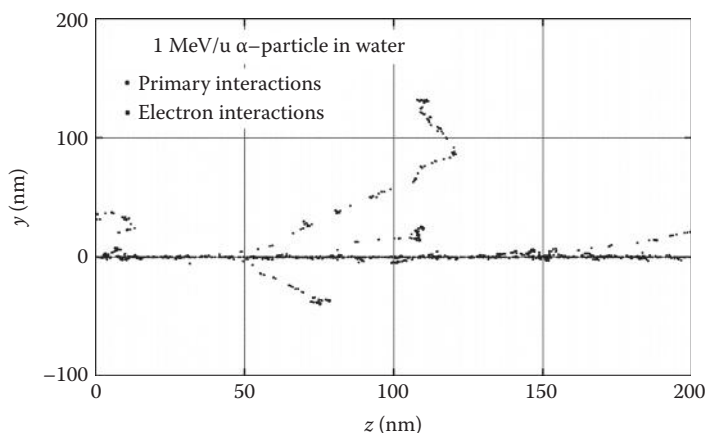


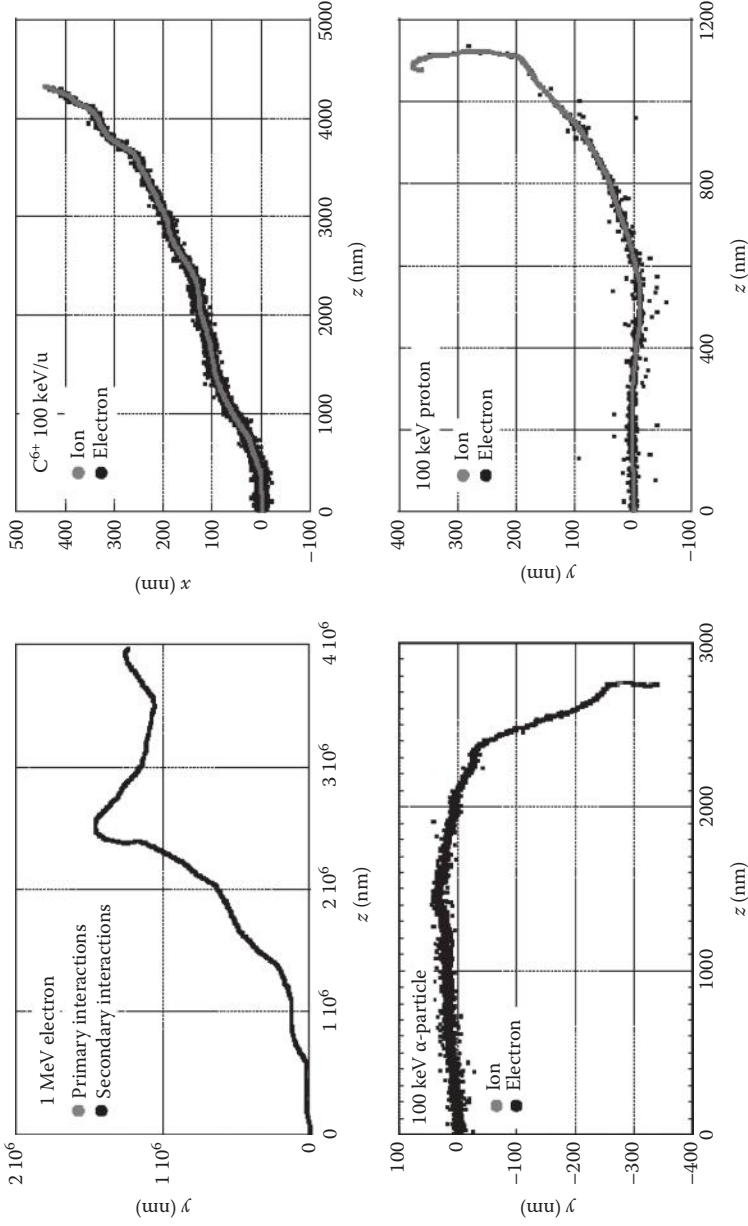
FIGURE 1.2 (SEE COLOR INSERT)

A short segment of the 1 MeV/u α -particle as in Figure 1.1.

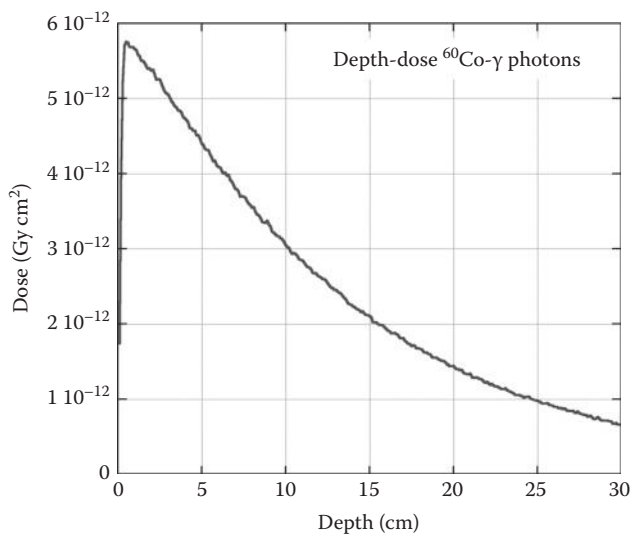
Figure 1.4 provides a more advanced application of Monte Carlo track structure codes to construct depth-dose curves for ^{60}Co - γ photons and 200 MeV protons, typical radiations used in therapy. Table 1.1 gives some of the relevant numbers in the Bragg peak area, and in Table 1.2 some specific details of tracks illustrated in Figure 1.3 are listed.

1.1 Radiation Transport Codes

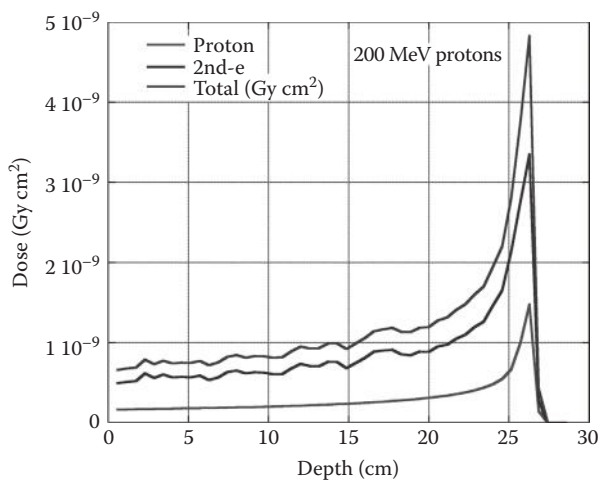
Tracks can be presented in many different ways. One of the earliest models of radiation track description is the linear energy transfer (LET). The concept of LET was originally introduced by Zirkle (1952), adopted from earlier notions of linear energy association (Zirkle 1940) and mean linear ion density (Gray 1947). Cormack and Johns (1952) introduced a more rigorous definition, but it did not separate the contributions of secondary electrons and the stochastic variations of energy loss along the track of the charged particles. Calculations of Burch and Bird (1956) and Burch (1957a,b) explicitly considered the contributions of secondary electrons generated by the interactions of the primary particle with atomic electrons along its trajectory. Burch's calculations were based on the particular criterion of 100 eV energy transfer, which was suggested by Gray (1947) as the dividing line between a primary and a secondary electron track. The secondary electrons resulting from interactions with a single energy transfer of >100 eV were considered to constitute a separate track. Energy transfers of ≤ 100 eV were considered to be deposited locally by the primary track. In radiation chemistry the chemical

**FIGURE 1.3**

Four examples of Monte Carlo tracks generated by the code KURBUC for 1 MeV electron, full slowing down of a 100 keV α -particle, full slowing down of a C^{6+} carbon ion, and a track of 100 keV proton. Tracks show points of energy depositions (ionizations and excitations) for the primary ion and the secondary electrons. All tracks were generated in water.



(a)



(b)

FIGURE 1.4 (SEE COLOR INSERT)

Depth-dose for ^{60}Co - γ photons and protons.

yield or number of molecules formed by reactions of energetic electrons is commonly expressed per 100 eV energy deposited by the track (Magee and Chatterjee 1987, Paretzke 1987).

A one-dimensional deterministic description of ion transport based on the solution of the Boltzmann transport equation has been developed at NASA Langley Research Center (Wilson et al. 1991). The development of these codes

TABLE 1.1
Number of Tracks Per Call

Radiation	Depth at	Dose (Gy cm ²)	Fluence for 1 cGy/cm ²	Average No. of Tracks per Cell
⁶⁰ Co-γ rays	Bragg peak	9e ⁻¹³	1.72	4,444
200 MeV protons	Bragg peak	4.7e ⁻⁹	2.13	8.5

dates back to pre-NASA history and the work on medical problems of high-altitude travel by pilots. Many decades later a greater concern and awareness of the radiation problems and radiation risk in manned space flights led to the development of computer codes at the Langley Research Center (Wilson et al. 1989, 1991, 1995). These codes (HZETRN, BRYNTRN) are used to predict the propagation and interactions of charged particles, including the transport of high-energy ions up to iron or higher charged ions.

1.1.1 Amorphous Track Codes

The Katz track structure model was first published by Butts and Katz (1967); reviews were done by Katz (2003) and Katz et al. (1993), as well as extended versions of the model (Cucinotta et al. 1999; Wilson et al. 1993) and a modified version of the model (Scholz and Kraft 1992, 2004). The latter model has been used in carbon ion therapy planning at GSI (Kraft et al. 1999). The model of Katz was the first to introduce the concept of the lateral extension or radial distribution of dose around the track of ionizing radiation. The model does not consider the track structure of individual interactions but the radial dose profile represented as a homogenous dose distribution in the irradiated sample. The radial dose profile is determined by the ratio of charge to the velocity of the particle.

1.1.2 Condensed History Monte Carlo (CHMC) Codes

Demand for high-level accuracy in dosimetry, for example, absolute dose distributions in patients in radiotherapy and shielding problems, has led to the generation of general purpose Monte Carlo transport codes for energetic electrons and photons, and more recently for stripped ions, for arbitrary geometries. To date, there are a number of these general purpose codes, based on CHMC or other methods, listed in Table 1.3. The most widely used among these codes that are in public domain include EGS4 (Nelson et al. 1985) for the simulation of photons and electrons; MCNP (Goorley et al. 2003) and MCNPx (Hendricks et al. 2008) for simulation of neutrons and light ions; PHITS (Niita et al. 2010), a general purpose code for simulation of heavy ions up to 200GeV; FLUKA (Fasso et al. 2005) for all heavy ion track simulation; GEANT4 (Agnostelli et al. 2003); the Monte Carlo track structure code

TABLE 1.2
Number and types of events in track

	Electrons 1 MeV FSD	Proton 100 keV FSD	α -Particle 100 keV/u FSD	Proton 1 MeV 1 μ m TS	Proton 1 MeV FSD	C ⁶⁺ 100 keV/u FSD
Total number of interactions	107,471	13,846	54,962	2,845	112,505	127,729
Ionization by primary particle	15,034(14%)	1569(11%)	7,478(14%)	356(13%)	13,895(12%)	14,106(11%)
Excitation by primary particle	6,335(5.9%)	1,121(8.1%)	2,656(4.8%)	160(5.6%)	6,585(5.9%)	5,239(4.1%)
Electron capture	0(0.0%)	738(5.3%)	1,311(2.4%)	0(0.0%)	862(0.8%)	5,412(4.2%)
Electron loss	0(0.0%)	737(5.3%)	1,295(2.4%)	0(0.0%)	861(0.8%)	5,406(4.2%)
Elastic (ions)	5,585(5.2%)	3204(23%)	13,344(24%)	306(11%)	13,094(12%)	8,659(6.8%)
Ionization by secondary electrons	18,846(18%)	933(6.7%)	4,681(8.5%)	497(18%)	17,814(16%)	18,748(15%)
Excitation by secondary electrons	27,653(26%)	2424(18%)	10,436(19%)	719(25%)	28,121(25%)	32,516(26%)
Subexcitation electrons	34,018(32%)	3120(23%)	13,004(24%)	807(28%)	31,272(28%)	37,641(30%)

Note: FSD = full slowing down track; TS = track segment (1 μ m).

TABLE 1.3

Partial List of General Purpose Monte Carlo Codes

Code	Particle	Energy Range	Reference
ETRAN	e ⁻ , phot	10 keV–1 GeV	Berger and Seltzer 1973
EGS4	e ⁻ , phot	10 keV–1 GeV	Nelson et al. 1985
FLUKA	p, n, Meson	1 keV–GeV	Fasso et al. 2005
GEANT4	p, n, Meson	250 eV–GeV	Agostinelli et al. 2003
MCEP	e ⁻ , phot	1 keV–30 MeV	Uehara 1986
MCNP5	n, phot, e ⁻	See ref.	Goorley et al. 2003
MCNPX	n, light ions	See ref.	Hendricks et al. 2005
PENPENELOPE	e ⁻ , e ⁺	100 eV–1 GeV	Salvat et al. 2008
PHITS	HZE	MeV–GeV	Niita et al. 2010
PEREGRINE	e ⁻ , phot	Therapy beams	Hartmann Siantar et al. 1998
PTRAN	Protons	<250 MeV	Berger 1993
SRIM	All ions	keV–2 GeV/u	Ziegler et al. 2003
SHIELD-HIT	1 < Z < 10	1 MeV ⁻¹ –1 TeV ⁻¹	Sobolovsky 2010

PENELOPE (Salvat et al. 2008) for performing simulation of coupled electron-photon transport in arbitrary materials and complex quadric geometries in the range of 100 eV to 1 GeV; and SHIELD-HIT (Sobolovsky 2010) for the simulation of heavy ions and complex geometries.

1.1.3 3D and 4D Monte Carlo Track Structure Codes

The full Monte Carlo track structure codes provide the distribution of coordinates of all interactions of the charged particle in space (three-dimensional (3D) codes) and with time (four-dimensional (4D) codes). The 3D codes provide the distribution of physical events (ionization, excitations, and elastic scatterings). This is usually called the *physical track*. In a biological medium, physical events lead to the generation of radicals. The 4D track or the *chemical track* describes the distribution of chemical events in the medium with time. The timeframe for the physical track is fixed from the time of the first interaction at 10^{-15} to 10^{-13} s.

Table 1.4 provides a list of some currently published track structure codes used at various research centers around the world. The majority of the codes use water as the medium for simulation. Most experimental data are obtained in water vapor, as water in any phase is not a tractable medium as a target in experiments. In Section III we discuss in some detail the inelastic interaction of charged particles in condensed media within the context of the dielectric theory, which represents the state of the art for track structure simulations in liquid water. In the codes for liquid water a mixture of data derived from liquid and vapor targets has been employed, as currently there are no direct experimental data for excitation and ionization cross sections for liquid water.

TABLE 1.4
Partial List of Monte Carlo Track Structure Code^a

Code	Particle	Energy Range	Reference
CPA100	e ⁻	10 eV–100 keV	Terrissol and Beaudre 1990
ETRACK	e ⁻ , p, α	10 eV–10 keV e ⁻	Ito 1987
KURBUC CODES	e ⁻	10 eV–10 MeV	Uehara et al. 1993
	p	1 keV–300 MeV	Uehara et al. 2001, Liamsuwan et al. 2011
	α	1 keV/u–2 MeV/u	Uehara and Nikjoo 2002
	C ions	1 keV/u–10 MeV/u	Liamsuwan et al. 2012
LEEPS	e ⁻ , e ⁺	≥10 eV–100 keV	Fernandez-Varea et al. 1996
MC4	e ⁻ , ions	≥10 eV e ⁻ , ions ≥ 0.3 MeV/u	Emfietzoglou et al. 2003
NOTRE DAME	e ⁻ , ions	≥10 eV e ⁻ , ions ≥ 0.3 MeV/u	Pimblott et al. 1990
PARTRAC ^a	e ⁻ , ions	≥10 eV e ⁻ , ions ≥ 0.3 MeV/u	Friedland et al. 2003
PITS99	e ⁻ , ions	≥ 10 eV e ⁻ , ions ≥ 0.3 MeV/u	Wilson and Nikjoo 1999
SHERBROOKE ^a	e ⁻ , ions	≥10 eV e ⁻ , ions > 0.3 MeV/u	Cobut et al. 2004

^a For more details, see Nikjoo et al. (2006).

QUESTIONS

1. Give five examples of the way a radiation track (for example, an α-particle track) can be characterized.
2. Given the depth-dose values in Table 1.1, calculate fluence values for ⁶⁰Co-γ photons and 200 MeV protons. For the cell assume 20 μm diameter/side, spherical or cubic.

References

Agostinelli A, Allison J, Amako K et al. 2003. GEANT4; A SIMULATION TOOLKIT. *Nuclear Instrum. Methods Phys. Res. A* 506. 250–303. <http://geant4.cern.ch/>

Berger MJ, Seltzer SM. 1973. ETRAN, Monte Carlo Code System for electron and photon transport through extended media. ORNL Documentation for RISC Computer code package CCC-107.

Berger MJ. 1993. Proton Monte Carlo transport program PTRAN. Report NISTIR-5113. National Institute of Standards and Technology (NIST). <http://www.nea.fr/abbs/html/ccc-0618.html>

Burch PRJ, Bird PM. 1956. Linear energy transfer calculations allowing for delta tracks. *Progress in Radiobiology*. Birmingham: The Keynoch Press, pp. 161–177.

Burch PRJ. 1957a. Some physical aspects of relative biological efficiency *Br. J. Radiology*. 30: 524–529.

- Burch PRJ. 1957b. Calculations of energy dissipation characteristics in water for various radiations. *Radiation Research*. 6: 289–301.
- Butts JJ, Katz R. 1967. Theory of RBE for heavy ion bombardment of dry enzymes and viruses. *Radiat. Res*. 30: 855–871.
- Cobut V, Cirioni L, Patau JP. 2004. Accurate transport simulation of electron tracks in the energy range 1keV-4MeV. *Nucl. Instrum. Methods. B*. 215: 57–68.
- Cormack DV, Johns HE. 1952. Electron energies and ion densities in water irradiated with 200 keV, 1 MeV and 25 MeV radiation. *Br. J. Radiol*. 25: 369.
- Cucinotta FA, Nikjoo H, Goodhead DT. 1999. Applications of amorphous track models in radiation biology. *Radiation and Environmental Biophysics*. 38: 81–92.
- Emfietzoglou D, Karava K, Papamichael G, Moscovitch M. 2003. Monte Carlo simulation of the energy loss of low-energy electron in liquid water. *Phys. Med. Biol*. 48: 2355–2371.
- Fasso A, Ferrari A, Ranft J, Sala P. 2005. Current version of FLUKA 2011.2.8. <http://fluka.org/>
- Fernandez-Varea JM, Liljequist D, Csillag S, Rdtty R, Salvat F. 1996. Monte Carlo simulation of 0.1-100 keV electron and positron transport in solids using optical data and partial wave methods. *Nucl. Instrum. Methods. B*. 108: 35–50.
- Friedland W, Bernhard P, Jacob P, Paretzke HG, Dingfelder M. 2003. Simulation of DNA damage after proton irradiation. *Radiat. Res*. 159: 401–410.
- Goorley T, Brown F, Cox LJ. 2003. MCNP5™ Improvements for Windows PCs. Proc. M&C 2003: A Century in Review, A Century Anew. Gatlinburg, Tennessee. (LA-UR-02-7162) <http://mcnp-green.lanl.gov/>
- Gray LH. 1947. The distribution of the ions resulting from the irradiation of living cells. *Br. J. Radiol*. (Suppl 1): 7.
- Hartmann-Siantar CL, Moses EI. 1998. The PEREGRINE programmer: using physics and computer simulation to improve radiation therapy for cancer. *Eur. J. Phys*. 19: 513–521. <http://www.llnl.gov/str/Moses.html>
- Hendricks JS, McKinney GW, Trellue HR, et al. 2008. MCNPx. Version 2.6.0. (LA-UR-08-2216.pdf) <http://mcnp.x.lanl.gov/>
- Ito A, 1987. Calculation of double strand break probability of DNA for low LET radiations based on track structure analysis. Nuclear and atomic data for radiotherapy and related radiobiology. International Atomic Energy Agency, IAEA, Vienna.
- Katz R, Cucinotta FA, Wilson JW, Shinn JL, Ngo DM. 1993. A model of cell damage in space flight. In: Swenberg CE, Horneck G, Stassinopoulos EG (Eds.). *Biological Effects and Physics of Solar and Galactic Cosmic Radiation*. Part A. Plenum Press, New York pp. 235–268.
- Katz R. 2003. The parameter-free track structure model of Scholz and Kraft for heavy-ion cross sections. *Radiat. Res*. 160: 724–728.
- Kraft G, Scholz M, Bechtold U. 1999. Tumour therapy and track structure *Radiat. Environ. Biophys*. 38: 229–237.
- Liamsuwan T, Nikjoo H. 2012. An energy-loss model for low- and intermediate-energy carbon projectiles in water, *Int. J. Radiat. Biol*. 88: 45–49.
- Liamsuwan T, Uehara S, Emfietzoglou D, Nikjoo H. 2011. Physical and biophysical properties of proton tracks of energies 1 keV to 300 MeV in water. *Int. J. Radiat Biol*. 87: 141–160.
- Magee JL, Chatterjee A. 1987. Track reactions of radiation chemistry in: Kinetics of nonhomogeneous processes. (Ed) GR Freeman, John Wiley and Sons, New York.

- Nelson WR, Hirayama H, Rogers DWO. 1985. The EGS4 code system (SLAC report 265). <http://rcwww.kek.jp/research/egs/>
- Niita K, Matsuda N, Iwamoto Y, Iwase H, Sato T, Nakashima H, Sakamoto Y, Sihver L. 2010. PHITS: Particle and Heavy Ion Transport code System, Version 2.23. JAEA-Data/Code 2010-022 (2010) <http://phits.jaea.go.jp/>
- Nikjoo H, Uehara S, Emfietzoglou D, Cucinotta FA. 2006. Track-structure codes in radiation research. *Radiat. Measure.* 41: 1052–1074.
- Paretzke HG. 1987. Radiation track structure theory, in: Kinetics of nonhomogeneous processes. (Ed) GR Freeman. John Wiley and Sons, New York.
- Pimblott SM, La Verne JA, Mozumder A, Green NJB. 1990. Structure of electron tracks in water. 1. Distribution of energy deposition events. *J. Phys. Chem.* 94: 488–495.
- Salvat F, Fernandez-Varea JM, Sempau J. 2008. PENELOPE-2008: A code system for Monte Carlo simulation of electron and photon transport. Issy-les-Moulineaux: OECD Nuclear Energy Agency. <http://www.nea.fr/lists/penelope.html>
- Scholz M, Kraft G. 1992. A parameter-free track structure model for heavy ion action cross sections. In: *Biophysical modeling of radiation effects*. (Eds) Chadwick KH, Moschini G, Varma MN. EUR pub no. 13848 EN. Scientific and Technical Communication Unit, Commission of the EC, Directorate General Telecommunications, Information Industries and Innovation, Luxembourg, 185–192.
- Scholz M, Kraft G. 2004. The physical and radiobiological basis of the local effect model: a response to the commentary by R. Katz. *Radiat. Res.* 161: 612–620.
- Sobololevsky N. 2010. SHIELD-Hit: multipurpose hadron transport code. <http://www.inr.ru/shield/>
- Terrissol M, Beaudre BA, 1990. Simulation of space and time evolution of radiolytic species induced by electrons in water. *Radiat. Protec. Dosim.* 31: 175–177.
- Uehara S, Nikjoo H, Goodhead DT. 1993. Cross-sections for water vapour for Monte Carlo electron track structure code from 10 eV to 10 MeV region. *Phys. Med. Biol.* 38: 1841–1858.
- Uehara S, Nikjoo H. 2002. Monte Carlo track structure code for low-energy alpha particles in water. *J. Phys. Chem.* 106: 11051–11063.
- Uehara S, Toburen LH, Nikjoo H. 2001. Development of a Monte Carlo track structure code for low-energy protons in water. *Int. J. Radiat. Biol.* 77: 138–154.
- Uehara S. 1986. The development of a Monte Carlo code simulating electron-photon showers and its evaluation by various transport benchmarks. *Nucl. Instrum. Methods B.* 14: 559–570.
- Wilson JW, Badavi FF, Cucinotta FA, Shinn JL, Badhwar GD, Silberberg R, Tsao CH, Townsend LW, Tripathi RK. 1995. HZETRN: description of a free-space ion and nucleon transport and shielding computer program. NASA Technical paper 3495.
- Wilson JW, Cucinotta FA, Shinn JL. 1993. Cell kinetics and track structure. In: Swenberg CE, Horneck G, Stassinopoulos EG (Eds). *Biological effects and physics of solar and galactic cosmic radiation*. Part A. Plenum Press, New York, 295–338.
- Wilson JW, Townsend LW, Chen SY, Buck WW, Khan F, Cucinotta FA. 1989. BRYNTRN: baryon transport computer code. NASA TM 4037 and NASA TP 288.
- Wilson JW, Townsend LW, Schimmerling W, Khandelwal GS, Khan F, Nealy JE, Cucinotta FA, Simonsen LC, Norbury JW. 1991. Transport methods and interactions for space radiations. RP1257, NASA Washington DC.

- Wilson WE, Nikjoo H. 1999. A Monte Carlo code for positive ion track simulation. *Radiat. Environ. Biophys.* 38: 97–104.
- Ziegler JF, Biersack JP, Littmark U. 2003. The stopping and ranges of ions and solids. Pergamon Press, New York. <http://www.srim.org>
- Zirkle RE, Marchbank DF, Kuck KD. 1952. Exponential and sigmoid survival curves resulting from alpha and x-irradiation of *Aspergillus* spores. *J. Cell Comp. Physiol.* 39 (Suppl. 1): 75–85.
- Zirkle RE. 1940. The radiobiological importance of the energy distribution along ionization tracks. *J. Cell. Comp. Physiol.* 16: 221–235.

2

Basic Knowledge of Radiation

2.1 Definitions of Radiation

Radiation originally meant α -rays, β -rays, and γ -rays emitted from natural radioactive isotopes. At present, elementary particles, nuclei, electrons, and photons, moving with speeds comparable to or higher than the rays from radioactive isotopes, are called radiation. The reason for using the term *rays* is that the path of particles has direction. When radiation passes through matter, it has the capability of direct or indirect ionization of atoms and molecules. Hence we use the term *ionizing radiation*.

Radiation is separated into charged particles and noncharged particles. The former is called direct ionizing radiation because that directly ionizes atoms and molecules with its electric charge. X-rays, γ -rays, and neutrons belong to the latter. Since those do not have the electric charge, they cannot ionize using the electric force directly. However, particles interact with matter and generate secondary charged particles. These particles are called indirect ionizing radiation because secondary charged particles ionize atoms and molecules. Table 2.1 shows a list of radiation relevant to medical and clinical fields.

Radiation is defined as the particles with sufficient energy to cause ionization. If an accelerator is used, all ions are qualified as radiation. Therefore, all elements from hydrogen to uranium can be called radiation. In practice, heavy ions up to neon are utilized in the clinical field. The generation source of radiation is the accelerator or radionuclides except cosmic rays. The radiation sources are as follows:

X-rays: X-ray tube, linear accelerator, synchrotron radiation.

γ -Rays: Radioisotopes.

Electrons: Linear accelerator, betatron, microtron.

β -Rays: Radioisotopes.

Heavy ions: Linear accelerator, cyclotron, synchrotron.

Neutrons: Cyclotron, nuclear reactor, Cf-254, Cf-252.

TABLE 2.1
Ionizing Radiation

Name	Symbol	Electric Charge (<i>e</i>)	Mass (<i>m_e</i>)	Mean Life (s)	Production Method	Remarks
γ-Ray	γ	0	0		Radioisotope (RI)	Single energy
X-ray	X	0	0		Accelerator	Continuous energy
Neutrino	ν	0	~0		Radioisotope	β-decay
Electron (β ⁻ ray)	e ⁻ , β ⁻	-1	1		Accelerator, RI	β-ray is continuous energy
Positron (β ⁺ ray)	e ⁺ , β ⁺	+1	1		Accelerator, RI	Annihilation quanta
Proton	p	+1	1,836		Accelerator	
Neutron	n	0	1,839	1.1 × 10 ³	Accelerator, Nuclear reactor	
Deuteron	d	+1	3,670		Accelerator	
Triton	t	+1	5,479	10 ⁹	Accelerator	
α-Particle	α	+2	7,249		Accelerator, RI	
Muon	μ [±]	±1	207	2.15 × 10 ⁻⁶	High energy nuclear reaction	
Pion (charged)	π [±]	±1	273	2.65 × 10 ⁻⁸	High-energy nuclear reaction	
Pion (neutral)	π ⁰	0	264		High energy nuclear reaction	
Fission fragment (light)		~36	~96 <i>m_p</i>		Nuclear fission	
Fission fragment (heavy)		~56	~140 <i>m_p</i>		Nuclear fission	

2.2 Electron Volt

When an electric charge *q* accelerates through an electrostatic potential difference of *V*, the mechanical work *W* where the electric field acts on the charge is given by

W = qV

(2.1)

This quantity is independent of the distance between both electrodes. The electric charge gains the kinetic energy corresponding to W . Since electric charge in nature cannot be divided infinitely, the minimum unit is called the elementary electric charge. An electron (e^-) has a negative elementary electric charge, $-e$.

$$e = 1.602177 \times 10^{-19} \text{ C} \quad (2.2)$$

The electron rest mass m_e is

$$m_e = 9.10939 \times 10^{-31} \text{ kg} \quad (2.3)$$

The kinetic energy that an electron obtains in motion between the potential of 1 V is defined by 1 eV (electron volt). The relationship between energy units eV and J using Equation (2.1) becomes

$$1 \text{ eV} = 1.602177 \times 10^{-19} \text{ J} \quad (2.4)$$

EXAMPLE 2.1

If an x-ray tube works with an electrical potential of 120 kV, what is the electron potential energy on the cathode surface?

SOLUTION 2.1

$$W = qV = (-1.6 \cdot 10^{-19} \text{ C})(-120 \text{ kV}) = 1.92 \cdot 10^{-14} \text{ J}$$

2.3 Special Theory of Relativity

The special theory of relativity was proposed in 1905 by Albert Einstein. It was constructed based on two fundamental principles:

1. The physical basic laws are not affected for all inertial frames (the principle of relativity).
2. Light in vacuum propagates with the speed c (a fixed constant) in terms of any system of inertial coordinates, regardless of the state of motion of the light source (the principle of invariant light speed).

Once we accept the principle of invariant light speed, a significant change on the concept of time and space must be made. For example, it is assumed that a light is emitted from the jet plane with a supersonic speed of v to the same direction as the plane. The light speed should be $c + v$ if the generally accepted theory is applied. However, the new principle gives the solution of c . In order to realize this principle, a new transformation of the coordinate system is required to take into account that time is needed. According to the

special theory of relativity, the mass of body is revised. If a body with the rest mass m_0 moves with speed v , the mass of body m is represented by

$$m = \frac{m_0}{\sqrt{1 - v^2/c^2}} \quad (2.5)$$

In addition, total energy of the body and its mass are related by the equation

$$E = \frac{m_0 c^2}{\sqrt{1 - v^2/c^2}} = mc^2 \quad (2.6)$$

in which the equation $E = mc^2$ shows the mass m and energy E are equivalent. If the body rests, i.e., $v = 0$, E becomes $m_0 c^2$, which is called the rest energy. The relativistic momentum $p = mv$ is represented by

$$p = \frac{m_0 v}{\sqrt{1 - v^2/c^2}} \quad (2.7)$$

Combining Equations (2.6) and (2.7),

$$E^2 = m_0^2 c^4 + p^2 c^2 \quad (2.8)$$

is obtained.

For photons the rest mass is 0. Inserting $m_0 = 0$ into Equation (2.8),

$$E = pc \quad (2.9)$$

This equation means the energy and the momentum have nonzero finite value even for the particle of $m_0 = 0$.

EXAMPLE 2.2

What is the energy equivalent of the electron and proton with masses $9.109384 \cdot 10^{-31}$ kg and $1.672623 \cdot 10^{-27}$ kg ?

SOLUTION 2.2

$$E = mc^2$$

$$\begin{aligned} E_e &= (9.109384 \cdot 10^{-31} \text{ kg})(2.998 \cdot 10^8 \text{ m/s})^2 = (8.1875 \cdot 10^{-14} \text{ J}) \frac{1 \text{ MeV}}{1.602 \cdot 10^{-13} \text{ J}} \\ &= 0.511 \text{ MeV} \end{aligned}$$

$$\begin{aligned} E_p &= (1.672623 \cdot 10^{-27} \text{ kg})(2.998 \cdot 10^8 \text{ m/s})^2 = (1.5033 \cdot 10^{-10} \text{ J}) \frac{1 \text{ MeV}}{1.602 \cdot 10^{-13} \text{ J}} \\ &= 938 \text{ MeV} \end{aligned}$$

EXAMPLE 2.3

Compare the relativistic and nonrelativistic kinetic energy of an electron traveling with a speed of 0.01, 0.1, 0.5, and 0.9 of the speed of light.

SOLUTION 2.3

The relativistic kinetic energy is

$$T_{rel} = m_0c^2 \left(\frac{1}{\sqrt{1-\frac{v^2}{c^2}}} - 1 \right) .$$

The nonrelativistic kinetic energy is given by $T_{non-rel} = \frac{1}{2} m_0 v^2$.
 m_0 is the rest mass of the electron ($m_0 = 9.10938 \cdot 10^{-31}$ kg),
 $c = 2.99792 \cdot 10^8$ m/s is the speed of light, and e is the elementary charge.
Results are given in the following table:

Table Example 2.3

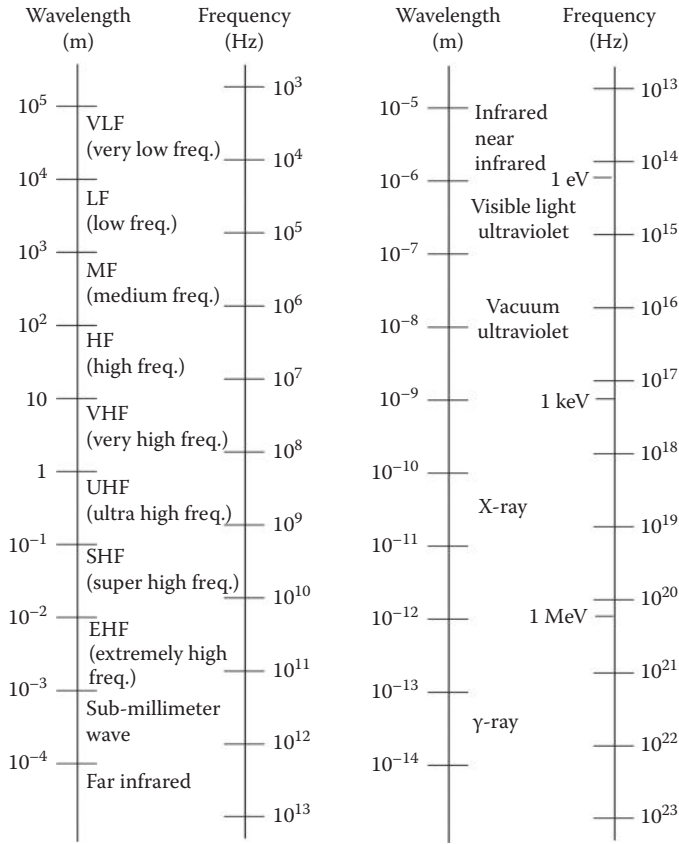
$\frac{v}{c}$	$\frac{1}{\sqrt{1-\frac{v^2}{c^2}}} - 1$	T_{rel} (J)	T_{rel} (eV) = T_{rel} (j)/ e	$T_{non-rel}$ (J)	$T_{non-rel}$ (eV)= $T_{non-rel}$ (j)/ e	Deviation of $T_{non-rel}$ from T_{rel} (%)
0.01	5.0004E-05	4.0939E-18	2.5587E+01	4.0936E-18	2.5585E+01	0.0075
0.1	5.0378E-03	4.1245E-16	2.5778E+03	4.0936E-16	2.5585E+03	0.7506
0.5	1.5470E-01	1.2665E-14	7.9159E+04	1.0234E-14	6.3962E+04	19.1987
0.9	1.2942E+00	1.0595E-13	6.6221E+05	3.3158E-14	2.0724E+05	68.7055

2.4 Electromagnetic Wave and Photon

In classical electromagnetism, Maxwell’s equations are a set of four equations that describe the properties of the electric and magnetic fields and relate them to their sources, charge density, and current density. The variation of the electric and magnetic field relates mutually. Even if the electric charge or the electric current varies, the electromagnetic field generated in the surrounding space cannot vary by a whole field in a moment. The field close to the current varies immediately; however, the variation will delay at the distant space. This means the variation of the electric and magnetic field propagates with a finite speed. This is the electromagnetic wave.

The propagation velocity of the electromagnetic wave, v , is given by

$$v = \frac{1}{\sqrt{\epsilon_0 \mu_0}} \tag{2.10}$$

**FIGURE 2.1**

Name, wavelength, and frequency of electromagnetic wave.

where ϵ_0 and μ_0 are the permittivity of free space and permeability of free space, respectively. Putting v into c ,

$$c = 2.998 \times 10^8 \text{ ms}^{-1} \quad (2.11)$$

is equal to the light speed. Therefore, the electric and magnetic field is the wave motion with the light velocity c inducing mutually. The electromagnetic wave is classified into various names, depending on its origin. Figure 2.1 shows the name, wavelength, and frequency of the electromagnetic wave.

On the other hand, Einstein constructed the photon theory in order to explain the photoelectric effect using Planck's idea of energy quantum. The light with the frequency ν and the wavelength λ can be regarded with a particle having energy and momentum such as

$$E = h\nu, \quad p = h/\lambda = h\nu/c \quad (2.12)$$

where h is Planck's constant with the value of 6.626×10^{-34} Js, which is an important physical constant appearing in the law of microscopic nature. This particle is called a light quantum or a photon. The photon theory was completely recognized by a successful explanation for the Compton effect discovered by Compton in 1923. On the other hand, we cannot abandon the idea of electromagnetic wave in order to interpret the phenomena such as interference and diffraction of light. Therefore, we need to accept the wave-particle duality for the property of light. A unified theory describing both properties was constructed by quantum mechanics. A relationship between the photon energy E (keV) and the wavelength λ (nm) is derived from Equation (2.12).

$$\lambda = \frac{ch}{E} = \frac{1.240}{E} \quad (2.13)$$

EXAMPLE 2.4

Calculate the frequency and the wavelength of 1 MeV x-rays.

SOLUTION 2.4

$$\begin{aligned} \nu &= \frac{E}{h} = \frac{(1\text{MeV}) \frac{1.602 \cdot 10^{-13} \text{ J}}{1\text{MeV}}}{6.626 \cdot 10^{-34}} = 2.417 \cdot 10^{20} \text{ Hz} \\ \lambda &= \frac{c}{\nu} = \frac{2.998 \cdot 10^8}{2.417 \cdot 10^{20}} = 1.24 \cdot 10^{-12} \text{ m} \end{aligned}$$

2.5 Interaction Cross Sections

Rutherford carried the classical mechanics calculations on scattering of α -particles by a positively charged nucleus. This calculation is a typical example of scattering of atomic or molecular collisions. That is very useful for understanding the concept of interaction cross sections. First, the concept of cross section is explained. The intensity of incident particles is assumed to be I , which gives the number of particles passing through a vertical unit area during a unit time. The direction of incident particle is changed by the collision with a target. That is called scattering. The probability of scattering into a given direction is represented by the differential cross section $d\sigma/d\Omega$. Its definition is as follows:

$$\frac{d\sigma}{d\Omega} = \frac{\text{number of particles scattered into the solid angle } d\Omega \text{ a unit time}}{\text{intensity of the incident particles}} \quad (2.14)$$

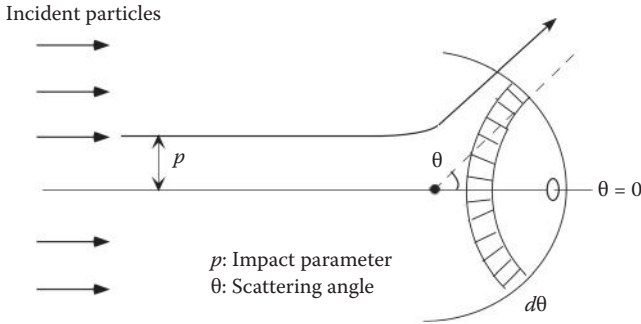


FIGURE 2.2
Scattering of the projectile by a central force.

As shown in Figure 2.2, the elementary solid angle is usually given by

$$d\Omega = 2\pi \sin \theta d\theta \quad (2.15)$$

because of the symmetrical property around the incident axis of particles. The term *cross section* arises because σ has the dimension of area.

The magnitude of scattering is determined by an impact parameter p . The number of particles scattered into the solid angle $d\Omega$ between θ and $\theta + d\theta$ should be equal to the number of incident particles with the corresponding impact parameter between p and $p + dp$. Therefore,

$$2\pi I p dp = -2\pi I \frac{d\sigma}{d\Omega} \sin \theta d\theta \quad (2.16)$$

If p increases by dp , then the force acting on the particle becomes weaker and the scattering angle reduces by $d\theta$. This is the reason for the minus sign on the right-hand side. From Equation (2.16), $d\sigma/d\Omega$ becomes

$$\frac{d\sigma}{d\Omega} = -\frac{p}{\sin \theta} \frac{dp}{d\theta} \quad (2.17)$$

The differential cross section can be evaluated using this formula if the relationship between p and θ is obtained. The total cross section σ_t is provided by integrating over the full solid angle.

$$\sigma_t = \int_{4\pi} \frac{d\sigma}{d\Omega} d\Omega = 2\pi \int_0^\pi \frac{d\sigma}{d\Omega} \sin \theta d\theta \quad (2.18)$$

Next, Rutherford scattering is explained. The problem is the motion of two positive charges acting on each other by the electric force as inverse square of distance. Because the nucleus is heavier than the α -particle, the nucleus

can be regarded as the center of the force fixed in the space. The α -particle approaches the nucleus from an infinite far distance and changes the direction and goes away to an infinite far distance; therefore, its orbit becomes a hyperbola. Here, we show just the solution, omitting the mathematical procedures. The differential cross section of the Rutherford scattering is represented by

$$\frac{d\sigma}{d} = \frac{1}{16} \frac{zZe^2}{4\pi\epsilon_0 E}^2 \frac{1}{\sin^4 \frac{\theta}{2}} \quad (2.19)$$

in which the scattering angle is θ , the nuclear charge is Z , the charge of the α -particle is z , the mass is m , and $E = mv^2/2$. Since this formula does not include the screening effect by orbital electrons, the total cross section σ_t calculated using Equation (2.18) diverges to infinity. If the screening effect is taken into account, it does not diverge.

EXAMPLE 2.5

In the Rutherford's scattering experiment, it was found that the fraction of α -particles scattered through an angle θ by a gold foil is $3.7 \cdot 10^{-7}$. The gold foil is $2.1 \cdot 10^{-5}$ cm thick. The scattered α -particles were counted on a screen of 1 mm^2 area placed at a distance of 1 cm from the scattering foil. What is the differential cross section of this collision at the angle θ ?

SOLUTION 2.5

From Equation (2.14), the differential cross section can be written as

$$\frac{d\sigma}{d} = \frac{N_s}{N_i} \frac{S}{N_t}$$

where N_i and N_s are the number of incident and scattered α -particles, respectively; $\Delta\Omega$ is the solid angle through which the particles were scattered; and N_t is the number of scattering centers.

Assuming that the area ΔS of the gold foil was impinged by the beam of α -particles, this foil has the thickness d , the density ρ , and the atomic weight A . Thus, N_t is calculated using

$$N_t = \frac{\rho N_A d S}{A}$$

where N_A is the Avogadro's constant. The solid angle can be written as

$$= \frac{a}{r^2}$$

where Δa is the counting area placed at a distance r from the gold foil.

Finally, the differential cross section of this collision is given by

$$\begin{aligned}\frac{d\sigma}{d} &= \frac{N_s}{N_i} \frac{Ar^2}{\rho N_A d a} \\ &= (3.5 \cdot 10^{-7}) \frac{(0.197 \text{ kg/mol})(10^{-2} \text{ m})^2}{(1.93 \cdot 10^4 \text{ kg/m}^3) \cdot (6.022 \cdot 10^{23} \text{ mol}^{-1})(2.1 \cdot 10^7 \text{ m})(10^{-6} \text{ m}^2)} \\ &= 2.825 \cdot 10^{-27} \text{ m}^2 = 28.25 \text{ b}\end{aligned}$$

2.6 Quantities and Units of Radiation

When we discuss radiation interaction with matter, we need to know the definition and units of radiation quantities. The present descriptions are based on the recommendations of ICRU Report 33 (1980) and Report 51 (1993).

2.6.1 Relevant to Radiation Fields

1. Particle number (N): The number of particles emitted, penetrated, or incident. The unit is 1.
2. Radiant energy (R): The energy of particles emitted, penetrated, or incident. (The rest energy is not included.) The unit is J.
3. Particle flux (\dot{N}):

$$\dot{N} = \frac{dN}{dt} \quad (2.20)$$

dN is the increment of particles within the time dt . The unit is s^{-1} .

4. Energy flux (\dot{R}):

$$\dot{R} = \frac{dR}{dt} \quad (2.21)$$

dR is the increment of radiant energy within the time dt . The unit is W.

5. Particle fluence (Φ):

$$\Phi = \frac{dN}{da} \quad (2.22)$$

Φ is the quotient of the particle number dN incident on the sphere divided by da , the sphere cross section. The unit is m^{-2} .

6. Energy fluence (Ψ):

$$\Psi = \frac{dR}{da} \quad (2.23)$$

Ψ is the quotient of the radiant energy dR incident on the sphere divided by da , the sphere cross section. The unit is Jm^{-2} .

7. Particle fluence rate (ϕ):

$$\phi = \frac{d\Phi}{dt} = \frac{d^2N}{dadt} \quad (2.24)$$

$d\Phi$ is the increment of particle fluence within the time dt . The unit is $\text{m}^{-2}\text{s}^{-1}$.

8. Energy fluence rate (ψ):

$$\psi = \frac{d\Psi}{dt} = \frac{d^2R}{dadt} \quad (2.25)$$

$d\Psi$ is the increment of energy fluence within the time dt . The unit is $\text{W m}^{-2}\text{s}^{-1}$.

2.6.2 Relevant to Interactions

2.6.2.1 Cross Section (σ)

$$\sigma = \frac{P}{\Phi} \quad (2.26)$$

P is the probability of interaction with a target (an atom or a molecule) when the particle fluence Φ hits. The unit is m^2 . The unit frequently used is barn (10^{-28}m^2).

2.6.2.2 Mass Attenuation Coefficient (μ/ρ)

The mass attenuation coefficient for noncharged particles is given by

$$\frac{1}{\rho} = \frac{1}{\rho N} \frac{dN}{dl} \quad (2.27)$$

N is the number of particles that entered the layer with the thickness dl and the density ρ . dN means the number of particles that interacted in this layer and varied their energies or directions. The unit is $\text{m}^2 \text{kg}^{-1}$. For x-rays and γ rays,

$$\frac{1}{\rho} = \frac{\tau}{\rho} + \frac{\sigma_c}{\rho} + \frac{\sigma_{\text{coh}}}{\rho} + \frac{\kappa}{\rho} \quad (2.28)$$

Each term on the right-hand side represents the mass attenuation coefficients for photoelectric effect, Compton effect, incoherent scattering, and electron pair creation, respectively.

2.6.2.3 Mass Energy Transfer Coefficient (μ_{tr}/ρ)

The mass energy transfer coefficient for noncharged particles is given by

$$\frac{\mu_{tr}}{\rho} = \frac{1}{\rho EN} \frac{dE_{tr}}{dl} \quad (2.29)$$

E is the total energy, except the rest energy, of noncharged particles that entered the layer with the thickness dl and the density ρ . dE_{tr} means the sum of kinetic energy generated in this layer. The unit is $m^2 kg^{-1}$.

2.6.2.4 Mass Energy Absorption Coefficient (μ_{en}/ρ)

The mass energy absorption coefficient for noncharged particles is given by

$$\frac{\mu_{en}}{\rho} = \frac{\mu_{tr}}{\rho} (1 - g) \quad (2.30)$$

where g is the fraction of the energy lost by a secondary charged particle in matter by bremsstrahlung with the unit $m^2 kg^{-1}$. The difference between μ_{en}/ρ and μ_{tr}/ρ becomes significant when the kinetic energy of secondary charged particles is high and the atomic number of matter is large.

2.6.2.5 Total Mass Stopping Power (S/ρ)

The total mass stopping power of material for charged particles is given by

$$\frac{S}{\rho} = \frac{1}{\rho} \frac{dE}{dl} \quad (2.31)$$

dE is the energy loss of charged particles within the length dl in the matter with the density ρ . The unit is $Jm^2 kg^{-1}$. S means the total linear stopping power. In the energy region where nuclear interaction can be neglected, the total mass stopping power is represented by

$$\frac{S}{\rho} = \frac{1}{\rho} \frac{dE}{dl}_{col} + \frac{1}{\rho} \frac{dE}{dl}_{rad} \quad (2.32)$$

where $(dE/dl)_{col} = S_{col}$ is the linear collision stopping power, and $(dE/dl)_{rad} = S_{rad}$ is the linear radiative stopping power.

2.6.2.6 LET (Linear Energy Transfer) or Restricted Linear Collision Stopping Power (L_Δ)

The linear energy transfer (LET) for charged particles in matter is given by

$$L = \frac{dE}{dl} \quad (2.33)$$

Δ represents the energy of secondary electrons generated by collision. The equation means the collision stopping power due to secondary electrons having energy below Δ . For example, L_{100} is called the LET for the cutoff energy of 100 eV. If all secondary electrons are taken into account, Δ becomes ∞ . Therefore, L_∞ is equal to S_{col} . The unit is J m^{-1} . Usually the units are given in $\text{keV } \mu\text{m}^{-1}$ or g/cm^2 .

2.6.2.7 Radiation Chemical Yield (G)

The chemical yield of reaction products by absorption of radiation energy is called the G value.

$$G = \frac{n}{\epsilon} \quad (2.34)$$

in which $\bar{\epsilon}$ is the absorbed energy and n is the produced numbers of an atom or a molecule. The unit is mol J^{-1} .

2.6.2.8 Average Energy per Ion Pair (W)

The average energy dissipated to form an ion pair in a gas is called W value. The unit is eV.

$$W = \frac{E}{\bar{N}} \quad (2.35)$$

\bar{N} is the average number of produced ion pairs when the charged particle having the initial kinetic energy of E is completely dissipated in the gas.

2.6.3 Relevant to Doses

2.6.3.1 Energy Imparted (ϵ)

The radiation energy imparted to matter in a certain volume is given by

$$\epsilon = R_{\text{in}} - R_{\text{out}} + \sum Q \quad (2.36)$$

in which, R_{in} = sum of radiant energy of all charged and noncharged particles entered in this volume (except the rest energy), R_{out} = sum of radiant

energy of all charged and noncharged particles emitted from this volume (except the rest energy), and ΣQ = sum of the change of the rest energy caused by the nuclear transformation of nuclei and elementary particles in this volume.

The unit is J. The ϵ is a stochastic quantity, which is the fundamental quantity in microdosimetry.

2.6.3.2 Absorbed Dose (D)

The absorbed dose is defined by the division of mean energy deposition $d\bar{\epsilon}$ (this is a nonstochastic quantity) by a given mass dm of matter.

$$D = \frac{d\bar{\epsilon}}{dm} \quad (2.37)$$

The unit is J kg^{-1} . The specific name is gray (Gy): $1 \text{ Gy} = 1 \text{ J kg}^{-1}$.

2.6.3.3 Absorbed Dose Rate (\dot{D})

$$\dot{D} = \frac{dD}{dt} \quad (2.38)$$

dD is the increment of absorbed dose in the time dt . The specific unit name is $1 \text{ Gy s}^{-1} = 1 \text{ J kg}^{-1}$.

2.6.3.4 Kerma (K)

This is the abbreviation for kinetic energy released in material. Kerma is defined by the division of the sum of initial kinetic energy of all charged particles released by noncharged particles by a given mass dm .

$$K = \frac{dE_{tr}}{dm} \quad (2.39)$$

The unit is J kg^{-1} . The specific name is gray (Gy); $1 \text{ Gy} = 1 \text{ J kg}^{-1}$. Kerma is applicable only for noncharged particles. dE_{tr} is the initial energy of secondary charged particles; therefore, it includes energy loss not only by ionization and excitation but also to bremsstrahlung. In addition, energy of Auger electrons resulting from the photoelectric effect within the volume element is also included. For noncharged particles with energy E , a relationship between energy fluence Ψ and kerma K holds:

$$K = \Psi \frac{tr}{\rho} = \Phi E \frac{tr}{\rho} \quad (2.40)$$

where μ_{tr}/ρ is the mass energy transfer coefficient and $[E(\mu_{tr}/\rho)]$ is called kerma factor. If charged particle equilibrium holds in matter and bremsstrahlung loss can be ignored, absorbed dose D is equal to kerma K . For high-energy photons, charged particle equilibrium does not hold and K becomes slightly smaller than D .

2.6.3.5 Kerma Rate (\dot{K})

$$\dot{K} = \frac{dK}{dt} \quad (2.41)$$

2.6.3.6 Exposure (X)

It is assumed that all electrons (both negative and positive) generated by incident photons completely stop in air with the mass dm . Electron-ion pairs are produced during electron slowing down. If the total charge of one pair is dQ , the exposure is defined by

$$X = \frac{dQ}{dm} \quad (2.42)$$

The unit is $C\ kg^{-1}$. The charge generated by bremsstrahlung due to secondary electrons is not included in dQ . It is difficult to measure the exposure in the energy range lower than a few keV or higher than a few MeV photons. An alternative definition of the exposure is

$$X = \Psi \frac{e}{\rho} \frac{1}{W} \quad (2.43)$$

2.6.3.7 Exposure Rate (\dot{X})

$$\dot{X} = \frac{dX}{dt} \quad (2.44)$$

The unit is $C\ kg^{-1}\ min^{-1}$ or $C\ kg^{-1}\ h^{-1}$ usually.

2.6.4 Relevant to Radioactivities

2.6.4.1 Decay Constant (λ)

For a radionuclide at a specific energy state, the decay constant is the probability that the nucleus causes a spontaneous nuclear transition from that state. The unit is s^{-1} .

2.6.4.2 Activity (A)

The activity is the quantity of a radionuclide at a specific energy state at a time. It is assumed that the expectation value of the number of spontaneous nuclear transition from the state is dN within the time dt .

$$A = \frac{dN}{dt} \quad (2.45)$$

The unit is s^{-1} . The specific name is Bq. $1 \text{ Bq} = 1 \text{ s}^{-1}$. Here, a specific energy state specifies the nuclear ground state. The activity A for a radionuclide at the specific energy state is equal to the product of λ and the number of nucleus N at the state.

$$A = \lambda N \quad (2.46)$$

EXAMPLE 2.6

The activity of a cobalt-60 source was measured to be 620 kBq on November 1, 1986. What is the activity of this source on October 31, 2011?

SOLUTION 2.6

The half-life, $T_{1/2}$, of Co-60 is 5.26 years. The decay constant λ is calculated using

$$\lambda = \frac{\ln 2}{T_{1/2}} = \frac{\ln 2}{5.26 \text{ y}} = 0.131777 \text{ y}^{-1}$$

From Equations (2.45) and (2.46), the activity A is given by

$$A = \lambda N = \frac{dN}{dt}$$

$$N = N_0 e^{-\lambda t}$$

$$A = A_0 e^{-\lambda t}$$

where the index 0 denotes the initial number of radioactive atoms, N , or activity of the source. Therefore, the activity of the source on October 31, 2011 (25 years later) is

$$A = 620 \text{ kBq} \cdot \exp(-0.13777 \text{ y}^{-1} \cdot 25 \text{ y}) = 22.995 \text{ kBq}$$

EXAMPLE 2.7

Calculate the exposure of 1 MeV photon in air, given the photon fluence of 10^9 cm^{-2} .

SOLUTION 2.7

The W value for air is $W_{\text{air}} = 34 \text{ eV}$.

$$\begin{aligned}
 X &= \phi E \frac{en}{\rho} \frac{e}{W_{\text{air}}} \\
 &= 10^9 \text{ cm}^{-2} \cdot 10^6 \text{ eV} \cdot 0.0278 \frac{\text{cm}^2}{\text{g}} \frac{1.6 \cdot 10^{-19} \text{ C}}{34 \text{ eV}} \\
 &= 1.308 \cdot 10^{-7} \text{ C/g} = 1.308 \cdot 10^{-4} \text{ C/g}
 \end{aligned}$$

EXAMPLE 2.8

Calculate the dose that the same photon beam would deposit in liquid water.

SOLUTION 2.8

$$\begin{aligned}
 D &= \phi E \frac{en}{\rho} \\
 &= 10^9 \text{ cm}^{-2} \cdot 10^6 \text{ eV} \cdot 0.0309 \frac{\text{cm}^2}{\text{g}} \\
 &= 3.09 \cdot 10^{13} \text{ eV/g} = 4.944 \cdot 10^{-3} \text{ Gy}
 \end{aligned}$$

2.6.4.3 Air Kerma Rate Constant (Γ_{δ})

A point source with the activity A is located at the distance l from the point of interest. At this point the air kerma rate constant for photons having energy greater than δ is given by

$$\Gamma_{\delta} = \frac{l^2 \dot{K}_{\delta}}{A} \quad (2.47)$$

where \dot{K}_{δ} is the air kerma rate. The unit is $\text{m}^2\text{Gy Bq}^{-1} \text{ s}^{-1}$.

2.6.4.4 Exposure Rate Constant (Γ_δ)

The activity A is located at the distance l from the point of interest. At this point the exposure rate constant for photons having an energy greater than δ is given by

$$\Gamma_\delta = \frac{l^2}{A} \frac{dX}{dt}_\delta \quad (2.48)$$

The relevant photons include γ -rays, characteristic x-rays, and bremsstrahlungs.

2.6.5 Relevant to Radiation Protection

2.6.5.1 Dose Equivalent (H)

The effect of radiation action on biological material is different depending on the radiation type, even if for the same absorbed dose. In order to indicate the differences, the term *relative biological effectiveness* (RBE) has been used (Nikjoo and Lindborg 2010). The dose equivalent (H) is represented by

$$H = QD \quad (2.49)$$

in which D is the absorbed dose at a point in tissue and Q is the quality factor at that point. The unit of the dose equivalent is Sv if the unit of absorbed dose is Gy; 1 Sv = 1 Gy. Table 2.2 shows the summary of radiation quantities and units.

EXAMPLE 2.9

What is the kerma in air produced by the photon beam?

SOLUTION 2.9

$$\begin{aligned} K &= \phi E \frac{-tr}{\rho}_{air} \\ &= 10^9 \text{ cm}^{-2} \cdot 10^6 \text{ eV} \cdot 0.028 \frac{\text{cm}^2}{\text{g}} \\ &= 2.8 \cdot 10^{13} \text{ eV/g} = 4.48 \cdot 10^{-3} \text{ Gy} \end{aligned}$$

TABLE 2.2

Radiation Quantities and Units

Name	Symbol	SI Unit	Specific Name of Unit	Special Unit
Particle number	N	1		
Radiant energy	R	J		
Particle flux	\dot{N}	s^{-1}		
Energy flux	\dot{R}	W		
Particle fluence	Φ	m^{-2}		
Energy fluence	Ψ	$J m^{-2}$		
Particle fluence rate	ϕ	$m^{-2} s^{-1}$		
Energy fluence rate	ψ	$W m^{-2}$		
Particle radiance	p	$m^{-2} s^{-1} sr^{-1}$		
Energy radiance	γ	$W m^{-2} sr^{-1}$		
Cross section	σ	m^2		b
Mass attenuation coefficient	μ/ρ	$m^2 kg^{-1}$		
Mass energy transfer coefficient	μ_{tr}/ρ	$m^2 kg^{-1}$		
Mass energy absorption coefficient	μ_{en}/ρ	$m^2 kg^{-1}$		
Total mass stopping power	S/ρ	$J m^2 kg^{-1}$		$eV m^2 kg^{-1}$
Linear energy transfer	L_{Δ}	$J m^{-1}$		$eV m^{-1}$
Radiation chemical yield	$G(x)$	$mol J^{-1}$		
Mean energy per ion pair	W	J		eV
Energy imparted	ε	J		
Lineal energy	y	$J m^{-1}$		$eV m^{-1}$
Specific energy	z	$J kg^{-1}$	Gy	rad
Absorbed dose	D	$J kg^{-1}$	Gy	rad
Absorbed dose rate	\dot{D}	$J kg^{-1} s^{-1}$	$Gy s^{-1}$	$rad s^{-1}$
Kerma	K	$J kg^{-1}$	Gy	rad
Kerma rate	\dot{K}	$J kg^{-1} s^{-1}$	$Gy s^{-1}$	$rad s^{-1}$
Exposure	X	$C kg^{-1}$		R
Exposure rate	\dot{X}	$C kg^{-1} s^{-1}$		$R s^{-1}$
Decay constant	λ	s^{-1}		
Activity	A	s^{-1}	Bq	Ci
Air kerma rate constant	Γ_{δ}	$m^2 J kg^{-1}$	$m^2 Gy Bq^{-1} s^{-1}$	$m^2 rad Ci^{-1} s^{-1}$
Dose equivalent	H	$J kg^{-1}$	Sv	rem
Dose equivalent rate	\dot{H}	$J kg^{-1} s^{-1}$	$Sv s^{-1}$	$rem s^{-1}$

2.7 Summary

1. Energetic elementary particles, nucleus, and photon moving in space and matter are called radiation.
2. When radiation travels in matter, particles with sufficient energy to ionize atoms and molecules are called ionizing radiation.

3. Charged particles are called directly ionizing radiation. Uncharged particles such as photons and neutrons are called indirectly ionizing radiation.
4. The energy of radiation is generally represented by electron volt (eV) units.
5. The theory of relativity changes the concepts of time, space, and mass. Therefore, energy and momentum in mechanics are represented in the manner of the relativistic theory.
6. The electromagnetic wave is derived from Maxwell's equations. X-rays and γ -rays are a kind of electromagnetic wave. Simultaneously, γ -rays and x-rays are also called photons because they have the characteristics of particles.
7. Energy and momentum of a photon having the frequency ν is $h\nu$ and $h\nu/c$, respectively.
8. Probability of reaction is represented by cross section. Energy spectrum or angular distribution is represented by the differential cross section.

QUESTIONS

1. The sequence of elements by atomic weight is Cl, K, Ar, and by atomic number using Mosely's law, Cl, Ar, K. Explain which is the correct sequence.
 2. What is radiation pressure?
 3. What can be seen on a screen if a flame is placed between two charged plates and a shadow of it is observed on the screen?
-

References

- ICRU. 1980. *Radiation Quantities and Units*. ICRU Report 33.
- ICRU. 1993. *Quantities and Units in Radiation Protection Dosimetry*. ICRU Report 51.
- Nikjoo H, Linborg L. 2010. RBE of low energy electrons and protons. *Phys. Med. Biol.* 55: R65.
-

For Further Reading

- Goldstein H. 1950. *Classical Mechanics*. Reading, MA: Addison-Wesley.
- Johns HE, Cunningham JR. 1974. *The Physics of Radiology*, 3rd ed. Springfield, IL: Charles C. Thomas Publisher.
- Turner JE. 1995. *Atoms, Radiation, and Radiation Protection*, 2nd ed. New York: John Wiley & Sons.

3

Atoms

3.1 Atomic Nature of Matter

At the beginning of the nineteenth century, the English chemist John Dalton discovered important laws that are the basis of modern chemistry. The first is the law of definite proportions. This law states that a chemical compound always contains exactly the same proportion of elements by mass. For example, oxygen makes up 8/9 of the mass of any sample of pure water, while hydrogen makes up the remaining 1/9 of the mass. In the case other than this ratio between oxygen and hydrogen, the elements do not make water, but whichever excess element remains. The second is the law of multiple proportions. The law states that when chemical elements combine, they do so in a ratio of small whole numbers. For example, a reaction of carbon of 12 g with oxygen of 32 g makes carbon dioxide (CO_2). Carbon monoxide (CO) is a combination of carbon of 12 g with oxygen of 16 g. In comparison with these two compounds, oxygen jumps by twice the amount, from 16 g to 32 g. Dalton's atomic model constructed the modern view for materials that compounds are produced by combination of atoms with the mass. This idea was supported by contemporary scientists. Gay-Lussac's law of combining volumes states that a simple integer ratio holds between the volumes of individual gases before reaction and the volumes of produced gases under the condition of constant pressure and temperature. This law means the volume of the gas is in proportion to the number of molecules under the above condition. Avogadro proposed the hypothesis that all gases of the same volume are the group of molecules with the same number. The mass of a material, A gram, consisting of an element with the atomic mass A is 1 g atom of the material. The mass of a compound, M gram, consisting of the molecular mass M is 1 g molecule or 1 mole. The number of atoms (molecules) included in the material of 1 g atom (molecule) is the common constant for all materials, called the Avogadro constant, N_A . The value of N_A is $6.022 \times 10^{23} \text{ mol}^{-1}$.

The chemical element forms a series of characteristic lines peculiar to each element and is called element spectrum. The element absorbs the light of the same wavelength as the emitted light. Discharging a hydrogen atom contained in the gas discharge tube, a lot of spectral lines are observed using

the spectrometer. A semiempirical formula giving the wavelength for the hydrogen spectrum was proposed by Balmer.

$$\frac{1}{\lambda} = R \left(\frac{1}{2^2} - \frac{1}{n^2} \right) \quad (3.1)$$

where $R = 1.09737 \times 10^7 \text{ m}^{-1}$ is called the Rydberg constant and n represents the integers greater than 2. This relationship was theoretically derived by Niels Bohr in 1913.

A few thousand volts is applied between two electrodes enclosed in a long and slender glass tube. Discharge occurs as the air pressure in the tube is reduced. At the pressure of 0.01 mmHg, a kind of radiation is ejected from the cathode. This is called the cathode ray. J.J. Thomson measured the ratio of its charge to the mass, e/m , called the specific charge. This is documented as the experimental discovery of the electron. The e/m value he obtained was about 1,700 times that of the hydrogen atom. The latest value is $1.7588 \times 10^{11} \text{ C kg}^{-1}$.

3.2 Rutherford's Atomic Model

α -, β -, and γ -rays are used as probes to investigate the material structure. Rutherford and his students, Geiger and Marsden, worked on the α -particles' penetration of the material. When the collimated α -particle beam of 7.69 MeV hits the thin gold foil, penetrated α -particles are observed at various angles. Almost all of them deviate a little bit from the incident direction. However, large-angle scattering and back scattering rarely occurred. A very strong electric field or magnetic field is required to reverse the direction of high-speed particles. Rutherford thought that such a large-angle deflection is the evidence of the existence of a small and heavy nucleus having the positive charge. Light electrons in the atom move around the nucleus rapidly. An atom is almost an empty space. Therefore, almost all α -particles penetrated the foil without scattering. From these considerations, he calculated, assuming an α -particle is scattered, the Coulomb force from a point mass with positive charge. The Rutherford scattering formula was then derived. The calculated angular distributions were in good agreement with the experimental data. The nuclear radius for mass number A is approximately represented by

$$R \approx 1.3A^{1/3} \times 10^{-15} \text{ m} \quad (3.2)$$

Therefore, the radius of a gold nucleus becomes $7.56 \times 10^{-15} \text{ m}$. The radius of a gold atom is $1.79 \times 10^{-10} \text{ m}$. The atomic model of Rutherford is called the solar system model.

3.3 Bohr's Quantum Theory

An object not moving with a constant speed and in the same direction is accelerated. From the viewpoint of classical mechanics, such an accelerated charge emits an electromagnetic wave. In this case, why is an atom of the Rutherford model stable? To explain this, Bohr proposed a theory that explains the spectrum of hydrogen. The theory of Bohr is based on three hypotheses:

1. The energy of an orbital electron is not continuous but one of discrete values peculiar to the atom, $E_1, E_2, E_3, \dots, E_n$. These states, called the stationary states, do not emit light. The above energies are called the energy levels. The stationary state of the lowest energy is the ground state and the upper stationary states are the excited states.
2. An atom emits or absorbs the light when an electron jumps from a stationary state to another stationary state. If the electron state transfers from E_i to E_f , a photon of frequency ν is emitted.

$$h\nu = E_i - E_f \quad (3.3)$$

This is called the Bohr's frequency condition.

3. An electron in the stationary state moves according to Newtonian mechanics. Bohr found that the correct energy level of an electron is obtained if the angular momentum of the electron around the nucleus is assumed to be the Planck's constant \hbar times an integer, in which $\hbar = h/2\pi$. The circular motion of an electron around the hydrogen nucleus having the angular momentum of rmv , equal to $n\hbar$, is therefore

$$rmv = n\hbar \quad (3.4)$$

This is called the quantum rule. The integer n is called the quantum number.

The Coulomb force acting on an electron is equal to the centripetal force of the circular motion with the same speed; therefore,

$$m \frac{v^2}{r} = \frac{e^2}{4\pi\epsilon_0 r^2} \quad (3.5)$$

is obtained. From this equation, r becomes

$$r = \frac{4\pi\epsilon_0 \hbar^2}{me^2} n^2 \quad (3.6)$$

If $n = 1$, the radius is called Bohr's radius. This is usually noted a with the value of 0.529×10^{-10} m, and represents the radius of a hydrogen atom. The electron energy E is the sum of the kinetic energy and the Coulomb potential.

$$E = \frac{1}{2}mv^2 - \frac{e^2}{4\pi\epsilon_0 r} \quad (3.7)$$

Using Equations (3.5) and (3.6), the electron energy traveling the n th circular orbit becomes

$$E_n = -\frac{e^2}{8\pi\epsilon_0 r} = -\frac{e^2}{8\pi\epsilon_0 a} \frac{1}{n^2} = -\frac{13.6}{n^2} \text{ [eV]} \quad (n = 1, 2, 3, \dots) \quad (3.8)$$

This represents the energy level of a hydrogen atom. The light frequency ν accompanying the transition $n_i \rightarrow n_f$ is represented from Bohr's frequency condition,

$$h\nu = \frac{e^2}{8\pi\epsilon_0 a} \left(\frac{1}{n_f^2} - \frac{1}{n_i^2} \right) \quad (3.9)$$

Using the relationship of $c = \lambda\nu$,

$$\frac{1}{\lambda} = R \left(\frac{1}{n_f^2} - \frac{1}{n_i^2} \right) \quad (3.10)$$

If $n_f = 2$, then the Balmer's series is derived.

$$R = \frac{e^2}{8\pi h \epsilon_0 a c} = \frac{me^4}{8\epsilon_0^2 h^3 c} \quad (3.11)$$

is the theoretical equation of the Rydberg constant. In addition to the Balmer series, the Lyman series for $n_f = 1$, $n_i = 2, 3, 4, \dots$, and the Paschen series for $n_f = 3$ were predicted by Bohr's theory. Bohr's quantum theory explained satisfactorily the spectrum of a hydrogen atom. The existence of the stationary state of an orbital electron in an atom was confirmed by the electron collision experiment carried out by Franck and Hertz. Bohr's theory mediated between the classical mechanics and the quantum mechanics. Nowadays this theory is called the old quantum theory.

EXAMPLE 3.1

Calculate the wavelengths of the first through third Lyman, Balmer, and Paschen lines.

SOLUTION 3.1

From Equations (3.10) and (3.11),

$$\frac{1}{\lambda} = R \left(\frac{1}{n_f^2} - \frac{1}{n_i^2} \right)$$

$$R = \frac{me^4}{8\epsilon_0^2 h^3 c} = \frac{(9.109 \cdot 10^{-31} \text{ kg})(1.602 \cdot 10^{-19} \text{ C})^4}{8(8.854 \cdot 10^{-12} \text{ C}^2 \text{V}^{-1} \text{m}^{-1})^2 (6.626 \cdot 10^{-34} \text{ Js})^3 (3 \cdot 10^8 \text{ ms}^{-1})}$$

$$= 1.096 \cdot 10^7 \text{ m}^{-1}$$

For the Lyman series, $n_f = 1$, $n_i = 2, 3, 4$; therefore,

$$\lambda_{n_i \rightarrow n_f} = \frac{1}{R \left(\frac{1}{n_f^2} - \frac{1}{n_i^2} \right)} = \frac{1}{R \left(1 - \frac{1}{n_i^2} \right)} = 121.64, 102.63, \text{ and } 97.31 \text{ nm}$$

For the Balmer series, $n_f = 2$, $n_i = 3, 4, 5$:

$$\lambda_{n_i \rightarrow n_f} = \frac{1}{R \left(\frac{1}{4} - \frac{1}{n_i^2} \right)} = 656.84, 486.54, \text{ and } 434.41 \text{ nm}$$

For the Paschen series, $n_f = 3$, $n_i = 4, 5, 6$:

$$\lambda_{n_i \rightarrow n_f} = \frac{1}{R \left(\frac{1}{9} - \frac{1}{n_i^2} \right)} = 1876.67, 1282.88, 1094.73 \text{ nm}$$

3.4 Quantum Mechanics

3.4.1 de Broglie Wave of Electrons

Light has the nature of wave-particle duality. DE Broglie considered that an electron regarded as a particle classically may have a wave nature. The wave-accompanying electron is called the electron wave. Generally, a wave accompanied by a particle is called a matter wave or de Broglie wave. When the energy E and the momentum p of the matter particle are given, the frequency and wavelength of the matter wave are written as

$$\nu = \frac{E}{h}, \quad \lambda = \frac{h}{p} \quad (3.12)$$

This is called the de Broglie's relation. Assuming the electron mass m , the charge e , and the accelerating voltage V , the electron velocity becomes $v = \sqrt{2eV/m}$. The de Broglie wavelength becomes

$$\lambda = \frac{h}{\sqrt{2meV}} \quad (3.13)$$

The de Broglie's relation was confirmed by the experiment of Davisson and Germer, in which electrons showed a diffraction phenomenon similar to that of x-rays.

EXAMPLE 3.2

What is the de Broglie wavelength of an electron accelerated by an electric potential of 54 V? Compare the electron's wavelength with the wavelength of a ball of 200 g moving with 50 m/s.

SOLUTION 3.2

For the electron:

$$\begin{aligned} \lambda &= \frac{h}{\sqrt{2meV}} = \frac{(6.626 \cdot 10^{-34} \text{ Js})}{\sqrt{2 \cdot (9.109 \cdot 10^{-31} \text{ kg})(1.602 \cdot 10^{-19} \text{ C}) \cdot V}} \\ &= \frac{1.227 \text{ nm}}{\sqrt{V(\text{volt})}} = \frac{1.227 \text{ nm}}{\sqrt{54}} = 1.67 \text{ nm} \end{aligned}$$

For the ball:

$$\lambda = \frac{h}{mv} = \frac{(6.626 \cdot 10^{-34} \text{ Js})}{(0.2 \text{ kg})(50 \text{ m/s})} = 6.626 \cdot 10^{-26} \text{ nm}$$

The ball's wavelength is 26 orders of magnitude shorter than the electron's wavelength. (Therefore, the wave nature has little effect on ordinary objects.)

3.4.2 Uncertainty Principle

Light, which was considered a wave, exhibits a particle-like property, and an electron, which was considered a particle, exhibits a wave-like property. It is a fact that all matter exhibits both wave-like and particle-like properties; however, these are apparently not compatible. Consequently, the concept that light is a particle is restricted by its wave-like property. Similarly, the concept that a matter particle is a wave is restricted by its particle-like property. That means we cannot use the property of wave or particle for all matter without restriction. The rule that brings the restriction is called the uncertainty principle discovered by Heisenberg. The fundamental attributes of particles are the position in the space and the momentum, and that of

waves is the wavelength. Momentum can be used in place of wavelength because of $p = h/\lambda$ between the wavelength λ and the momentum p . The uncertainty principle states both the position and the momentum of the matter particle cannot be determined at the same time. A relationship between the uncertainty of the position Δx and that for the momentum Δp holds:

$$\Delta x \cdot \Delta p \geq \hbar \quad (3.14)$$

If Δp becomes smaller, Δx becomes larger. In opposition, if Δx becomes smaller, Δp must become larger. Accurate quantities for two parameters cannot be determined at the same time. This means wave-like and particle-like properties restrict each other, and unrestricted use of one property is not permitted. If we investigate the particle-like property for photons and electrons, their wave-like property is disturbed. There is a similar relationship between time Δt and energy ΔE , i.e.,

$$\Delta t \cdot \Delta E \geq \hbar \quad (3.15)$$

EXAMPLE 3.3

What would be the annihilation time of an electron and a positron according to the uncertainty principle? How long would it take for a proton-antiproton pair?

SOLUTION 3.3

The positron and electron mass energy equivalent is 0.511 MeV and the Planck constant (\hbar) is $4.136 \cdot 10^{-15}$ eV·s. Thus, from the uncertainty principle, the lifetime of an electron-positron pair is

$$t \geq \frac{4.136 \cdot 10^{-15} \text{ eV} \cdot \text{s}}{2 \cdot 3.14159} \cdot \frac{1}{2 \cdot 0.511 \cdot 10^6 \text{ eV}} = 6.44 \cdot 10^{-22} \text{ s}$$

The proton mass is 1,836 times larger than the electron mass; therefore, for a proton-antiproton pair it would take

$$t \geq \frac{6.44 \cdot 10^{-22} \text{ s}}{1836} = 3.5 \cdot 10^{-25} \text{ s}$$

3.4.3 Schrödinger Equation

In 1925, the theory of quantum mechanics was completed by Heisenberg and independently by Schrödinger. The formalism of Heisenberg is called matrix mechanics and that of Schrödinger wave mechanics. These two mechanics are equivalent in spite of different mathematical formalism. The same results

are obtained. Here we give a simple introduction to wave mechanics. One of the objectives of quantum mechanics is to understand the concept of the wave-particle duality. It is assumed E is the electron energy, p the electron momentum, and ν and λ the frequency and wavelength of the de Broglie wave, respectively. The relationships $\nu = E/h$ and $\lambda = h/p$ are transformed into a convenient form:

$$E = \hbar\omega, \quad p = \hbar k \quad (3.16)$$

where $\omega = 2\pi\nu$ and $k = 2\pi/\lambda$, which is called the wavenumber vector. Wave is a phenomenon that a wave quantity such as the displacement from the average level propagates in a direction without changing the spatial shape. If the quantity is assumed to be ϕ , the classical wave equation that describes the variation in time and space is represented by

$$\frac{1}{c^2} \frac{\partial^2 \phi}{\partial t^2} = \frac{\partial^2 \phi}{\partial x^2} + \frac{\partial^2 \phi}{\partial y^2} + \frac{\partial^2 \phi}{\partial z^2} \equiv \Delta \phi \quad (3.17)$$

in which Δ is the Laplace operator,

$$\Delta = \frac{\partial^2}{\partial x^2} + \frac{\partial^2}{\partial y^2} + \frac{\partial^2}{\partial z^2} \quad (3.18)$$

In the case of the sine wave propagating along the wavenumber vector k , ϕ is given by

$$\phi = A \sin(kr - \omega t) \quad (3.19)$$

where r is the position vector. For this ϕ ,

$$\frac{\partial^2 \phi}{\partial t^2} = -\omega^2 \phi \quad (3.20)$$

$$\Delta \phi = -k^2 \phi \quad (3.21)$$

Inserting these two equations into Equation (3.17), $\omega = ck$ is obtained.

A complex solution can be considered in place of Equation (3.19), which is a real solution.

$$\phi = A \exp[i(kr - \omega t)] \quad (3.22)$$

In analogy with classical mechanics, it is assumed that the de Broglie wave is represented by an appropriate wave quantity ψ . This is called the wavefunction. The energy of an electron is $E = p^2/2m$ in the absence of a net force. Inserting this equation into Equation (3.16),

$$\omega = \hbar k^2/2m \quad (3.23)$$

is obtained. The function ψ represents the de Broglie wave and is written as in Equation (3.22). If so, $\psi = -k^2\psi$ holds. Therefore, Equation (3.23) is changed by multiplying ψ and using $E = \hbar\omega$,

$$-\frac{\hbar^2}{2m} \psi = E\psi \quad (3.24)$$

This is called Schrödinger's wave equation, which is a fundamental equation to obtain the energy level or the energy eigenvalue. If there is a potential $U(x, y, z)$, the above equation becomes

$$-\frac{\hbar^2}{2m} \psi + U\psi = E\psi \quad (3.25)$$

The solution of E derived from this equation for a hydrogen atom with the potential $U = -e^2/4\pi\epsilon_0 r$ agrees exactly with the solution of Bohr's theory (Equation 3.8).

3.4.4 Wavefunction

In Bohr's theory an electron exists just on a circular orbit with a certain radius, while the solution of the Schrödinger equation extends to around this circular orbit. If an electron exists somewhere in the space, its mass and charge exist there. Namely, an electron is an individual particle. The distributed wavefunction in space and the individuality of an electron is inconsistent. Bohr proposed an interpretation for this question. The probability $p(x, y, z, t)$ that a particle exists in a small volume $dx dy dz$ at a point (x, y, z) at a time t is given by

$$p(x, y, z, t) dx dy dz = |\psi(x, y, z, t)|^2 dx dy dz \quad (3.26)$$

ψ does not depend on t for the stationary state; therefore, the probability over the whole space becomes

$$\iiint |\psi(x, y, z)|^2 dx dy dz = 1 \quad (3.27)$$

It is understood that the wavefunction decides the statistical behavior of a particle.

EXAMPLE 3.4

What is the general solution of the wavefunction for a constant potential U ? Consider a one-dimensional problem.

SOLUTION 3.4

From Equation (3.25), the Schrodinger equation for a one-dimensional problem is given by

$$-\frac{\hbar^2}{2m} \frac{\partial^2 \Psi}{\partial x^2} + U\Psi = E\Psi$$

$$\frac{\partial^2 \Psi}{\partial x^2} = -\frac{2m}{\hbar^2} (E - U)\Psi$$

where A and B are constants, and $k = \sqrt{\frac{2m}{\hbar^2} (E - U)}$.

Therefore:

$$\text{If } k > 0, \Psi = A \exp(-ikx) + B \text{ (wave form)}$$

$$\text{If } k \leq 0, \Psi = A \exp(\pm kx) + B$$

To have a finite solution at infinitely large x , the solution for this case is $\Psi = A \exp(-kx) + B$ (the wavefunction is decreasing with the distance $x \Rightarrow$ tunneling).

3.5 Atomic Structure

3.5.1 Electron Orbit

Quantum mechanics provides the strict solution just for the hydrogen atom ($Z = 1$). However, it is impossible to provide strict solutions for atoms with $Z \geq 2$. Adequate approximations are applied to these atoms. The outline for atomic structure obtained by these methods is described here. The energy level of an atom is specified by a set of three quantum numbers (n, l, m). The principal quantum number n is allowed $n = 1, 2, 3, \dots$, corresponding to the magnitude of the electron orbit. The azimuthal quantum number l , which represents the magnitude of angular momentum of an electron, is allowed, $l = 0, 1, \dots, n - 1$, for a given n . The alternative notation is s, p, d, f, \dots . The third quantum number m is called the magnetic quantum number, which was introduced to explain the split of spectrum under the magnetic field (Zeeman effect). The values of m corresponding to the components of angular momentum are allowed $m = 0, \dots, \pm(l - 1), \pm l$. A state specified (n, l, m) is called the orbit. According to quantum mechanics, the distribution of electrons extends like a cloud with a spherical shell. The spherical shells are called K-shell, L-shell, M-shell, N-shell, etc., corresponding to $n = 1, 2, 3, 4, \dots$. Energy levels depend on n and l but not m . The value of energy level, E_{nl} , is higher as n is larger for the same l and is higher as l is larger for the same n . On the E_{2p} state, three states of $m = -1,$

0, 1 are allowed even if the same energy. Such a state is called a degenerate energy level.

3.5.2 Pauli's Exclusion Principle

In consideration of atomic structure Pauli's exclusion principle plays an important role. The number of electrons included in an orbit specified by (n, l, m) is restricted to at most two. Moreover, if two electrons are included in an orbit, the direction of electron spin should be reversed. According to this principle, the ground state is realized by filling electrons starting with the lowest level. Table 3.1 shows the electron configuration for the ground state of atoms up to Kr ($Z = 36$). For example, the electron configuration is represented as $(1s)^2$ for He ($Z = 2$). The Li ($Z = 3$) has such a configuration of one electron at the 2s orbit added to the closed shell of He. Based on the energy level diagram, the periodic table of elements and their chemical properties are understood.

TABLE 3.1

Electron Configuration for the Ground State of Atoms up to Kr ($Z = 36$)

Z	Element	Energy Level							
		K	L		M			N	
		1s	2s	2p	3s	3p	3d	4s	4p
1	H	1							
2	He	2							
<hr/>									
3	Li	2	1						
4	Be	2	2						
5	B	2	2	1					
6	C	2	2	2					
7	N	2	2	3					
8	O	2	2	4					
9	F	2	2	5					
10	Ne	2	2	6					
<hr/>									
11	Na	2	2	6	1				
12	Mg	2	2	6	2				
13	Al	2	2	6	2	1			
14	Si	2	2	6	2	2			
15	P	2	2	6	2	3			
16	S	2	2	6	2	4			
17	Cl	2	2	6	2	5			
18	Ar	2	2	6	2	6			

(continued)

TABLE 3.1 (CONTINUED)

Electron Configuration for the Ground State of Atoms up to Kr ($Z = 36$)

Z	Element	Energy Level							
		K	L		M			N	
		1s	2s	2p	3s	3p	3d	4s	4p
19	K	2	2	6	2	6		1	
20	Ca	2	2	6	2	6		2	
21	Sc	2	2	6	2	6	1	2	
22	Ti	2	2	6	2	6	2	2	
23	V	2	2	6	2	6	3	2	
24	Cr	2	2	6	2	6	4	1	
25	Mn	2	2	6	2	6	5	2	
26	Fe	2	2	6	2	6	6	2	
27	Co	2	2	6	2	6	7	2	
28	Ni	2	2	6	2	6	8	2	
29	Cu	2	2	6	2	6	10	1	
30	Zn	2	2	6	2	6	10	2	
31	Ga	2	2	6	2	6	10	2	1
32	Ge	2	2	6	2	6	10	2	2
33	As	2	2	6	2	6	10	2	3
34	Se	2	2	6	2	6	10	2	4
35	Br	2	2	6	2	6	10	2	5
36	Kr	2	2	6	2	6	10	2	6

EXAMPLE 3.5

What is the electron configuration of an oxygen atom? How many L-electrons does it have?

SOLUTION 3.5

An oxygen atom has in total eight electrons: $(1s)^2(2s)^2(2p)^4$, of which six electrons are the L-electrons ($n = 2$).

3.6 Summary

1. Dalton’s law in chemical reaction (the law of definite proportions and the law of multiple proportions) is a pioneer of modern atomic theory.
2. The spectrum of a hydrogen atom was explained by Bohr’s quantum theory.

3. In quantum mechanics, the square of the absolute value of a wave-function represents the existence probability of particles.
4. The uncertainty principle states that the position and the momentum of a particle cannot be determined accurately at the same time.
5. The energy level of an atom is specified by the principal quantum number n , the azimuthal quantum number l , and the magnetic quantum number m . One state specified (n, l, m) is called the orbit.

QUESTIONS

1. Describe ways in which atoms of a gas can be excited to emit light with frequencies that are of the characteristic line spectrum of the element involved.
 2. Under what condition does an electron remain in an orbit without emitting energy?
 3. Compare binding energy and ionization potential of an α -particle.
 4. What is the value of the ionization potential of hydrogen?
 5. Using the uncertainty principle, explain numerically why the hydrogen atom is stable rather than an electron merging into a proton.
 6. Using the uncertainty principle, explain why a hydrogen atom exists as H_2 rather than H .
 7. Calculate the radius of a Bohr atom.
 8. Calculate the velocity of an electron in the first Bohr orbit.
 9. What is the ratio of the Bohr velocity to the velocity of light known as? Obtain its numerical value of α .
 10. Equation $\Delta t \cdot \Delta E \approx h/2\pi$ permits a temporary violation of conservation of energy. How long is a violation of 0.03 eV tolerated?
 11. What is the closest approach an α -particle of 5.3 MeV energy can make to a water molecule?
 12. Calculate the number and show the configuration of the number of electrons allowed in the M-shell.
-

For Further Reading

- Johns HE, Cunningham JR. 1974. *The Physics of Radiology*, 3rd ed. Springfield, IL: Charles C. Thomas Publisher.
- Turner JE. 1995. *Atoms, Radiation, and Radiation Protection*, 2nd ed. New York: John Wiley & Sons.

4

Atomic Nucleus

4.1 Constituents of Nucleus

A nucleus of the atomic number Z and the mass number A consists of Z protons and $N = A - Z$ neutrons. The mass number A is the sum of nucleons (protons and neutrons) in a nucleus. A nucleus identified by A and Z is called a nuclide. The notation of a nuclide is ${}^A_Z\text{E}$, in which E is an element, for example, ${}^{16}_8\text{O}$. At the present time, there exist about 300 stable nuclides and about 1,700 unstable radioactive nuclides. The classification of nuclides is as follows:

1. Isotope has the same Z . Chemical properties are the same because the number of orbital electrons and that of electron configurations are the same. Radioisotopes are unstable in energy; therefore, a nuclide decays to another nuclide by emitting radiation. This ability is called radioactivity.
2. Isobar has the same A .
3. Isotone has the same N .
4. Isomer has the same Z and the same N .

4.2 Binding Energy of Nucleus

There is a relationship between atomic mass unit (u) and energy (MeV). From the definition the ${}^{12}\text{C}$ atom is 12 u. Because its gram-atomic weight is 12 g,

$$1\text{u} = 1/(6.022 \times 10^{23}) = 1.6605 \times 10^{-27} \text{ kg} \quad (4.1)$$

This corresponds to 931.5 MeV using Einstein's formula, $E = mc^2$. If the mass ΔM is lost, the released energy Q becomes $(\Delta M)c^2$. The mass of a neutral atom specified by A and Z is $M(A, Z)$, and the mass of a hydrogen atom, M_H . If

the electron binding energy is ignored, the total binding energy of a nuclide (A, Z), B , is given by

$$B = \{ZM_H + (A - Z)M_n - M(A, Z)\}c^2 = \Delta Mc^2 \quad (4.2)$$

where ΔM is called the mass defect. Using the atomic mass units, M_H and M_n are 1.007825 u and 1.008665 u, respectively. An alternative representation, the mass deviation can be used to obtain B .

$$B = \Delta Mc^2 = M - A \quad (4.3)$$

in which M is the mass and A is an integer mass number. That for ^{12}C becomes $\Delta = 0$ from the definition. The binding energy means the decrease of the total energy when a nucleus is formed by combining isolated free nucleons. In other words, that is the energy released when nucleons bind as a nucleus. The value of B for ^4He atom becomes

$$B = [(2 \times 1.007825 + 2 \times 1.008665) - 4.002603] \times 931.5 = 28.30 \text{ MeV} \\ = 7.07 \text{ MeV/n} \quad (4.4)$$

The energy of chemical reaction is at most a few eV. For ^4He , an energy of about 10 million times the chemical reaction is dissipated for binding the nucleons. The binding energy of a nucleon is denoted by B/A . Figure 4.1 shows B/A for the stable nuclides as a function of A . In the region of $A \geq 40$,

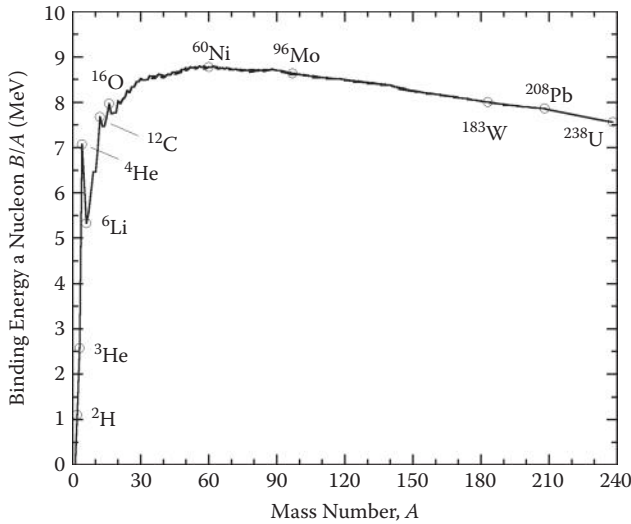


FIGURE 4.1

Mean binding energy of a nucleon.

for example, for ^{56}Fe $B/A = 8.8$, B/A is almost constant, ~ 8 MeV/n. This is called the saturation of the binding energy. The binding energy is the largest, namely, the most stable, for nuclides of $A = 55 \sim 60$. If an unstable nucleus is converted to a more stable nucleus, enormous energy is released. One method is the nuclear fusion by making a helium nucleus from hydrogen isotopes. Another example is the nuclear fission, by breaking a heavy nucleus like uranium into two light nuclei.

EXAMPLE 4.1

Obtain the absolute value of the atomic mass unit for 1 mole of ^{12}C (0.012 kg).

SOLUTION 4.1

$0.012 \text{ kg} = N_A \cdot 12 m_u$; therefore, $1u = 1.661 \times 10^{-27} \text{ kg} \equiv 931.48 \text{ MeV}$.

4.3 Nuclear Models

4.3.1 Liquid Drop Model

To understand various overall properties of nuclei, various models have been created, such as the shell model and the liquid drop model. The liquid drop model can satisfactorily explain many of the nuclear phenomena. This model arose from saturation phenomena of the nuclear density and the binding energy being analogous with the liquid drop. Here, the nuclear binding energy corresponds to the intermolecular force in the liquid. Nuclear reactions and nuclear fission are explained by the liquid drop model. When a projectile enters the nucleus, the energy enhances the temperature of the nucleus and particles are emitted similar to evaporation. Nuclear fission looks like separation into two liquid drops when energy is given to a large liquid drop. Weizsäcker and Bethe proposed a semiempirical mass formula representing the mass $M(A, Z)$ for a neutral atom of $A > 15$.

$$M(A, Z) = ZM_{\text{H}} + (A - Z)M_{\text{n}} - a_{\text{V}}A + a_{\text{S}}A^{2/3} + a_{\text{C}}\frac{Z^2}{A^{1/3}} + a_{\text{a}}\frac{(A/2 - Z)^2}{A} + \delta(A, Z) \quad (4.5)$$

where the parameters a_{V} , a_{S} , a_{C} , a_{a} , and $\delta(A, Z)$ are determined to fit to the measured data.

EXAMPLE 4.2

Use the Bethe-Weizsäcker mass formula to calculate the binding energy of a U-235 nucleus, given that

$$a_V = 15.75 \text{ MeV}, a_S = -17.8 \text{ MeV}, a_C = 0.711 \text{ MeV}, a_a = 23.7 \text{ MeV}, \text{ and}$$

$$\begin{aligned} & -\frac{11.18 \text{ MeV}}{\sqrt{A}}, & Z \text{ and } N \text{ are even numbers} \\ \delta = & 0, & \text{either } Z \text{ or } N \text{ are even numbers} \\ & +\frac{11.18 \text{ MeV}}{\sqrt{A}}, & Z \text{ and } N \text{ are odd numbers} \end{aligned}$$

Calculate B/A and the nuclear mass.

SOLUTION 4.2

$$\begin{aligned} B &= [Z \cdot M_H + (A - Z)M_n] - M(A, Z) \\ &= (15.75 \text{ MeV}) \cdot 235 - (17.8 \text{ MeV}) \cdot 235^{2/3} - (0.711 \text{ MeV}) \cdot \frac{92^2}{235^{1/3}} \\ &\quad - (23.7 \text{ MeV}) \cdot \frac{(235 - 2 \cdot 92)^2}{235} + 0 \\ &= 1785.9 \text{ MeV} \end{aligned}$$

$$B/A = 1785.9 \text{ MeV}/235 = 7.6 \text{ MeV/n}$$

$$\begin{aligned} M &= [Z \cdot M_H + (A - Z)M_n] - B \\ &= [92 \cdot (1.007825 \text{ u}) + (235 - 92) \cdot (1.008665 \text{ u})] - \frac{1785.9 \text{ MeV}}{931.5 \text{ MeV/u}} \\ &= 235.0418 \text{ u} \end{aligned}$$

4.3.2 Shell Model

The shell model originates from the accumulation of a lot of experimental data showing the existence of a closed shell in a nuclear structure. In the case that the number of protons Z or that of neutrons N is 2, 8, 20, 28, 50, 82, and 126, the nucleus lies especially stable. Therefore, it is thought that

the nucleus forms the closed shell for Z or N of these numbers. These numbers are called the magic number. The liquid drop model could not explain the magic number. The shell model was proposed to settle this problem. Discrete magic numbers remind us that atoms, like inert gases, are stable because of the closed shell structure of the orbital electrons. For atoms, the electron configuration of the ground state was obtained by filling electrons in order, starting with the lowest energy level. A similar method was applied to the nucleus. This model assumes individual nucleons move independently in the average potential replacing the nuclear force. In addition, Mayer and Jensen (1955) introduced the spin-orbit coupling potential. They succeeded in explaining all magic numbers as the closed shell. Their potential is given by

$$V(r) = V_0(r) + f(r)L \cdot S \quad (4.6)$$

in which L and S are the orbital angular momentum and spin quantum number, respectively. The potential $V_0(r)$ was assumed to be an intermediate type between the harmonic oscillator and the well. The spin-orbit coupling potential generates the splitting of the energy levels. Figure 4.2 shows the energy levels calculated by the shell model. Because the value of $f(r)$ is negative, the level with the total angular momentum $I = L + 1/2$ is lower than the level with $I = L - 1/2$. Each level is represented as nL_I , where n is the principal quantum number. The occupancy number in a level I is $2I + 1$ for the same kind of particle. The total number becomes 2, 8, 20, ..., at the levels $1s_{1/2}$, $1p_{1/2}$, $1d_{3/2}$, ..., when nucleons are filled in order from the lowest level. It is found that the energy gap between these levels and their upper levels is large in comparison with other gaps; therefore, these levels form the closed shell.

4.3.3 Collective Model

The electric quadrupole moment of the nucleus is determined by distributions of charge and current in the nucleus. We understand the nuclear size, the shape, and the density from this. The shell model could not explain this quantity. Bohr and Mottelson proposed the collective model in which the shape of a closed shell is not spherical symmetry but deformed spheroid. The deformed nucleus rotates around the axis perpendicular to the symmetry axis of a spheroid if energy is given. Consequently, rotational levels of the quantized rigid top may appear. The electric quadrupole moment and the excited levels called the rotational band calculated using the theory of Bohr-Mottelson were in agreement with the experimental values. In addition, the collective model explained the vibrational excited mode assuming the vibration of nuclear matter.

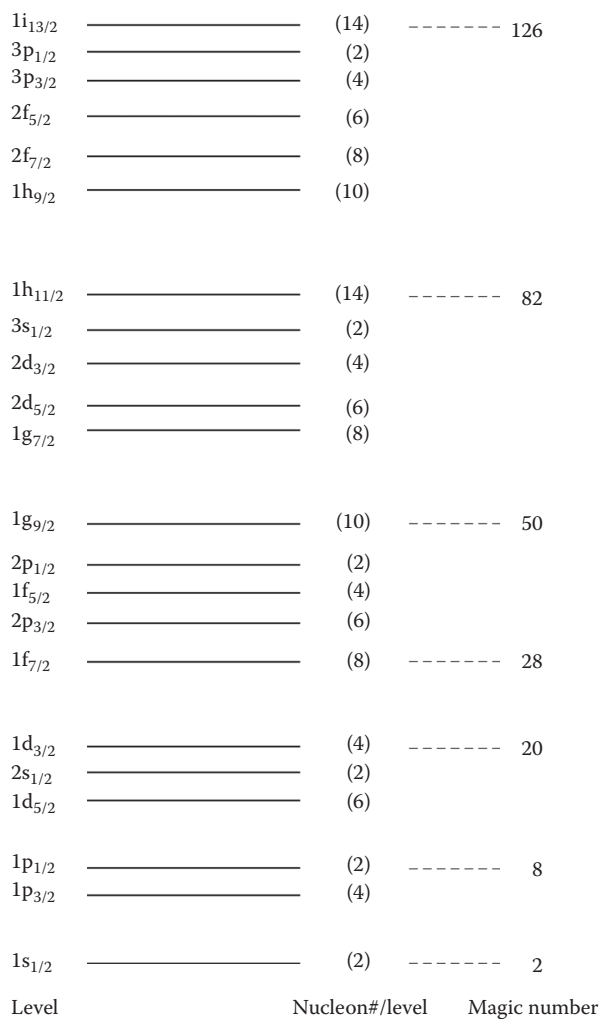


FIGURE 4.2
Energy level scheme of a nuclear shell model.

4.4 Nuclear Reaction

4.4.1 Characteristics

When particles collide with the nucleus, various phenomena arise by the interaction between the target nucleus and the projectile. Those are generally called a nuclear reaction. For the purposes of study of a nucleus and nuclear transformation, nuclear reactions using the projectiles of protons, neutrons, heavy ions, and electrons and photons, too, are performed. After the

interaction of the projectile a with the target nucleus A , the emitted particle b and the residual nucleus B are produced. This reaction is written as $a + A \rightarrow B + b$ or $A(a, b)B$. There are various kinds of interactions. In a reaction the target nucleus is converted into another nucleus. Inelastic scattering accompanies the change of inner state of the target nucleus. Elastic scattering changes the direction of the projectile. Classification of a direct reaction or compound reaction is made from the difference in the reaction mechanism.

4.4.2 Cross Section

Projectiles incident on the target do not always induce reaction. Even if reaction occurs, not a specific reaction but many different reactions occur. A specific reaction occurs with a certain probability. This probability is called the cross section. It is assumed that a thin target with the volume $V \text{ m}^3$, including a nucleus with a density of $n \text{ m}^{-3}$, is put in the uniform stream of the incident particles. If the fluence rate of the particle is $\phi \text{ m}^{-2}\text{s}^{-1}$, the number of reaction in the unit time, $N \text{ s}^{-1}$, is given by

$$N = \sigma \phi n V \quad (4.7)$$

in which σ represents the cross section. Its unit is m^2 or barn (b) ($1\text{b} = 10^{-28} \text{ m}^2$). A partial cross section is for a specific reaction type, and a total cross section is the sum of all possible reactions. The value of a cross section does not mean a simple geometrical area but depends on the incident energy and the nuclear structure of the target. The rough value for the nuclear reaction is estimated at $\sim 10^{-30} \text{ m}^2$ because of the diameter of nucleus $\sim 10^{-15} \text{ m}$. The differential cross section $d\sigma/d\Omega$ is defined to describe the angular distribution of the ejected particles. The differential cross section in energy $d\sigma/d\varepsilon$ describes the energy distribution.

EXAMPLE 4.3

5 MeV neutrons with the fluence rate $10 \text{ m}^{-2}\text{s}^{-1}$ are emitted to a water tank. Calculate number of neutron interactions in 1 m^3 water.

SOLUTION 4.3

$$\sigma_O = 1.55 \times 10^{-28} \text{ m}^2,$$

$$\sigma_H = 1.5 \times 10^{-28} \text{ m}^2$$

$$\begin{aligned} N &= \sigma_O \phi \frac{\rho}{A} n_A f_O + \sigma_H \phi \frac{\rho}{A} n_A f_H \\ &= (1.55 \times 10^{-28} \text{ m}^2) \cdot (10 \text{ m}^{-2}\text{s}^{-1}) \cdot \frac{1000}{0.016} \cdot 6.02 \times 10^{23} \cdot \frac{1}{3} \\ &\quad + (1.5 \times 10^{-28} \text{ m}^2) \cdot (10 \text{ m}^{-2}\text{s}^{-1}) \cdot \frac{1000}{0.001} \cdot 6.02 \times 10^{23} \cdot \frac{2}{3} \\ &= 621 (\text{s}^{-1}) \end{aligned}$$

4.4.3 Threshold Value of Reaction

We consider a reaction $X + a \rightarrow Y + b$ or $X(a, b)Y$. The energy released in the reaction is called the Q value of reaction. If $Q < 0$, namely, energy is absorbed, the reaction is called the endothermic reaction. If $Q > 0$, it is called the exothermic reaction. The reaction including Q is written as

$$X + a \rightarrow Y + b + Q \quad (4.8)$$

Extra energy is required in order to cause the endothermic reaction. The threshold energy of reaction, E_{th} , is calculated from the kinematical relationships. Assuming the head-on collision of the projectile a , with a mass M_a on the target M_X in rest, M_Y and M_b are produced after collision. The difference of the rest energy becomes

$$Q = M_a + M_X - (M_b + M_Y) \quad (4.9)$$

If an endothermic reaction, the sign of Q is minus. Since the total energy is conserved,

$$E_a = E_Y + E_b - Q \quad (4.10)$$

is obtained in which E represents the kinetic energy. From the momentum conservation,

$$p_a = p_Y + p_b \quad (4.11)$$

is obtained. If E_Y and E_b are deleted from the above equations, the threshold energy E_a is obtained

$$E_{th} = -Q \left(1 + \frac{M_a}{M_Y + M_b - M_a} \right) \quad (4.12)$$

For positively charged projectiles, the actual threshold is greater than E_{th} due to the Coulomb's repulsive force. The projectile needs acceleration to some extent even if $Q > 0$. Various reactions are easily caused for the case of neutrons without the Coulomb barrier.

EXAMPLE 4.4

Calculate the Q value and the threshold energy of the projectile for the reactions $^{13}\text{C}(d, t)^{12}\text{C}$ and $^{14}\text{C}(p, n)^{14}\text{N}$. Are these reactions endothermic or exothermic?

Atomic mass can be found at <http://t2.lanl.gov/data/astro/molnix96/massd.html>.

SOLUTION 4.4

For $^{13}\text{C}(\text{d}, \text{t})^{12}\text{C}$:

$$\begin{aligned} Q &= (13.00335503 + 2.01410174) \text{ u} - (3.01604939 + 12) \text{ u} \\ &= 0.001407 \text{ u} = 1.3157 \text{ MeV} \end{aligned}$$

Exothermic reaction: No threshold energy is required.

For $^{14}\text{C}(\text{p}, \text{n})^{14}\text{N}$:

$$\begin{aligned} Q &= (14.00324154 + 1.007825) \text{ u} - (1.008665 + 14.00307369) \text{ u} \\ &= -0.00063 \text{ u} = -0.59 \text{ MeV} \end{aligned}$$

Endothermic reaction: The threshold energy is

$$\begin{aligned} E_{\text{th}} &= 0.59 \text{ MeV} \cdot 1 + \frac{1.007825}{14.00307369 + 1.008665 - 1.007825} \\ &= 0.63 \text{ MeV} \end{aligned}$$

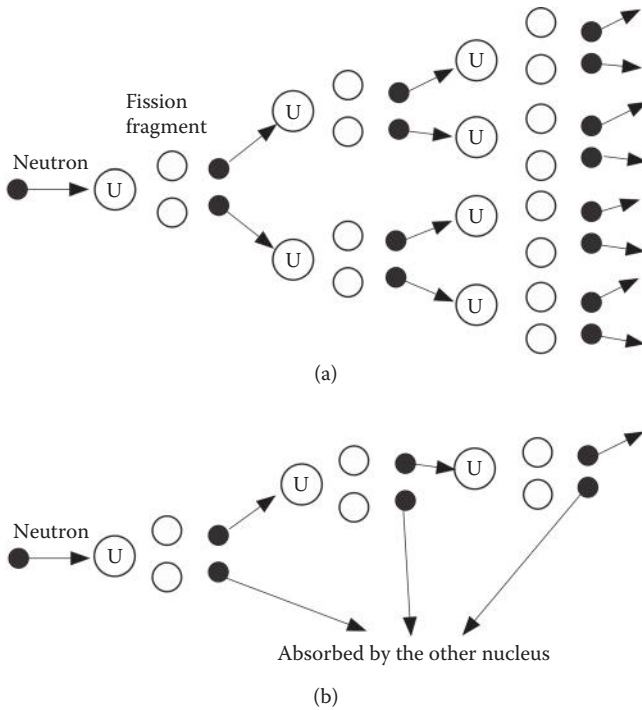
4.5 Nuclear Fission

When slow neutrons hit $^{235}_{92}\text{U}$, two more light nuclides are produced. This phenomenon is called nuclear fission. The binding energy B/A is ~ 7.6 MeV in the uranium region ($A \sim 240$). On the other hand, that value is ~ 8.5 MeV in the region of $A \sim 120$. It is estimated, therefore, the released energy is $240 \times (8.5 - 7.6) = 210$ MeV. A major part of this is converted into the kinetic energy of the fission products. The fission products do not separate in two right away but show an unsymmetrical pattern in the mass distribution. The fission fragments usually have excess neutrons; therefore, successive β -decays occur. The number of emitted neutrons in a fission reaction was confirmed. That was important from the viewpoint of the chain reaction of nuclear fission. Table 4.1 lists the average distribution of energies ~ 200 MeV released by the fission of ^{235}U . Two kinds of neutrons are ejected from the fission fragments.

TABLE 4.1

Average Distribution of Energies Released by Nuclear Fission of ^{235}U

Kinetic energy of fission fragments ($A \sim 96, A \sim 140$)	$165 \pm 5 \text{ MeV}$
Kinetic energy of fission neutrons ($2 \sim 3$)	5 ± 0.5
Energy of prompt γ -rays (~ 5)	6 ± 1
Energy of β -rays from fission fragments (~ 7)	8 ± 1.5
Energy of γ -rays from fission fragments (~ 7)	6 ± 1
Energy of neutrinos from fission fragments	12 ± 2.5
Total energy of nuclear fission	$202 \pm 6 \text{ MeV}$

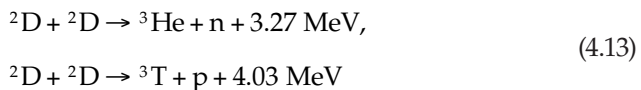
**FIGURE 4.3**

Schemes of chain reaction: (a) uncontrolled and (b) controlled.

One is the prompt neutrons ejected immediately ($\sim 10^{-12}$ s), and the other is the delayed neutrons after 1 s \sim 1 min. When the fission of ^{235}U occurs by a slow neutron, the mean number of emitted neutrons is 2.47. This value suggests successive chain reaction due to produced neutrons. Figure 4.3 shows the schemes of chain reactions, uncontrolled and controlled. If all emitted two more neutrons are absorbed by ^{235}U , the chain reaction abruptly increases and results in an explosion (the atomic bomb). The controlled chain reaction always uses one neutron under the constant rate in time.

4.6 Nuclear Fusion

The formation of the intermediate nuclei combining the light nuclei is called nuclear fusion, in which nuclear energy is also released. The most efficient nuclear fusion is



Moreover, such a fusion occurs using ^3T ,



EXAMPLE 4.5

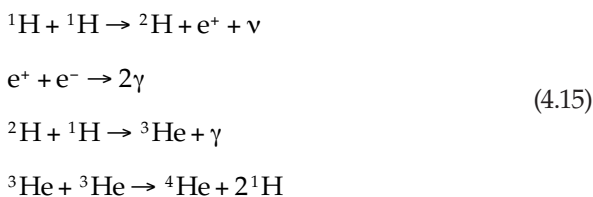
Calculate the Q value for the $^2\text{D} + ^3\text{T} \rightarrow ^4\text{He} + \text{n}$ fusion reaction.

SOLUTION 4.5

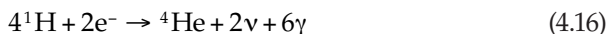
$$Q = (3.016049 + 2.014102 - 4.002604 - 1.008665) \times 931.5 = 17.58 \text{ MeV}$$

It is important for us to control these nuclear fusions. At very high temperature, thermonuclear reactions are sustained because nuclei in matter having thermal energy collide with each other. By the way, the average energy of a thermal motion is kT . The temperature T becomes $1 \times 10^7 \text{ K}$ for 1 keV . The problem is to keep such a high temperature as $10^7 \sim 10^9 \text{ K}$. This problem has not yet been solved.

The origin of radiation energy of the sun is the following nuclear fusion:



From the above reactions,



is obtained. Consequently ^4He is formed from four protons accompanied by γ -ray emission of 27 MeV .

4.7 Summary

1. A nucleus of the atomic number Z and the mass number A consists of Z protons and $A - Z$ neutrons.
2. Radioactive isotopes convert into a different element emitting radiations. Radioactivity means this capability.
3. The binding energy represents a reduction of the whole energy when a nucleus is formed by binding of isolated free nucleons.

4. The shell model of a nucleus explains the magic numbers 2, 8, 20, 28, 50, ..., for Z or N at which the nucleus is stable.
5. The energy released in the nuclear reaction is called the Q value. The endothermic and exothermic reactions occur for $Q < 0$ and $Q > 0$, respectively.

QUESTIONS

1. Complete the table.

Radiation	nature	Atomic mass (u)	Charge	Energy (MeV)	Velocity (c)	Range in Air	Range in Water	Range in Al	Ionization relative to α -particle
λ									
β									
α									

2. The Weizsäcker semiempirical mass formula is given by Equation 4.5
- a. Identify each term in the equation.

b. Derive an equation in MeV for M according to even and odd A .

c. What is the value of δ ?
3. What is the intrinsic parity of (a) photon, (b) electron, (c) proton, and (d) neutron? In the case of a photon, comment on the origin of the photon.
4. What is the work done in MeV for two protons separated by 5 F (1 fermi = 10^{-15} m). How does this energy compare with the nuclear force between the two protons?

For Further Reading

Mayer M, Jensen J. 1955. *Elementary Theory of Nuclear Shell Structure*. New York: John Wiley & Sons.

Turner JE. 1995. *Atoms, Radiation, and Radiation Protection*, 2nd ed. New York: John Wiley & Sons.

5

Radioactivity

5.1 Types of Radioactivity

5.1.1 α -Decay

An unstable atomic nucleus spontaneously loses energy by emitting ionizing particles and radiation. This process is called the decay of the nucleus. Almost all heavy elements of $Z \geq 83$ spontaneously emit α -rays, which is the nucleus of ${}^4\text{He}$. Both the atomic number Z and the number of neutron N decrease by 2. An example of the α -decay is



The energy released in this decay, namely, the Q value, is given by

$$Q = M(A, Z) - [M(A - 4, Z - 2) + M(2, 2)] \quad (5.2)$$

where M represents the atomic mass. This energy is shared by the α -particle and the recoil nucleus. From the kinematical relationship between them, it is understood that the kinetic energy of the α -particle is discrete. Even α -particles with lower energy than the barrier of Coulomb potential can jump out of nucleus owing to the tunnel effect. Figure 5.1 shows the potential for α -particles and the scheme of the tunnel effect. The Coulomb potential is

$$U(r) = \frac{2Ze^2}{4\pi\epsilon_0 r} \quad (5.3)$$

If $r = 1 \times 10^{-12}$ cm, $Z = 85$, then the magnitude of the barrier $U \approx 25$ MeV is obtained. This value is much higher than ordinary α -particle energies of a few MeV. α -Particles cannot pass through the barrier from the classical viewpoint. The quantum theory for the tunnel effect settled the problem. The penetration rate P is given by

$$P = e^{-G}, \quad G = \frac{2}{\hbar} \int_R^b \sqrt{2m_\alpha(U(r) - E)} \, dr \quad (5.4)$$

in which R and b are the radii, as shown in the figure. The value of P is nonzero.

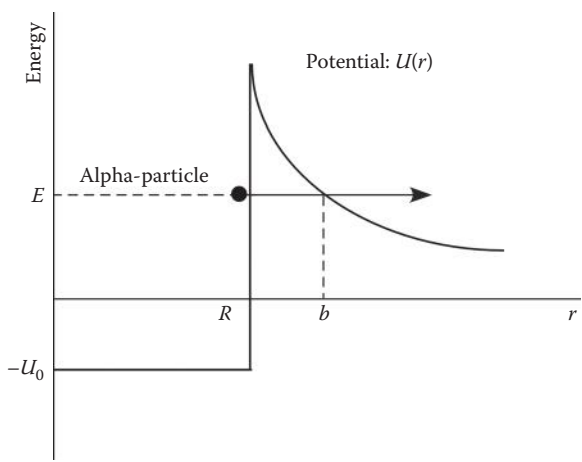


FIGURE 5.1
Potential energy of a nucleus for an α -particle.

For example, α -decay of $^{230}_{90}\text{Th}$ is shown as



Figure 5.2 shows the decay scheme of a decay of ^{230}Th . The released energy, $Q = 4.771\text{ MeV}$, is the nuclear mass difference between Th and Ra + He.

$$Q = M_{\text{Th}} - (M_{\text{Ra}} + M_{\alpha}) \tag{5.6}$$

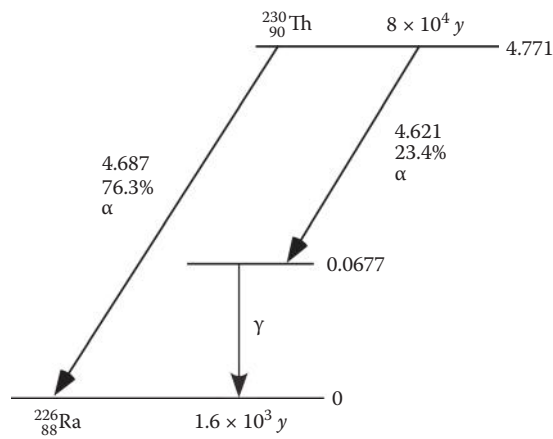


FIGURE 5.2
Decay scheme of ^{230}Th (Lederer et al. 1978).

This energy is shared between the α -particle and the recoiled radium. The magnitude of momentum of Ra is equal to that of α , and they go to opposite directions. Assuming the velocities V and v for Ra and α , respectively, the momentum conservation is represented by

$$M_{\alpha}v = M_{\text{Ra}}V \quad (5.7)$$

The relationship for energy is given by

$$Q = \frac{1}{2}M_{\alpha}v^2 + \frac{1}{2}M_{\text{Ra}}V^2 \quad (5.8)$$

From these equations, the energies of α -particle and radium become

$$E_{\alpha} = \frac{M_{\text{Ra}}Q}{M_{\alpha} + M_{\text{Ra}}}, \quad E_{\text{Ra}} = \frac{M_{\alpha}Q}{M_{\alpha} + M_{\text{Ra}}} \quad (5.9)$$

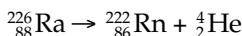
Inserting $Q = 4.771$ MeV into the first equation, $E_{\alpha} = 4.688$ MeV is obtained. It is understood that the α -particle has the discrete energy.

EXAMPLE 5.1

Calculate the value and energy of the α -particle and the daughter nucleus, originating from the decay of $^{226}_{88}\text{Ra}$.

SOLUTION 5.1

The decay of $^{226}_{88}\text{Ra}$ is



$$\begin{aligned} Q &= M(^{226}_{88}\text{Ra}) - M(^{222}_{86}\text{Rn}) - M(^4_2\text{He}) \\ &= (226.0254 - 222.0176 - 4.0026) \text{ u} \\ &= 0.0052 \text{ u} = 0.0052 \cdot 931.5 \text{ MeV} = 4.8438 \text{ MeV} \end{aligned}$$

The α -particle has the energy of

$$\begin{aligned} E_{\alpha} &= \frac{M_{\text{Rn}}Q}{M_{\text{Rn}} + M_{\alpha}} = \frac{222.0176 \cdot 4.8438 \text{ MeV}}{222.0176 + 4.0026} = 4.758 \text{ MeV} \\ E_{\text{Rn}} &= (4.8438 - 4.758) \text{ MeV} = 0.0858 \text{ MeV} \end{aligned}$$

5.1.2 β^- Decay

β^- decay is a phenomenon that a neutron changes into a proton following the emission of an electron (β^-) and an antineutrino.

$$n \rightarrow p + e^- + \bar{\nu}_e \quad (5.10)$$

When this decay occurs within a nucleus, the atomic number changes from Z to $Z + 1$. Generally, β^- decay occurs for the nuclide having excess neutrons other than the stable isotopes. For example,



The Q value for the β^- decay is given by

$$\begin{aligned} Q &= [M(A, Z) - Zm_e] - [M(A, Z + 1) - (Z + 1)m_e + m_e] \\ &= M(A, Z) - M(A, Z + 1) \end{aligned} \quad (5.12)$$

in which M represents the atomic mass and m_e the electron mass. This energy is shared by a β^- -particle and antineutrino.

$$E_{\beta^-} + E_{\bar{\nu}} = Q \quad (5.13)$$

Both E_{β^-} and $E_{\bar{\nu}}$ distribute from 0 to Q . Therefore, the energy spectrum of β^- -particle becomes a continuous spectrum. According to Fermi's theory, the energy spectrum of β^- -particles is given by

$$\frac{dn}{dT} \propto (Q - T)^2 (T + mc^2) \sqrt{T(T + 2mc^2)} \quad (5.14)$$

where dn = the relative intensity, T = the kinetic energy, and m = the mass of β^- -particle. Figure 5.3 shows the energy spectrum for the β^- rays from ${}^{40}\text{K}$ decay with $Q = 1,314$ keV (100%). If a single Q , then the average energy is $\sim Q/3$. For ${}^{40}\text{K}$, the average energy of β^- particles is 536 keV.

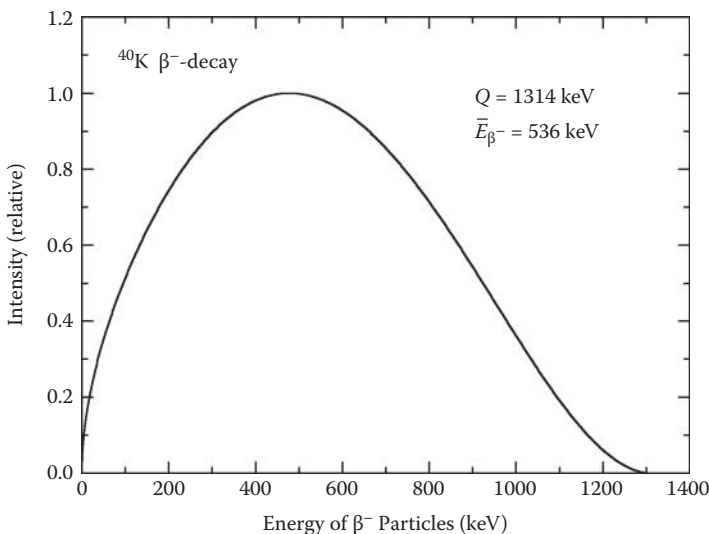


FIGURE 5.3

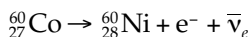
Energy spectrum of β^- particles ejected by β^- decay of ${}^{40}\text{K}$.

EXAMPLE 5.2

Calculate the value for the decay of Co-60.

SOLUTION 5.2

The decay of Co-60 is



The antineutrino mass can be neglected. Therefore,

$$\begin{aligned} Q &= M({}_{27}^{60}\text{Co}) - M({}_{28}^{60}\text{Ni}) \\ &= (59.93382 - 59.93079) \text{ u} \\ &= 0.00303 \text{ u} = 0.00303 \cdot 931.5 \text{ MeV} = 2.82 \text{ MeV} \end{aligned}$$

The nickel-60 nucleus is in an excited state; therefore, it will emit a γ -ray to attain its ground state.

5.1.3 γ -Decay

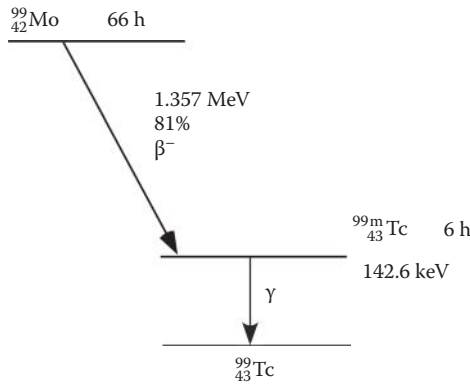
One or several γ photons are emitted from the excited states of the daughter nucleus produced by the α - or β -decay. In the γ -transition, Z and A both do not change. The γ -ray spectrum is discrete and specific to the nuclide. The lifetime of the nuclear excited states is usually $\sim 10^{-10}$ s; therefore, γ -rays are promptly emitted after the decay. However, there are some exceptions due to the selection rule for photon emission. The half-life of the excited state of ${}_{56}^{137}\text{Ba}$ produced by the decay of ${}_{55}^{137}\text{Cs}$ is 2.55 minutes. Such a long life state is called a metastable state. The relevant state is denoted by ${}_{56}^{137\text{m}}\text{Ba}$. Another example of the metastable nuclide is ${}_{43}^{99\text{m}}\text{Tc}$ produced by the β^{-} decay of ${}_{42}^{99}\text{Mo}$. This state with the half-life of 6 h causes the isomeric transition (IT) to the ground state.



The energy of γ -ray is equal to the difference between the metastable state and the ground state. Figure 5.4 shows the decay scheme of ${}_{42}^{99}\text{Mo}$.

5.1.4 Internal Conversion

In internal conversion an electron is ejected from the atom by transferring the energy of the excited state to an electron in the K- or L-shell of the atom. This is regarded as an alternative to photon emission. The kinetic energy of ejected electron E_e , or E_{IC} , becomes $E_{\gamma} - E_B$, in which E_B is the binding energy. The process of internal conversion occurs in competition with γ -decay. The relative proportion of the two processes is given by the total conversion

**FIGURE 5.4**

Decay scheme of ^{99}Mo (Lederer et al. 1978).

coefficient, α . The internal conversion coefficient α is defined by the ratio of the number of conversion electrons N_e to that of competing photons N_γ

$$\alpha = N_e/N_\gamma$$

$$= \alpha_K + \alpha_{L1} + \alpha_{L2} + \dots \quad (5.16)$$

where α_K , α_{L1} , and α_{L2} are the partial conversion coefficients for the individual subshells. The magnitude of a vacancy cascade depends on the individual subshells. The partial conversion coefficients are given by Rosel et al. (1978), Coursol et al. (2000), and Gorozhankin et al. (2002). For ^{137}Cs , 95% of β -decay goes to the metastable state lying at 662 keV of ^{137}Ba . The relative intensity of the γ -rays emitted at this time is 85%. Internal conversion accounts for the 10% difference. The energies of conversion electrons for the K-shell and L-shell of ^{137}Ba are 624 keV and 656 keV, respectively. These are the line spectrum. Of particular interest is the Auger electron emitting the radioisotopes ^{123}I , ^{124}I , and ^{125}I (Kassis 2004; Nikjoo et al. 2008).

5.1.5 β^+ Decay

β^+ decay is a phenomenon that a proton changes into a neutron following the emission of a positron (β^+) and a neutrino.

$$p \rightarrow n + e^+ + \nu_e \quad (5.17)$$

When this decay occurs within a nucleus, the atomic number changes from Z to $Z - 1$. Generally, β^+ decay occurs for the nuclide having excess protons other than the stable isotopes. For example,

$$^{18}_9\text{F} \rightarrow ^{18}_8\text{O} + e^+ + \nu_e \quad (5.18)$$

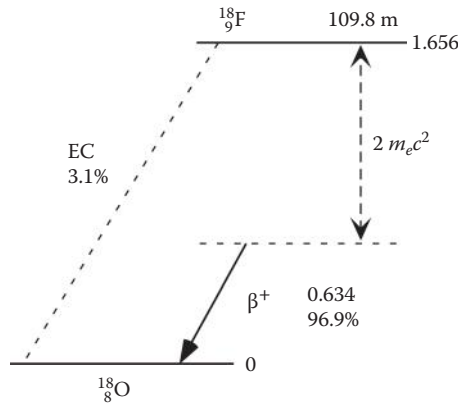
**FIGURE 5.5**Decay scheme of ^{18}F (Lederer et al. 1978).

Figure 5.5 shows the decay scheme of ^{18}F . The Q value for the β^+ decay is given by

$$\begin{aligned} Q &= [M(A, Z) - Zm_e] - [M(A, Z - 1) - (Z - 1)m_e + m_e] \\ &= M(A, Z) - M(A, Z - 1) - 2m_e \end{aligned} \quad (5.19)$$

in which M represents the atomic mass and m_e the electron mass. In order to result in positron emission, therefore, the mass of the parent atom must be greater than that of the daughter atom by at least $2mc^2 = 1.022 \text{ MeV}$. The released energy Q is used for the kinetic energy of the positron and neutrino. The nuclide that emits positrons is called the positron emitter. The peculiar phenomenon of the positron emitter in matter is to accompany two annihilation photons of 511 keV. They are in opposite directions of each other.

5.1.6 Electron Capture

Electron capture (EC) is a phenomenon that a proton changes into a neutron by capturing an orbital electron following the emission of a neutrino and characteristic x-ray.



When this decay occurs within a nucleus, the atomic number changes from Z to $Z - 1$. Generally, EC occurs for the nuclide having excess protons other than the stable isotopes. EC competes with β^+ decay, which results in the same change. For example,



The Q value for EC is given by

$$\begin{aligned} Q &= [M(A, Z) - Zm_e + m_e] - [M(A, Z - 1) - (Z - 1)m_e] \\ &= M(A, Z) - M(A, Z - 1) - B \end{aligned} \quad (5.22)$$

where B is the mass equivalent to the binding energy of the atomic shell. In order for the EC to occur, therefore, the mass of the parent atom must be greater than that of the daughter atom by the binding energy. The orbital electron in the K-shell is usually captured. The vacancy is necessarily generated in the inner shell; therefore, the characteristic x-ray of the daughter nucleus is always emitted. EC is detected by observation of the characteristic x-rays and the Auger electrons. In calculations related to Auger electron cascades the relative proportion of vacancies created by EC in the individual subshells representing the distribution of initial vacancies in the decaying isotope is needed. The electron capture probabilities for i- and j-shells is given, for example, for subshells K and L_1 by

$$\frac{P_{L1}}{P_K} = \frac{n_{L1} q_{L1}^2 B_{L1} \beta_{L1}^2}{n_K q_K^2 B_K \beta_K^2} \quad (5.23)$$

and

$$\frac{q_{L1}}{q_K} = \frac{E_{EC} - E_{L1}}{E_{EC} - E_K} \quad (5.24)$$

For radionuclide decay by EC the sum of probabilities for EC in each individual subshell is equal to unity:

$$P_{EC} = P_K + P_{L1} + P_{L2} + P_{L3} + \dots = 1 \quad (5.25)$$

EXAMPLE 5.3

Calculate the difference between the values for the positron emission of ^{18}F and electron capture by the same nucleus.

SOLUTION 5.3

For positron emission (Equation (5.18)),

$$\begin{aligned} Q &= M(^{18}_9\text{F}) - M(^{18}_8\text{O}) - 2m_e \\ &= (18.000938 - 17.99916 - 2 \cdot 5.4858 \cdot 10^{-4}) \text{ u} \\ &= 6.8084 \cdot 10^{-4} \text{ u} = 6.8084 \cdot 10^{-4} \cdot 931.5 \text{ MeV} = 0.634 \text{ MeV} \end{aligned}$$

On the other hand, for electron capture (Equation (5.21)), the value is calculated from

$$\begin{aligned} Q &= M(^{18}\text{F}) - M(^{18}\text{O}) - B \\ &= (18.000938 - 17.99916) \text{ u} - 696.7 \text{ eV} \\ &= 0.001778 \cdot 931.5 \text{ MeV} - 6.967 \cdot 10^{-6} \text{ MeV} = 1.6562 \text{ MeV} \end{aligned}$$

where B is the K-shell electron binding energy of fluorine (tabulated in, for instance, Cardona and Ley 1978).

The difference in the values obtained from both processes is 1.022 MeV (which is about twice the electron mass energy equivalent; in this case, the binding energy of the K-shell electron is much lower than the nuclear mass difference).

5.1.7 Radiative and Nonradiative Transitions

Absorption of photons through the photoelectric effect or the interaction of ions with the target results in ionization and excitation and creation of vacancy in the inner shells of the atom. Subsequently, the vacancy may be filled by radiative (x-ray) or nonradiative (Auger) processes. Electron vacancies are generated when an atom is ionized by an incident electron beam and electrons are knocked out from their shells. This process is called inner shell ionization. When an electron vacancy is created, the atom is said to be in an excited state. The atom in such an excited state returns to the ground state by filling the electron vacancy by an electron from one of the atomic subshells. For example, if the K-shell is excited, the Auger electron may originate in the L-shell. The second way of creating a vacancy is by internal conversion (IC). In internal conversion the excitation energy of the nucleus is transferred to an atomic electron, which is subsequently emitted with the energy $E_g - E_b$, where E_g is the excitation energy and E_b the binding energy of the electron in its atomic shell. And the third way of generating electron vacancy is by electron capture (EC). In the process of electron capture the orbital electron of an atom interacts with a nucleus proton to form a neutron, and a neutrino is emitted. The probability of such an interaction depends on the overlap between the atomic electron and the nucleus. This is highest for the K-shell. If the filling of the vacancy is accompanied by the emission of X-photon, it is said to be a radiative transition. If the filling of the vacancy is accompanied by the emission of an electron, it is a nonradiative transition. Above the K-shell, if the filling electron originates from the same family of subshells, it is called a Coster-Kronig transition.

Figure 5.6 shows various scenarios leading to the emission of photons or electrons from an atom when in an excited state. The relative probability of Auger emission and photon emission is measured by the fluorescence yield

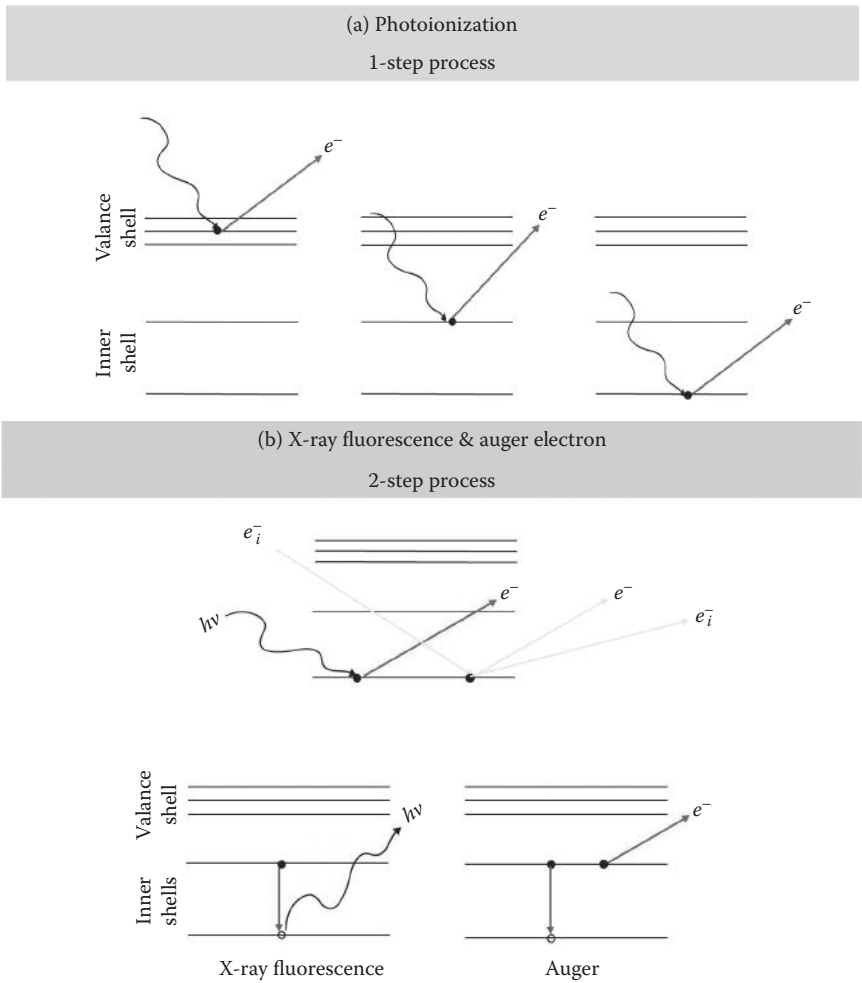


FIGURE 5.6
Various scenarios leading to the emission of photons or electrons from an atom when in an excited state.

such that $\omega + a + f = 1$, where a and f refer to Auger and Coster-Kronig yields. Fluorescence yield is the relative probability of Auger emission and x-ray such that, for the K-shell, ω is the number of K-photons/number of K-shell vacancies. For the heavy atoms x-radiation is the more probable because of the high nuclear charge. For light atoms the Auger effect is predominant. Other processes that may be of importance are super Coster-Kronig transitions, autoionization, double Auger effect, Auger-Coster-Kronig transitions, interatomic Auger effect, electron shake-up and shake-off, and plasma excitations.

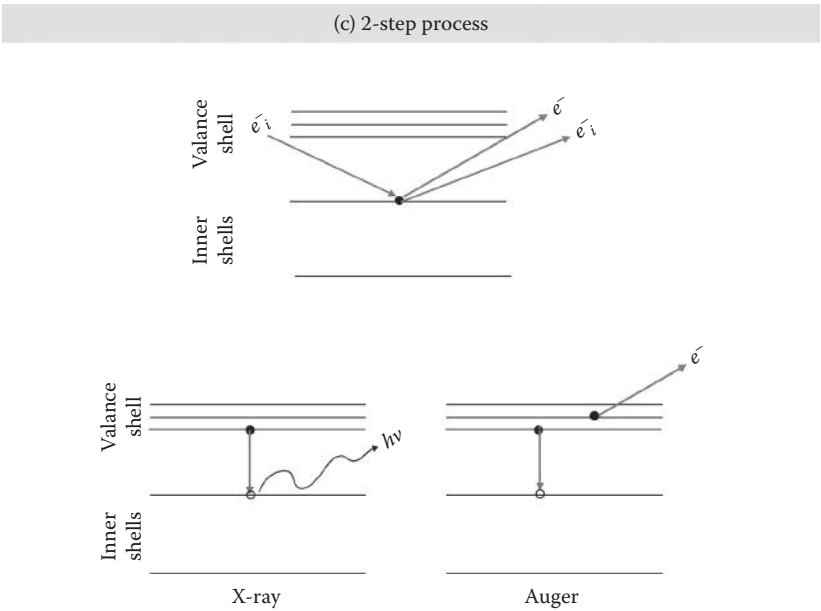


FIGURE 5.6
(Continued)

EXAMPLE 5.4

Calculate the Auger electron energy following the K-shell ionization of water vapor.

SOLUTION 5.4

The K-shell binding energy (B_K) of water vapor is 539.7 eV, and the first ionization energy (B_1) is 12.62 eV. Therefore, the Auger electron energy is

$$E_e = B_K - 2 \cdot B_1 = (539.7 - 2 \cdot 12.62) \text{ eV} = 514.46 \text{ eV}$$

5.2 Formulas of Radioactive Decay

5.2.1 Attenuation Law

The disintegration rate of radioactive nuclides is represented by activity. The unit of activity Bq is defined by the number of disintegrated atoms per second. The activity of a radioisotope decreases exponentially in time.

Assuming the number of radioactive nuclides in a sample N , the variation of the number dN in time dt is given by

$$dN = -\lambda N dt \quad (5.26)$$

where λ is a constant specific to a radioactive nuclide called the decay constant. The activity A becomes

$$A = \frac{-dN}{dt} = \lambda N \quad (5.27)$$

Solving Equation (5.26),

$$N = N_0 e^{-\lambda t} \quad (5.28)$$

is obtained, in which N_0 is the number at $t = 0$. The same form can be applied to the activity A . Figure 5.7 shows the exponential decay pattern for the activity as a function of the time. The time at which the activity reduces by one-half is called the half-life. The relationship between the half-life T and λ becomes

$$T = \frac{\ln 2}{\lambda} = \frac{0.693}{\lambda} \quad (5.29)$$

The attenuation law is written by

$$\frac{A}{A_0} = e^{-0.693t/T} = \frac{1}{2}^{t/T} \quad (5.30)$$

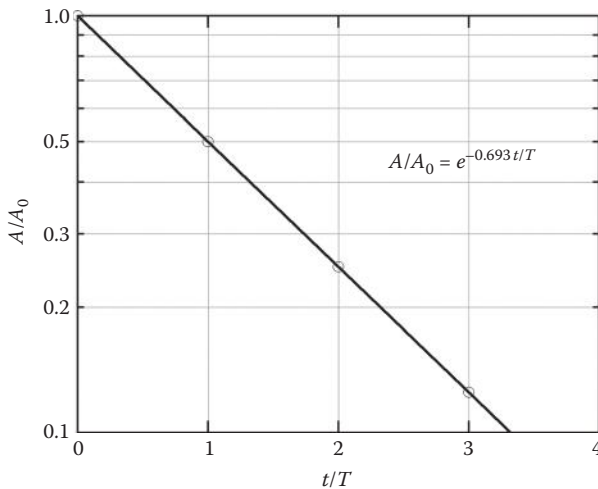


FIGURE 5.7
Exponential decay of radioactivity.

EXAMPLE 5.5

^{60}Co source is a γ -emitter, which is used in medicine and industry. The half-life of the ^{60}Co source is 5.3 years. In order to account for the source strength decrease, a correction factor could be applied. Calculate the source strength decrease each year.

SOLUTION 5.5

$$\frac{A}{A_0} = \frac{1}{2}^{t/T} = \frac{1}{2}^{1/5.3} = 0.877$$

The activity of the source after a year is 87% of the initial activity.

5.2.2 Specific Activity

The specific activity of a sample is defined by the activity per unit mass. The specific activity S is determined by T and atomic mass M . Because the number of atoms per gram is $6.022 \times 10^{23}/M$, Equation (5.27) is changed into

$$S = \frac{4.17 \times 10^{23}}{MT} \quad (5.31)$$

The unit of S is Bq g^{-1} if T s.

EXAMPLE 5.6

What is the specific activity of ^{60}Co and ^{226}Ra ?

SOLUTION 5.6

$$S(^{60}\text{Co}) = \frac{4.17 \times 10^{23}}{MT} = \frac{4.17 \times 10^{23}}{60 \times 5.4 \times 365 \times 24 \times 3600} = 4.08 \times 10^{13}$$

The specific activity of ^{226}Ra is 1 Ci/g or 3.7×10^{10} Bq/g.

5.2.3 Radioactive Equilibrium**5.2.3.1 Secular Equilibrium**

A parent nucleus with the half-life of T_1 decays to a daughter nucleus with the half-life of T_2 . It is assumed that T_1 is much longer than T_2 , namely, $T_1 \gg T_2$. The parent activity A_1 is regarded as constant in the short time. The variation of the number of daughter atoms is given by

$$\frac{dN_2}{dt} = A_1 - \lambda_2 N_2 \quad (5.32)$$

The solution A_2 is obtained putting the initial condition for the daughter as N_{20} at $t = 0$.

$$A_2 = A_1(1 - e^{-\lambda_2 t}) + A_{20}e^{-\lambda_2 t} \quad (5.33)$$

If starting from the pure parent, $A_{20} = 0$ at $t = 0$. This condition is called the secular equilibrium.

5.2.3.2 General Formula

When the relative magnitudes of T_1 and T_2 are unrestricted, the differential equation for N_1 and N_2 becomes

$$\frac{dN_2}{dt} = \lambda_1 N_1 - \lambda_2 N_2 \quad (5.34)$$

The first term of the right side is

$$\lambda_1 N_1 = \lambda_1 N_{10} e^{-\lambda_1 t} \quad (5.35)$$

Therefore, Equation (5.34) is changed into

$$\frac{dN_2}{dt} + \lambda_2 N_2 = \lambda_1 N_{10} e^{-\lambda_1 t} \quad (5.36)$$

The solution of this equation is obtained assuming the initial condition $N_{20} = 0$ at $t = 0$.

$$N_2 = \frac{\lambda_1 N_{10}}{\lambda_2 - \lambda_1} (e^{-\lambda_1 t} - e^{-\lambda_2 t}) \quad (5.37)$$

EXAMPLE 5.7

Calculate the activity of ^{222}Rn from a 1 g ^{226}Ra sample after a week (half-life of $^{226}\text{Ra} = 1,600$ years, half-life of $^{222}\text{Rn} = 3.8$ days).

SOLUTION 5.7

$$A_{\text{Rn}} = A_{\text{Ra}} (1 - e^{-\lambda_{\text{Rn}} t}) = 3.7 \times 10^{10} (\text{Bq/g}) \times 1(\text{g}) \times \left(1 - e^{-\frac{0.693}{3.8} \times 7}\right) = 2.67 \times 10^{10} \text{Bq}$$

5.2.3.3 Transient Equilibrium

For the case of $T_1 \geq T_2$ and $N_{20} = 0$, $A_2 = \lambda_2 N_2$ increases slowly. The second term in the bracket can be neglected in comparison with the first term as time goes by.

$$\lambda_2 N_2 = \frac{\lambda_1 \lambda_2 N_{10} e^{-\lambda_1 t}}{\lambda_2 - \lambda_1} \quad (5.38)$$

Because $A_1 = \lambda_1 N_{10} e^{-\lambda_1 t}$ is the activity of the parent, the above equation is written as

$$A_2 = \frac{\lambda_2 A_1}{\lambda_2 - \lambda_1} \quad (5.39)$$

This condition is called the transient equilibrium.

5.2.3.4 Nonequilibrium

For the case of $T_1 < T_2$, the activity of the daughter nucleus becomes maximum and attenuates. The parent soon decays and the daughter remains. The equilibrium is not realized.

5.3 Summary

1. The process where a nucleus transfers to more stable states is called the disintegration of the nucleus, in which excess energies are emitted as various types of radiation.
2. Emitted radiations following the decay are α , β^- , β^+ , γ , internal conversion electrons, and so on. Electron capture is detected by observing the characteristic x-rays and Auger electrons.
3. Activity in Bq units attenuates exponentially as a function of time. The time when the activity reduces to half is called the half-life.
4. Half-lives of the parent nucleus and the daughter nucleus are assumed to be T_1 and T_2 , respectively. If $T_1 \gg T_2$, then the secular equilibrium is realized. If $T_1 \geq T_2$, then the transient equilibrium is realized.

QUESTIONS

1. Write the decay of tritium. How much of 10 g tritium is left after 25 years?
2. A luminous watch dial contains 5 microcuries of the isotope radium. How many decays per second are taking place?
3. A fresh sample of ^{210}Bi weighs 1 pg and decays to ^{210}Po by emitting a β^- particle with a $T_{1/2}$ of 5 days. ^{210}Po decays to ^{206}Pb by emitting an α -particle with a $T_{1/2}$ of 140 days. Calculate the maximum mass of ^{210}Po present at any time and the activity.

4. If two radioactive nuclei A and B, produced in the process of nuclear fission, are characterized by the disintegration constants λ_1 and λ_2 , and if the probability that a time less than T elapses between the subsequent disintegrations of A and B is represented by $W(T)$, show that $W(T) = 1 - (\lambda_1 + \lambda_2)^{-1} (\lambda_1 e^{-\lambda_2 T} + \lambda_2 e^{-\lambda_1 T})$.
-

References

- Cardona M, Ley L. 1978. *Photoemission in Solids. I. General Principles*. Berlin: Springer-Verlag. With additional corrections.
- Coursol N, Gorozhankin VM, Yakushev EA, Briançon C, Vylov T. 2000. Analysis of internal conversion coefficients. *Appl. Radiat. Isot.* 52(3): 557–567.
- Gorozhankin VM, Coursol N, Yakushev EA, Vylov Ts, Briançon C. 2002. New features of the IC(4) code and comparison of internal conversion coefficient calculations. *Appl. Radiat. Isot.* 56(1–2): 189–197.
- Kassis AI. 2004. The amazing world of Auger electrons. *Int. J. Radiat. Biol.* 80(11–12): 789–803.
- Lederer CM, Shirley VS. 1978. *Table of Isotopes*, 7th ed. New York: John Wiley & Sons.
- Nikjoo H, Emfietzoglou D, Charlton DE. 2008. The Auger effect in physical and biological research. *Int. J. Radiat. Biol.* 84(12): 1011–1026.
- Rosel F, Fries HM, Alder K, Pauli HC. 1978. Internal conversion coefficients for all atomic shells. *At. Data Nucl. Data Tables* 21: 91 ± 289.
-

For Further Reading

- Turner JE. 1995. *Atoms, Radiation, and Radiation Protection*, 2nd ed. New York: John Wiley & Sons.

6

X-Rays

6.1 Generation of X-Rays

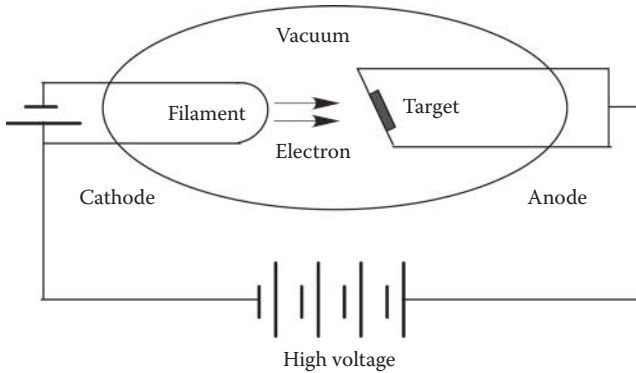
In 1895, German physicist W.C. Roentgen discovered a new type of radiation in the course of an experiment using the Crookes' vacuum tube. This radiation penetrated opaque materials such as black paper or wood. He named it x-ray and clarified its properties such as penetrability, fluorescence action, imaging ability, and ionization. The discovery of x-rays is the starting point of the investigation on ionizing radiation and its application to various fields.

X-rays are produced when electrons are incident on target. The electron collides with a target atom and loses a major part of its energy by ionization and excitation of an atom. In addition, the electron decelerated in the field of an atomic nucleus loses its energy by emitting the x-ray photons. An electron having the kinetic energy T can produce photons having the energy distributed less than T .

$$h\nu \leq T \quad (6.1)$$

As a result, monochromatic electron beams generate a continuous energy spectrum with the maximum energy equal to the beam energy. These continuous x-rays are called bremsstrahlung or braking radiation. Bremsstrahlung is likened to photons shaken off an electron that suffered from a sudden brake in the nuclear field.

Figure 6.1 shows the schematic diagram of an x-ray generator. This structure is called the Coolidge tube and consists of the cathode and anode. The atmospheric pressure is kept at less than 10^{-6} mmHg. Thermal electrons emitted from the cathode are accelerated and collide with the anode target. Only a few percent of electron kinetic energy is converted to x-rays. The major part of the remaining energy is converted to heat. The x-ray tube is usually used under the voltage less than 300 kV. Only 1% of the electron energy is converted to useful x-rays, and 99% is converted to heat and warms the anode. Therefore, tungsten having a high melting point is frequently used as the target. In addition, the structure of the anode is devised in such a way as to decrease the temperature.

**FIGURE 6.1**

Schematic diagram of x-rays generator.

For high-energy electrons, acceleration of electrons is made by magnetic field or microwave used in a betatron or linac. The higher the electron energy, the higher the generation efficiency that is achieved. The angular distributions of x-rays vary. Bremsstrahlung is emitted in all directions. That is a complex function of the energy of electrons and bremsstrahlung photons. Segre gave the average emission angle of x-rays as

$$\bar{\theta} \approx \frac{1}{1 + T/mc^2} \quad (\text{radian}) \quad (6.2)$$

in which T is the kinetic energy of electrons, and m is the electron rest mass. Therefore, the dominant angle is the forward direction for high-energy electrons and around 60° for low-energy electrons. The extraction direction is different between the x-ray tube and high-energy linac.

EXAMPLE 6.1

Common energy for x-ray tubes is about 120 kVp, and for radiotherapy accelerators is about 6 MV. What is the most probable emission angle for the two examples in order to design the target angle?

SOLUTION 6.1

$$\begin{aligned} \bar{\theta} &\approx \frac{1}{1 + T/mc^2} = \\ \frac{1}{1 + 120/511} &= 0.809(\text{radian}) = 46.4^\circ \\ \frac{1}{1 + 6000/511} &= 0.078(\text{radian}) = 4.5^\circ \end{aligned}$$

6.2 Continuous X-Rays

The x-ray intensity rapidly increases as the tube voltage increases if the current is kept constant. The wavelength of the photon with the maximum energy becomes the shortest. Using the relationship, $\lambda[\text{nm}] = 1.24/h\nu[\text{keV}]$, the minimum wavelength for the tube voltage 50 kV becomes $\lambda_{\min} = 1.24/50 = 0.0248 \text{ nm} = 0.248 \text{ \AA}$. Generally, the energy of x-rays is referred to by the peak voltage of the x-ray tube, kV_p . The maximum voltage V_{\max} in kV units and the minimum wavelength λ_{\min} in $\text{\AA}(=10^{-8}\text{cm})$ units is related by the Duane-Hunt's equation:

$$V_{\max} \times \lambda_{\min} = 12.4 \quad (6.3)$$

At the present it is rather convenient to represent the x-ray spectrum as a function of energy unit eV in place of wavelength. Figure 6.2 shows the measured energy spectrum extracted from a diagnostic x-ray of 80 kV_p . Figure 6.3 shows the energy spectrum for the therapeutic x-rays generated by 4 MV linac. Naturally the number of bremsstrahlung photons is smaller as the energy is lower. The reason is that the low-energy component is reduced because of the absorption by the metal filter and the target itself equipped in the apparatus. The energy spectrum not extracted from the x-ray tube but produced at the target is different. Detailed descriptions for the Koch-Motz's bremsstrahlung cross sections and the thick target spectrum are given in Section 12.5.

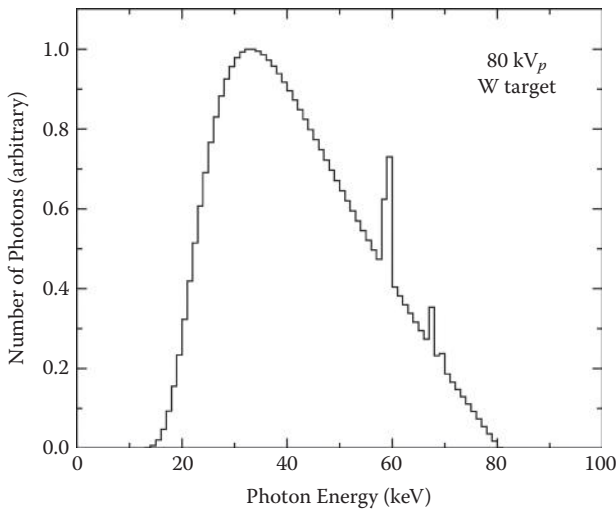
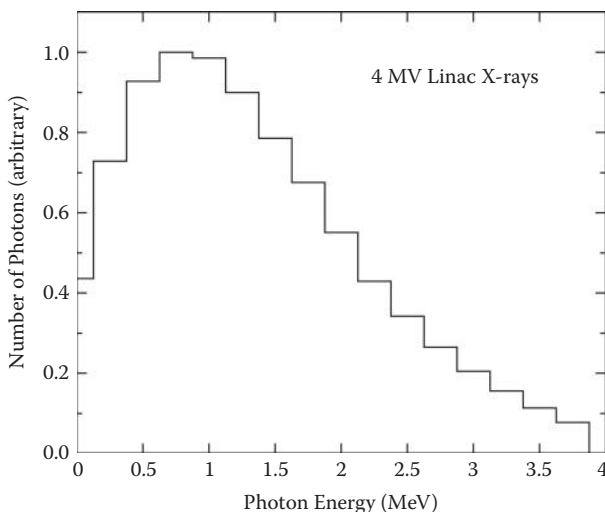


FIGURE 6.2

Energy spectrum of x-rays generated by the tube voltage of 80 kV.

**FIGURE 6.3**

Energy spectrum of x-rays generated by 4 MV linac.

6.3 Characteristic X-Rays

The binding energy of tungsten K-shell is $E_K = 69.525$ keV. If the tube voltage is higher than that, the projectile ejects an orbital electron of the target atom. Then, discrete or discontinuous x-rays are generated. These x-rays are emitted when the electrons of the outer orbit fill the vacancy of the inner shell. These are called the characteristic x-rays because those are characteristic of the target element. Figure 6.2 shows the characteristic x-rays as the lines overlying on the continuous bremsstrahlung spectrum. The K-shell vacancy is filled by the electron from L-shell and M-shell, etc., and the x-rays are marked by K_α and K_β , etc., respectively. For the L-shell vacancy, L_α and L_β x-rays are emitted. The orbital energies other than K-shell do not degenerate; namely, those differ a little with each other. Therefore, K x-ray has a fine structure. L-shell of tungsten consists of three subshells with the electron binding energies of LI = 12.098, LII = 11.541, and LIII = 10.204 keV. The transition LIII \rightarrow K produces $K_{\alpha 1}$ x-ray with the energy of $E_K - E_{LIII} = 69.525 - 10.204 = 59.321$ keV. The transition LI \rightarrow K produces $K_{\alpha 2}$ x-ray with the energy of 57.984 keV. The frequency of K_α x-ray is related to the atomic number by

$$\sqrt{\nu} = k(Z - S) \quad (6.4)$$

where Z = atomic number, and k and S are constants. This is called Moseley's law. This law played an important role in understanding the atom structure and the periodic table.

EXAMPLE 6.2

The binding energies of innermost shell electrons for molybdenum are as follows:

$$K = 20,000 \text{ eV}, \text{ LI} = 2,866 \text{ eV}, \text{ LII} = 2,625, \text{ and LIII} = 2,520 \text{ eV}$$

Calculate the characteristic x-ray $K_{\alpha 1}$, $K_{\alpha 2}$, $K_{\alpha 3}$ for this target.

SOLUTION 6.2

$$K_{\alpha 1}: \text{L}_{\text{III}} \rightarrow \text{K}: E_K - E_{\text{L}_{\text{III}}} = (20000 - 2520) \text{ eV} = 17.48 \text{ keV}$$

$$K_{\alpha 2}: \text{L}_{\text{II}} \rightarrow \text{K}: E_K - E_{\text{L}_{\text{II}}} = (20000 - 2625) \text{ eV} = 17.375 \text{ keV}$$

$$K_{\alpha 3}: \text{L}_{\text{I}} \rightarrow \text{K}: E_K - E_{\text{L}_{\text{I}}} = (20000 - 2866) \text{ eV} = 17.134 \text{ keV}$$

6.4 Auger Electrons

Even if an L electron of an atom moves to the vacancy of the K-shell, a photon is not necessarily emitted. This phenomenon frequently occurs for a small Z element. There is a probability of an alternative nonoptical transition in which an L electron is ejected from an atom. In consequence, two vacancies are generated in the L-shell. Such an ejected electron is called the Auger electron. Figure 6.4 illustrates the emission of an Auger electron on a water molecule. The downward arrow shows the transition of the electron from the $1b_1$ level to the oxygen-K-shell vacancy. Then, the energy of $E_{\text{OK}} - E_{1b_1}$ is released. In place of a photon emission, this energy is given to another electron on the $1b_1$ orbit. This electron is ejected from an atom with the kinetic energy of

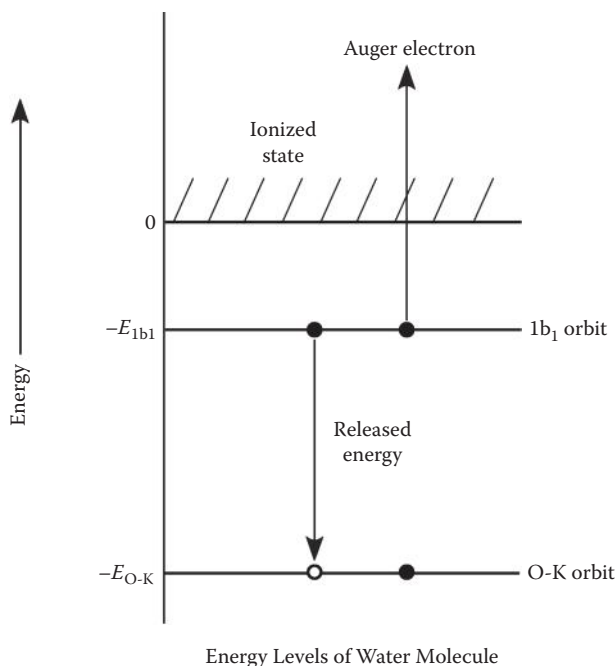
$$T = E_{\text{OK}} - E_{1b_1} - E_{1b_1} \quad (6.5)$$

For a water molecule with $E_{\text{OK}} = 539.7 \text{ eV}$ and $E_{1b_1} = 12.62 \text{ eV}$, the energy of the Auger electron becomes 514.5 eV .

The K fluorescence yield is defined by the number of KX-photon emission per K-shell vacancy. The yield Y_K as a function of Z is approximated by

$$Y_K = \frac{1}{1 + (33.6/Z)^{3.5}} \quad (6.6)$$

The yield for smaller Z is nearly 0, and that for larger Z nearly 1. On the contrary, emission of Auger electrons occurs frequently for the smaller Z in comparison with photon emission. The inner shell vacancy as the source of Auger electron emission is generated not only by electron collision but also by orbital electron capture, internal conversion, and photoelectric effect. The emission of an Auger electron increases one vacancy of atomic shell. The inner

**FIGURE 6.4**

Schematic diagram of Auger electron emission on water molecule.

shell vacancy is occupied by the Auger electron and a simultaneously weakly bound electron is ejected. Therefore, the Auger cascade occurs for a relatively heavy atom. An ion at first with only one inner shell vacancy changes to a highly charged ion by Auger cascade. This phenomenon is applied to the Auger therapy in radiology. An Auger emitter such as ^{125}I is taken in DNA or biological molecules. ^{125}I decays by electron capture. Auger cascades release about 20 electrons, which deposit plenty of energy (~ 1 keV) within a few nm. Highly charged ^{125}Te remains. As a result, biological effects such as DNA strand break, chromosome aberration, and cell death are induced.

6.5 Synchrotron Radiation

A phenomenon that was theoretically well known was that an electromagnetic wave is emitted when a charged particle moves with acceleration. In 1947, this was observed using electron synchrotron. Such an electromagnetic wave was named synchrotron radiation (SR) or synchrotron light. When high-energy relativistic electrons are forced to travel in a circular path by a magnetic field, synchrotron radiation is produced. If the speed of an electron

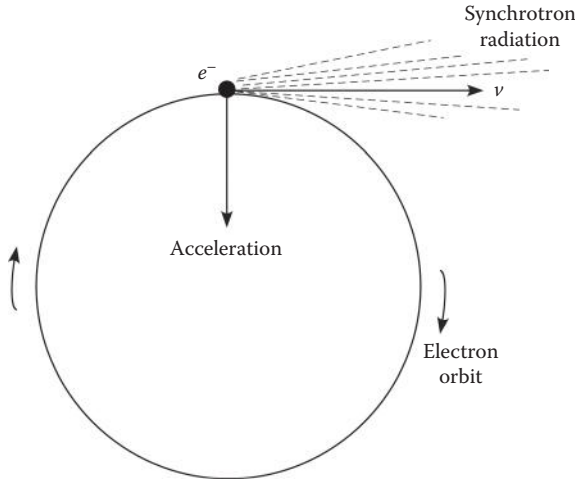


FIGURE 6.5
Schematic diagram of synchrotron radiation.

is near the speed of light, photons are emitted to the narrow angular region around the electron direction—i.e., the tangential direction. Figure 6.5 shows the scheme of synchrotron radiation. The radiation produced may range over the entire electromagnetic spectrum, from radio waves to infrared light, visible light, ultraviolet light, x-rays, and γ -rays. According to the detailed calculation, the intensity SR per unit time and unit wavelength is given by

$$I(\lambda, t) = 7.51 \times 10^{-8} \frac{E^7}{R^3} G(y) \text{ Js}^{-1} \text{ \AA}^{-1} \quad (6.7)$$

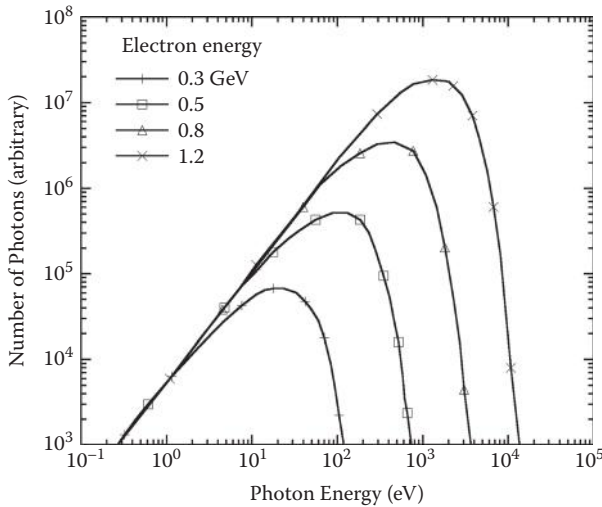
in which E (GeV) is the kinetic energy of electrons, R (m) is the orbital radius, and $G(y)$ is a function providing the spectrum shape. Figure 6.6 shows the SR spectra for various electron energies. The total radiant energy per unit time is given by

$$I(t) = 6.77 \times 10^{-7} \frac{E^4}{R^2} \text{ Js}^{-1} \quad (6.8)$$

The energy lost per turn is approximately

$$E = 88.5 \frac{E^4}{R} \text{ keV turn}^{-1} \quad (6.9)$$

ΔE becomes 5.53 MeV for $E = 5$ GeV and $R = 10$ m. Therefore, acceleration is needed to compensate the energy lost for large E and small R . The SR generated by an electron synchrotron or storage ring is a powerful light source covering a broad range of wavelength. It has characteristics superior to the conventional light sources: (1) a high-intensity continuous spectrum, (2) a good directivity, (3) a polarized light, and (4) a short time pulse.

**FIGURE 6.6**

Energy spectra of synchrotron radiation for various electron energies.

EXAMPLE 6.3

The European Synchrotron Radiation Facility (ESRF) is one of the synchrotron research facilities in Europe. The electron energy in the synchrotron storage ring is 6 GeV, and the storage ring is a semicircle with 844.4 m circumference. Calculate the total radiant energy per unit time and the energy lost per turn in the storage ring.

SOLUTION 6.3

$$I(t) = 6.77 \times 10^{-7} \frac{E^4}{R^2} = 6.77 \times 10^{-7} \frac{6^4}{(844.4/2\pi)^2} = 4.9 \times 10^{-8} \text{ Js}^{-1}$$

$$E = 88.5 \frac{E^4}{R} = 88.5 \frac{6^4}{844.4/2\pi} = 853.5 \text{ keV turn}^{-1}$$

6.6 Diffraction by Crystal

The penetrability of x-rays is used for various fields of application. The structure analysis of crystal uses the wave motion of x-rays. A solid forms a well-ordered crystal, unlike vapor or liquid. If solid atoms or solid molecules are spatially arranged in a regular manner, this is called the crystal lattice.

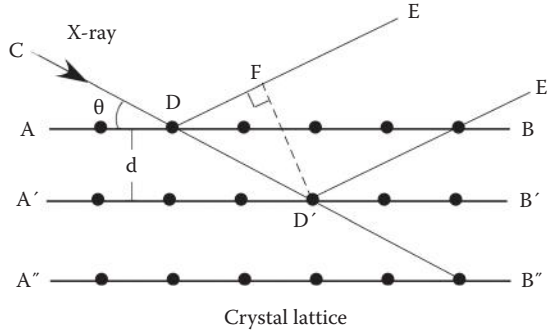


FIGURE 6.7
Bragg diffraction by crystal.

Each point in the crystal lattice is called the point of a lattice. The distance between the points of a lattice of a solid crystal is ordinarily a few nm. X-rays are used as a rule to measure the crystal structure because of the similarity of wavelength. When x-rays irradiate crystal, a major part of x-rays passes on the straight line. They are penetrated x-rays. A part of x-rays scattered by an atom becomes the diffracted x-rays enhancing each other at the specific direction. This phenomenon is similar to the diffraction of visible light impinging the diffraction lattice.

Assuming a plane in a crystal, there is a case that a lot of atoms are arranged in a regular manner on the plane. Such a plane is called the plane of atomic arrangement. Figure 6.7 shows the planes parallel forming with an equal distance d , which is called the lattice constant. It is assumed that x-rays with the wavelength λ impinge with the angle θ vs. AB from the direction CD and reflect the direction DE. A part of the remaining x-rays is reflected on the planes A'B' and A''B'' and goes to D'E' and D''E'' parallel to DE. The difference of path length of the reflected x-rays between a plane and the next one is equal to $DD' - DF$. Using

$$DD' = \frac{d}{\sin \theta}, \quad DF = \frac{d}{\sin \theta} \cos 2\theta \quad (6.10)$$

then

$$DD' - DF = \frac{d}{\sin \theta} (1 - \cos 2\theta) = 2d \sin \theta \quad (6.11)$$

is obtained. If this value is equal to the integer times the wavelength λ ,

$$2d \sin \theta = n\lambda \quad (n = 1, 2, 3, \dots) \quad (6.12)$$

is held and the reflected wave is enhanced by interference with each other. This is called the Bragg's reflection condition. The integer n is the order of

reflection. For known λ , the measurement of the lattice constant d is possible, while the wavelength of x-rays can be determined by measuring the position of *moire* (denoted by θ) if the lattice constant of crystal is known.

EXAMPLE 6.4

The d-spacing of a diamond is 1.075 Å. At which angle θ do we expect to detect the first-order interference pattern, given the impinging light has a wavelength of 1.54 Å? What is the maximum wavelength of light needed for detecting the interference pattern at the same angle for a crystal with the lattice constant of 1.261 Å?

SOLUTION 6.4

$$\sin(\theta) = \frac{1.54}{2 \cdot 1.075} = 0.716 \quad \theta = 45.75^\circ$$

For the d-spacing of 1.261 Å and the angle $\theta = 45.75^\circ$, the maximum wavelength is

$$\lambda_{\max} = 2 \cdot 1.261 \text{ Å} \cdot 0.716 = 1.806 \text{ Å}$$

6.7 Summary

1. When electrons hit the target material, electrons suffer a sharp breaking near the nucleus and generate x-rays.
2. Monochromatic electron beam generates the continuous x-ray spectrum whose maximum is the beam energy. This continuous x-ray is called bremsstrahlung.
3. The relationship $V_{\max} \times \lambda_{\min} = 12.4$ holds for the peak voltage V_{\max} (kV) and the minimum wavelength λ_{\min} (Å).
4. Electrons eject the orbital electron from the target atom. Either characteristic x-ray or Auger electron is emitted when the electrons of the outer shell occupy the inner shell vacancy.
5. High-speed electrons moving in circular orbit emit the synchrotron radiation toward the tangential direction. Synchrotron radiation is useful as the polychromatic light source, similar to bremsstrahlung.

QUESTIONS

1. Calculate a photon energy generated when an electron with the initial velocity of $0.8c$ is braked to $0.6c$ by the nuclear electric field.
 2. The efficiency of bremsstrahlung generation for diagnostic x-ray tube is represented by $\eta = kZV$, in which k is a constant, V is the tube voltage [kV] and Z is the atomic number of target. On an x-ray generator with W target, η is 0.74% for 100 kV. What is the bremsstrahlung output in Watt units for 80 kV and the tube current 200 mA.
 3. An x-ray beam generated by 150 kVp is hardened by a tin filter. What will be the best choices of a second and a third filter to stop fluorescent radiation?
-

For Further Reading

- Birch R, Marshall M, Ardran GM. 1979. *Catalogue of Spectral Data for Diagnostic X-Rays*. London: Hospital Physicists' Association.
- Johns HE, Cunningham JR. 1974. *The Physics of Radiology*, 3rd ed. Springfield, IL: Charles C. Thomas Publisher.
- Turner JE. 1995. *Atoms, Radiation, and Radiation Protection*, 2nd ed. New York: John Wiley & Sons.

7

Interaction of Photons with Matter

7.1 Types of Interaction

Energetic charged particles when moving steadily lose energy by the electric interactions with the atoms in matter. On the other hand, photons lose energy by a different manner than the electric interaction because of their charge neutralities. Namely, photons can go forward a certain distance before an interaction with an atom occurs. That distance is statistically dominated by the interaction probability per unit length, which depends on the medium and the photon energy. Sometimes interacted photons are absorbed and disappear, or are scattered and change direction. Both cases are possible, whether energy is lost or not. Thomson scattering and Rayleigh scattering are the processes of photon interaction with matter without energy transfer. The principal mechanisms of the energy deposition of photons in matter are photoelectric absorption, Compton scattering, pair creation, and photonuclear reaction.

7.1.1 Thomson Scattering

In Thomson scattering, a free electron oscillates in response to the electric vector of an electromagnetic wave. This type of scattering is important at low energies. The oscillating electron emits a radiation with the same frequency as the incident wave. No energy loss occurs in this process. Only the angle of deflection is changed in the collision. Quantum mechanics proves Thomson scattering is an extremity of Compton scattering when incident photon energy is brought to zero.

7.1.2 Photoelectric Effect

The photoelectric effect is a phenomenon in which electrons are emitted from matter after the absorption of energy from electromagnetic radiation such as x-rays or visible light. The emitted electrons can be referred to as photoelectrons. The energy of the emitted electrons does not depend on intensities of the incident radiation, but relates to the wavelength of radiation. As the wavelength is shorter, the electrons with larger energy are emitted. To elucidate

these experimental results, Einstein proposed that the incident radiation is a quantum (photon) having the energy of $E = h\nu$, and he assumed that the photoelectron is produced when an electron in matter completely absorbs a photon. The incident photon therefore disappears. The kinetic energy of a photoelectron, T , is represented by

$$T = h\nu - B \quad (7.1)$$

where B is the binding energy of an electron orbit.

EXAMPLE 7.1

What is the energy of a photoelectron emitted from lead by interaction with photons of 100 keV energy?

SOLUTION 7.1

$$B_{\text{Pb}} = 88.0 \text{ keV}, T_e = (100 - 88) \text{ keV} = 12 \text{ keV}$$

7.1.3 Compton Scattering

Compton scattering is the decrease in energy of an x-ray or γ -ray photon when it interacts with matter. Because of the change in photon energy, it is an inelastic scattering process. The effect is important because it demonstrates that light cannot be explained purely as a wave phenomenon. Thomson scattering, the classical theory of an electromagnetic wave scattered by charged particles, cannot explain low-intensity shift in wavelength. Light must behave as if it consists of particles in order to explain the Compton scattering. Compton's experiment verified that light can behave as a stream of particle-like quanta whose energy is proportional to the frequency.

Figure 7.1 shows the scheme for Compton scattering. The quantum model of Compton scattering is that a photon with the energy $h\nu$ and the

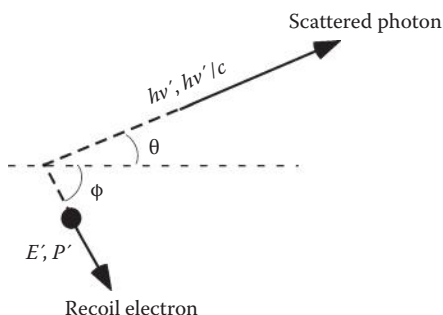


FIGURE 7.1

Definition of angles after collision.

momentum $h\nu/c$ directs at a free electron at rest. After collision, the photon is scattered through an angle θ having the energy $h\nu'$ and the momentum $h\nu'/c$, and an electron is ejected at an angle ϕ with the total energy E' and the momentum P' . The relativistic expression for E' and P' for the electron rest mass m and the velocity $\beta = v/c$ is as follows:

$$E = mc^2/\sqrt{1-\beta^2}, \quad P = mc\beta/\sqrt{1-\beta^2} \quad (7.2)$$

From the conservation laws for energy and momentum, the following equations are obtained.

$$\begin{aligned} h\nu + mc^2 &= h\nu' + E \\ \frac{h\nu}{c} &= \frac{h\nu'}{c} \cos \theta + P \cos \phi \\ \frac{h\nu}{c} \sin \theta &= P \sin \phi \end{aligned} \quad (7.3)$$

Using Equations (7.2) and (7.3) the energy of the scattered photon is obtained as

$$h\nu' = \frac{h\nu}{1 + \frac{h\nu}{mc^2}(1 - \cos \theta)} \quad (7.4)$$

The kinetic energy of the recoiled electron, T , becomes

$$T = h\nu - h\nu' = h\nu \frac{1 - \cos \theta}{1 - \cos \theta + mc^2/h\nu} \quad (7.5)$$

If $\theta = 180^\circ$ then the electron has the maximum energy:

$$T_{\max} = \frac{2h\nu}{2 + mc^2/h\nu} \quad (7.6)$$

In the field of γ -ray spectroscopy, T_{\max} is known as the Compton edge. It is found that T_{\max} approaches $h\nu$ for $h\nu \gg mc^2$. The relationship between θ and ϕ is given by

$$\cot \frac{\theta}{2} = 1 + \frac{h\nu}{mc^2} \tan \phi \quad (7.7)$$

When θ increases from 0° to 180° , ϕ decreases from 90° to 0° . This means that the photon is scattered through all directions, while the recoil angle of the electron is limited to the forward angles ($0 \leq \phi \leq 90^\circ$).

EXAMPLE 7.2

1. What is the maximum energy of the Compton electron for the incident photon of energy 1 MeV?
2. Calculate the wave length of the scattered photon through the angle of 45° .
3. At which angle is the Compton electron of energy 250 keV detected?

SOLUTION 7.2

$$1. T_{\max} = \frac{2 \cdot 1 \text{ MeV}}{2 + 0.511} = 0.796 \text{ MeV}$$

$$2. h\nu = \frac{1 \text{ MeV}}{1 + \frac{1 \text{ MeV}}{0.511 \text{ MeV}} (1 - \cos 45^\circ)} = 0.636 \text{ MeV}$$

The wavelength of the scattered photon is

$$\lambda = \frac{hc}{E} = \frac{1240 \text{ eV nm}}{0.636 \text{ MeV}} = 1.95 \cdot 10^{-3} \text{ nm}$$

$$3. \cos \theta = 1 - \frac{T \frac{mc^2}{h\nu}}{h\nu - T} = 1 - \frac{0.75 \cdot 0.511}{0.25} = -0.533 \quad \theta = 122.21^\circ$$

$$\tan \phi = \frac{\cot \frac{122.21^\circ}{2}}{(1 + 1/0.511)} = 0.187 \quad \phi = 10.57^\circ$$

7.1.4 Pair Creation

When photon energy is at least twice the electron rest mass ($h\nu \geq 2mc^2$), the photon is converted to a pair of electron-positron in the vicinity of a nucleus. Pair creation occurs in the field of atomic electron for the photon energy greater than $4mc^2$; however, its probability is very low. This process is called triplet pair creation because another recoiled electron is produced. In photon-nucleus pair creation, the recoiled energy of a heavy nucleus is negligible. Therefore, the photon energy $h\nu$ is converted to

$$h\nu = 2mc^2 + T_+ + T_- \quad (7.8)$$

where T_+ and T_- represent the kinetic energies of the positron and electron, respectively. The energy distribution of the electron and positron continuously varies in the range between 0 and $h\nu - 2mc^2$. Those energy spectra are almost the same. The threshold energy is 1.022 MeV.

The inverse process occurs such that photons are produced by annihilation of an electron-positron pair. The positron slows down and attracts an electron. Then, a positronium that resembles a hydrogen atom is formed. This survives $\sim 10^{-10}$ s before pair annihilation. The annihilation generates two photons with energy of 511 keV. These photons are emitted in opposite directions. The probability of in-flight annihilation is less than 10%.

7.1.5 Photonuclear Reaction

Photonuclear reaction is the process in which nucleons are ejected from nucleus-absorbing photons. For example, a neutron is emitted when a γ -ray is captured by a nucleus of $^{206}_{82}\text{Pb}$: the notation of this reaction is $^{206}_{82}\text{Pb}(\gamma, n)^{205}_{82}\text{Pb}$. For this to occur, photons should have sufficient energy greater than the binding energy of nucleons. Those are usually above several MeV. The kinetic energy of the emitted neutron is equal to the photon energy less the binding energy. The probability of a photonuclear reaction is much smaller in comparison with a photoelectric effect, Compton scattering, and pair creation. However, this reaction is important from the viewpoint of radiation protection because it produces neutrons. In addition, the residual nucleus after the reaction frequently becomes radioactive. From these reasons this reaction plays a significant role in the vicinity of high-energy electron accelerators. Table 7.1 shows the Q values of (γ, n) reactions that produce neutrons. The threshold energy for (γ, p) reactions is greater than that for (γ, n) reactions because higher energy is needed for protons to exceed the repulsive force of the Coulomb barrier. Reactions $(\gamma, 2n)$, (γ, np) , and (γ, α) occur other than (γ, n) and (γ, p) .

TABLE 7.1
 Q Values for (γ, n) Reactions

Reaction	Q Value (MeV)	Decay Mode of Product Nucleus
$^{12}\text{C}(\gamma, n)^{11}\text{C}$	-19.0	β^+
$^{14}\text{N}(\gamma, n)^{13}\text{N}$	-10.7	β^+
$^{16}\text{O}(\gamma, n)^{15}\text{O}$	-16.3	β^+
$^{23}\text{Na}(\gamma, n)^{22}\text{Na}$	-12.1	β^+
$^{27}\text{Al}(\gamma, n)^{26}\text{Al}$	-14.0	β^+
$^{40}\text{Ca}(\gamma, n)^{39}\text{Ca}$	-15.9	β^+
$^{56}\text{Fe}(\gamma, n)^{55}\text{Fe}$	-11.2	EC
$^{63}\text{Cu}(\gamma, n)^{62}\text{Cu}$	-10.9	β^+
$^{65}\text{Cu}(\gamma, n)^{64}\text{Cu}$	-10.2	EC(100), $\beta^-(38)$, $\beta^+(19)$
$^{206}\text{Pb}(\gamma, n)^{205}\text{Pb}$	-8.25	EC
$^{207}\text{Pb}(\gamma, n)^{206}\text{Pb}$	-6.85	Stable
$^{208}\text{Pb}(\gamma, n)^{207}\text{Pb}$	-8.1	Stable

7.2 Attenuation Coefficients

The penetration of photons in matter is statistically dominated by the interaction probability per unit length. This probability μ is called the linear attenuation coefficient or the macroscopic cross section. The dimension is the inverse of length (m^{-1}). The coefficient μ depends on both photon energy and matter. The mass attenuation coefficient is represented by μ/ρ ($\text{m}^2 \text{kg}^{-1}$), in which ρ is the density of matter. This denotes the interaction probability per thickness in kg.m^{-2} units. Monochromatic photons attenuate exponentially in a uniform target. It is assumed that the number N_0 of monochromatic photons with a narrow beam vertically enter a slab. Some photons are scattered and other photons are absorbed in the absorber. The number of photons reached at the depth x without any interactions is assumed $N(x)$. The number of interactions dN in the small interval dx is written by

$$dN = - \mu N dx \quad (7.9)$$

in which μ is the linear attenuation coefficient. Solving this equation,

$$N(x) = N_0 e^{-\mu x} \quad (7.10)$$

is obtained. The ratio $N(x)/N_0$ is the probability that the vertically incident photons traverse a slab with the thickness x without interaction. The linear attenuation coefficient can be measured using such a setup as shown in Figure 7.2. A small size detector with the diameter d is located at the distance R from the absorber ($R \gg d$). This condition is called a narrow beam or a good geometry. Only photons passed through without interaction are detected. Using Equation (7.10), the coefficient μ is obtained from measurements of $N(x)/N_0$ as a function of x . Figure 7.3 shows the linear attenuation

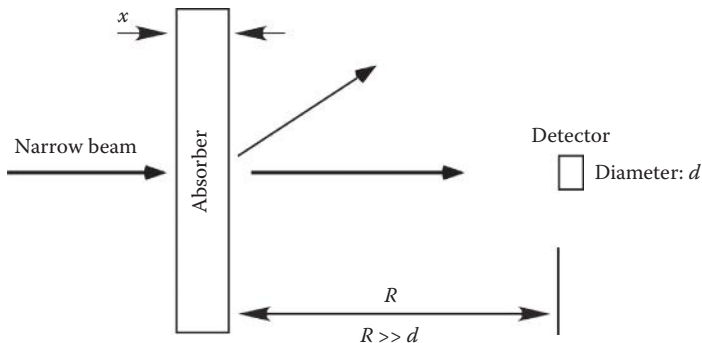
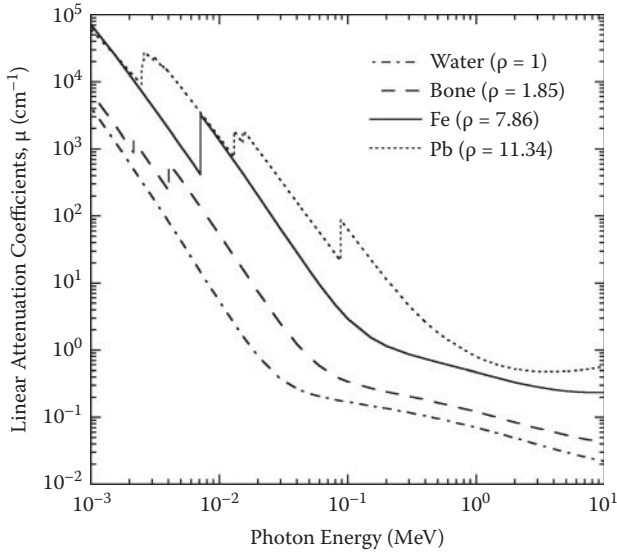


FIGURE 7.2

Measurements of attenuation coefficients using narrow beam.

**FIGURE 7.3**

Linear attenuation coefficients for various matter.

coefficients for various matters for photons with energies between 1 keV and 10 MeV.

The photon linear attenuation coefficient is the sum of contributions from various processes removing photons from the narrow beam.

$$= \tau + \sigma + \kappa \quad (7.11)$$

where τ , σ , and κ denote photoelectric effect, Compton effect, and pair creation, respectively. Here, Thomson scattering and photonuclear reaction are omitted. The mass attenuation coefficients for a matter with the density of ρ are τ/ρ , σ/ρ , and κ/ρ . Photoelectric effect is dominant at the lower-energy region. High Z material gives greater attenuation and absorption; however, these rapidly decrease as energies increase. Compton scattering becomes dominant above a few hundred keV. Pair creation increases above 1.022 MeV.

The linear attenuation coefficient is from photon cross sections in barn/atom units. μ is the product of the atomic density N_A by the total atomic cross section σ_A .

$$= N_A \sigma_A \quad (7.12)$$

The number of atoms N_A per 1 cm³ is given by $\rho N_0/A$ for the gram atomic mass A and Avogadro number N_0 .

$$\frac{\mu}{\rho} = \frac{N_0 \sigma_A}{A} \quad (7.13)$$

This equation gives a relationship between mass attenuation coefficients and atomic photon cross sections. For compound and mixture materials, contributions of each constituent element are summed:

$$\frac{\mu}{\rho} = \frac{N_0}{A} \sum_j f_j^i \sigma_A^j \quad (7.14)$$

where A is the gram molecular mass, f_j^i the number of the j th atom in a molecule, and σ_A^j the j th atomic cross section.

EXAMPLE 7.3

The total cross section of C for 1 MeV photons is 1.267 b. The atomic mass of C is 12.011 and the Avogadro number is 6.022×10^{23} . Calculate the mass attenuation coefficient.

SOLUTION 7.3

$$\frac{\mu}{\rho} = \frac{6.022 \times 10^{23}}{12.011} \times 1.267 \times 10^{-24} = 6.35 \times 10^{-2} \text{ cm}^2\text{g}^{-1}$$

EXAMPLE 7.4

Total cross sections of H and O for 1 MeV photons are 0.2112 b and 1.69 b, respectively. The atomic masses of H and O are 1 and 16, respectively. Calculate the mass attenuation coefficient for water.

SOLUTION 7.4

$$\frac{\mu}{\rho} = \frac{6.022 \times 10^{23}}{18} \times (2 \times 0.2112 + 1 \times 1.69) \times 10^{-24} = 7.06 \times 10^{-2} \text{ cm}^2\text{g}^{-1}$$

7.3 Half-Value Layer of X-Rays

The energy spectrum of x-rays used for diagnosis is not monochromatic. Since the lower-energy component is apt to be absorbed in matter, the fraction of high-energy photons rises in penetrating the matter. The attenuation for such polychromatic photons cannot be treated by counting the number of photons, while the exposure or exposure rate is measured. The attenuation is represented by the absorber (filter) thickness for which those quantities decrease by a half. This thickness is called the half-value layer (HVL). The

HVL measurement is extensively used for obtaining the properties of x-rays using narrow beams. If broad beams are used, the measured HVL is overestimated in comparison with the true value because of additional scattering from the filter. The exposure rate I for the filter thickness of x is given by

$$I = I_0 e^{-\mu x} \quad (7.15)$$

where I_0 is the rate for the case of filterless. From the definition, the HVL becomes the thickness x when $I/I_0 = 1/2$ is held.

$$\text{HVL} = \frac{\ln 2}{\mu} = \frac{0.693}{\mu} \quad (7.16)$$

If the HVL for a continuous spectrum of x-rays is equal to that for monochromatic photons for a filtration material, the photon energy is called the effective energy of continuous x-rays. The voltage of the x-ray generator is represented by the peak voltage. Generally, the effective voltage (the effective energy) is less than half of the peak voltage. X-rays passing through the HVL have higher energy than before penetration; that is, they become harder. The thickness of filter necessary for degrading the exposure rate after penetration by half again is called the second half-value layer. The second HVL is thicker than the first HVL.

EXAMPLE 7.5

The mass attenuation coefficient of Al ($\rho = 2.7 \text{ g cm}^{-3}$) for 60 keV photons is $0.2778 \text{ cm}^2 \text{ g}^{-1}$. Calculate the half-value layer in mm units of Al for 60 keV photons.

SOLUTION 7.5

$$\begin{aligned} \mu &= \mu_m \cdot \rho = 0.2778 \times 2.7 = 0.75 \text{ cm}^{-1} = 0.075 \text{ mm}^{-1} \\ \therefore \text{HVL} &= \frac{0.693}{0.075} = 9.24 \text{ mm} \end{aligned}$$

EXAMPLE 7.6

The mass absorption coefficient of 2.5 MeV x-rays in lead is $0.0042 \text{ m}^2 \text{ kg}^{-1}$. Find the thickness of tissue of density $11,300 \text{ kg m}^{-3}$ that will reduce the intensity of the radiation by a factor 10.

SOLUTION 7.6

$$I = I_0 e^{-\mu x}, \quad x = (\mu_m \rho)^{-1} \cdot \ln I_0/I = 0.0485 \text{ m}$$

7.4 Mass Energy Absorption Coefficients

The mechanism of energy loss of photons is considered in this section. In the photoelectric effect, a secondary electron with the initial kinetic energy $T = h\nu - B$ is produced absorbing a photon energy $h\nu$. After emission of the photoelectron, the inner shell is occupied and a characteristic x-ray or an Auger electron is emitted. The fraction of energy transferred to a photoelectron or Auger electron is $1 - \delta/h\nu$, in which δ is the average energy of fluorescent x-rays. If the mass attenuation coefficient of the photoelectric effect is τ/ρ , then the mass energy transfer coefficient becomes

$$\frac{\tau_{tr}}{\rho} = \frac{\tau}{\rho} \left(1 - \frac{\delta}{h\nu} \right) \quad (7.17)$$

Because the photoelectron and Auger electron generate bremsstrahlung photons to some extent, the energy transfer coefficient does not necessarily represent energy absorption. The mass energy transfer coefficient in Compton scattering for a monochromatic photon is given by

$$\frac{\sigma_{tr}}{\rho} = \frac{\sigma}{\rho} \frac{T_{avg}}{h\nu} \quad (7.18)$$

in which $T_{avg}/h\nu$ means the average fraction converted into the initial kinetic energy of Compton electrons. Bremsstrahlungs due to Compton electrons are not taken into account here. On pair creation, the sum of the initial kinetic energy of a pair is $h\nu - 2mc^2$. The mass energy transfer coefficient is therefore given by

$$\frac{\kappa_{tr}}{\rho} = \frac{\kappa}{\rho} \left(1 - \frac{2mc^2}{h\nu} \right) \quad (7.19)$$

The total mass energy transfer coefficient becomes

$$\frac{\tau_{tr}}{\rho} = \frac{\tau}{\rho} \left(1 - \frac{\delta}{h\nu} \right) + \frac{\sigma}{\rho} \frac{T_{avg}}{h\nu} + \frac{\kappa}{\rho} \left(1 - \frac{2mc^2}{h\nu} \right) \quad (7.20)$$

This coefficient determines the initial kinetic energy of all electrons generated directly and indirectly. The absorbed energy at the vicinity of the interaction point is equal to the transferred energy except bremsstrahlung. Putting the average fraction of energy emitted by bremsstrahlung g , the mass energy absorption coefficient is defined by

$$\frac{\mu_{en}}{\rho} = \frac{\tau_{tr}}{\rho} (1 - g) \quad (7.21)$$

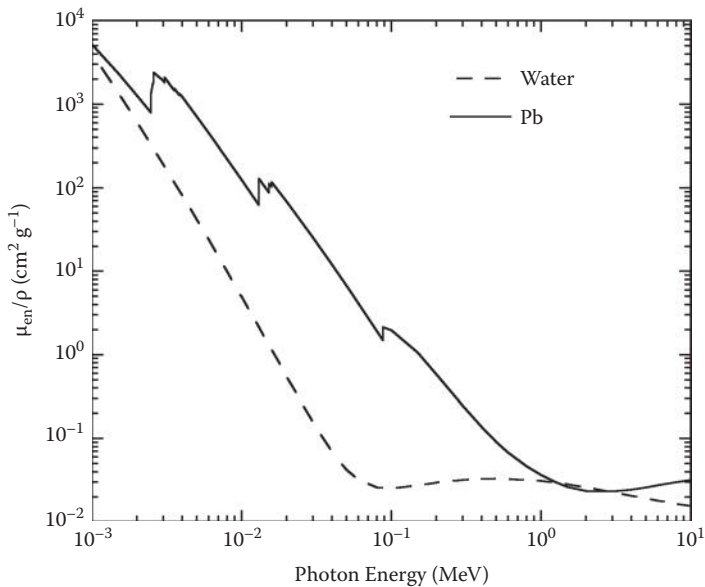


FIGURE 7.4
Comparison of mass energy absorption coefficients between water and Pb.

Figure 7.4 shows the mass energy absorption coefficients for various matter in the energy range 1 keV–10 MeV. Table 7.2 shows the differences between the coefficients for water and lead. Bremsstrahlungs for water is insignificant below 10 MeV. For lead, the difference between mass energy transfer coefficient and mass energy absorption coefficient can be explained by bremsstrahlung emission.

TABLE 7.2
Mass Attenuation Coefficients, Mass Energy Transfer Coefficients, and Mass Energy Absorption Coefficients of Photons for Water and Pb (cm²g⁻¹ units)

Photon Energy (MeV)	Water			Pb		
	μ/ρ	μ _{tr} /ρ	μ _{en} /ρ	μ/ρ	μ _{tr} /ρ	μ _{en} /ρ
0.01	5.33	4.95	4.95	131.0	126.0	126.0
0.10	0.171	0.0255	0.0255	5.55	2.16	2.16
1.0	0.0708	0.0311	0.0310	0.0710	0.0389	0.0379
10.0	0.0222	0.0163	0.0157	0.0497	0.0418	0.0325
100.0	0.0173	0.0167	0.0122	0.0931	0.0918	0.0323

The absorbed dose D in a medium is represented by the product of the energy fluence Ψ and the energy absorption coefficient μ_{en}/ρ under the condition of electron equilibrium, such as

$$D = \Psi \frac{\mu_{\text{en}}}{\rho} \quad (7.22)$$

A similar equation for the kerma K holds using the mass energy transfer coefficient τ_{tr}/ρ ,

$$K = \Psi \frac{\tau_{\text{tr}}}{\rho} \quad (7.23)$$

This relationship does not need the condition of electron equilibrium.

EXAMPLE 7.7

The mass attenuation coefficient of W for a photoelectric effect for 100 keV photons is $4.15 \text{ cm}^2 \text{ g}^{-1}$. The average energy of K-x-rays is 60.6 keV. Calculate the mass energy transfer coefficient for the photoelectric effect for 100 keV photons.

SOLUTION 7.7

$$\frac{\tau_{\text{tr}}}{\rho} = 4.15 \times \left(1 - \frac{60.6}{100}\right) = 1.64 \text{ cm}^2 \text{ g}^{-1}$$

EXAMPLE 7.8

The mass attenuation coefficient of water for Compton scattering for 0.5 MeV photons is $0.0966 \text{ cm}^2 \text{ g}^{-1}$. The average energy of scattered photons is 0.329 MeV. Calculate the mass energy transfer coefficient for Compton scattering for 0.5 MeV photons.

SOLUTION 7.8

The average energy of recoil electrons is $0.5 - 0.329 = 0.171 \text{ MeV}$.

$$\frac{\sigma_{\text{tr}}}{\rho} = 0.0966 \times \frac{0.171}{0.5} = 0.033 \text{ cm}^2 \text{ g}^{-1}$$

EXAMPLE 7.9

The mass energy transfer and mass energy absorption coefficients are 0.0271 and $0.0270 \text{ cm}^2 \text{ g}^{-1}$, respectively. Calculate the average fraction of energy emitted by bremsstrahlung.

SOLUTION 7.9

$$g = 1 - \frac{\text{en}}{\text{tr}} = 1 - \frac{0.0270}{0.0271} = 0.0037$$

EXAMPLE 7.10

The mass energy absorption coefficient of Al for 80 keV photons is $0.05511 \text{ cm}^2 \text{ g}^{-1}$. If the fluence is $1 \times 10^6 \text{ cm}^{-2}$, what is the absorbed energy?

SOLUTION 7.10

$$D = 80 \times 10^6 \times 0.05511 = 4.41 \times 10^6 \text{ keVg}^{-1}$$

Expressed in SI units,

$$D = \frac{4.41 \times 10^6 \text{ keV}}{\text{g}} \times 1.6 \times 10^{-16} \frac{\text{J}}{\text{keV}} \times 10^3 \frac{\text{g}}{\text{kg}} = 7.06 \times 10^{-7} \text{ Gy}$$

7.5 Summary

1. Photon interactions with matter are in the form of Thomson scattering, photoelectric effect, Compton scattering, electron pair creation, and photonuclear reaction.
2. The major process of energy deposition of photons in matter is photoelectric absorption in the low-energy region, Compton scattering in the medium-energy region, and electron pair creation in the high-energy region.
3. A photon travels a distance called the free path before interaction with an atom. The mean free path is determined by the attenuation coefficient.
4. The thickness of absorber that reduces a dose by a half is called the half-value layer (HVL). The HVL is used for representing radiation quality of the continuous x-rays.
5. Under the condition that electron equilibrium holds, the absorbed dose at a point in the medium is equal to the product of energy fluence by mass energy absorption coefficient.

QUESTIONS

1. a. Write an expression for the energy relation between the incident and the scattered photon.
b. Write a corresponding relation for the electron.
c. Derive an expression relating the energy of an incident and a scattered photon in a Compton process.
 2. Calculate the specific γ -ray constant for ^{60}Co in units R per h per Ci at a distance of 1 m.
 3. In a Compton interaction the scattered photon gets three times more energy than the ejected electron. Calculate the minimum incident photon energy.
 4. What is the energy of the back scattered photon from Compton interaction of ^{137}Cs γ (662 keV)?
 5. Calculate ^{137}Cs γ -ray attenuation by 1 cm lead and aluminum.
 6. Neutron contamination from accelerators in radiotherapy could cause secondary cancer. The photoneutron could be produced in the head of the accelerators when a photon hits the target, or collimators. The target and collimators are made of heavy atomic number materials like tungsten and lead. What is the minimum energy of the photon in order to avoid contamination of the neutron?
 7. Derive the minimum photon energy that can induce triplet production.
 8. Calculate the number of interactions that occur in lead 15 mm thick impinged perpendicularly by a narrow photon beam with 10^{15} photons of energy 10 MeV. The density of lead is 11.3 g/cm^3 .
-

For Further Reading

- ICRU. 1992. *Photon, Electron, Proton and Neutron Interaction Data for Body Tissues*. ICRU Report 46.
- Storm E, Israel HI. 1970. Photon cross sections from 1 keV to 100 MeV for elements $Z = 1$ to $Z = 100$. *Nuclear Data Tables A7*: 565–681.

8

Interaction of Electrons with Matter

8.1 Energy Loss of Charged Particles

When charged particles penetrate matter, their energies are lost by ionization and excitation of atoms or molecules of the medium. Moving charged particles act on atomic electrons through electromagnetic force and transfer energy to these electrons. The transferred energy may be sufficient for ionizing the atom by ejecting an orbital electron or may produce an excited state not ionized. Heavy charged particles lose a small part of their energies by a single collision. The deflection of the path when collision occurs can be ignored. Heavy charged particles travel almost in a straight line, continuously losing a small amount of energies by collision with the atomic electrons. Ionized or excited atoms are left on the track of penetration. Sometimes, the path is bent by the Rutherford scattering with the nucleus. Electrons and positrons lose energies almost continuously when being slowed down in matter. They lose a major part of energies by a single collision with the orbital electron. The path is largely bent because the scattering angle determined from the kinematics is usually large. Electrons are largely scattered by elastic scattering with the nucleus. Electrons and positrons do not advance in a straight line. In addition, electrons emit bremsstrahlung photons when the path is sharply bent. The contribution of bremsstrahlung to the stopping power becomes important at high-energy regions. For example, the radiative stopping power for water for 100 MeV electrons contributes almost half to the total stopping power.

The mean energy loss of charged particles per length in medium is important in the fields of radiation physics and radiation dosimetry. This quantity, noted by $-dE/dx$, is called the stopping power of the medium for the particle—or from the viewpoint of the particle, it is frequently represented by the linear energy transfer (LET). The unit of LET is usually $\text{keV } \mu\text{m}^{-1}$. The stopping power and LET are closely related to the dose given by the recoiled charged particles produced by the uncharged particles, such as photons and neutrons. In addition, those are related to the biological effect of various radiations. The stopping power is defined by the product of the mean energy loss per collision, Q_{av} and the collision probability per unit length, μ ,

in which μ is the macroscopic cross section whose dimension is the inverse of the length. The mean energy loss Q_{av} is then given by

$$Q_{av} = \int_{Q_{min}}^{Q_{max}} QW(Q)dQ \quad (8.1)$$

where $W(Q)$ is the energy loss spectrum for a collision. The minimum energy loss, Q_{min} , in the collision between charged particle and electron seems to be ~ 0 . The maximum energy loss, Q_{max} , can be roughly estimated from the kinematical relationship. If a charged particle having the mass M and the speed V collides with an electron having the mass m in rest, the energy transfer reaches maximum for the head-on collision. Solving the conservation laws of energy and momentum, Q_{max} is obtained as

$$Q_{max} = \frac{4mME}{(M + m)^2} \quad (8.2)$$

in which $E = MV^2/2$ is the initial kinetic energy of the charged particle. If the incident particle is an electron or positron, Q_{max} is E . It is experimentally confirmed that the energy transfer continuously distributes in the range $Q_{min} < Q < Q_{max}$ and Q_{av} is ~ 20 eV.

The linear stopping power is defined by

$$-\frac{dE}{dx} = Q_{av} = \int_{Q_{min}}^{Q_{max}} QW(Q)dQ \quad (8.3)$$

The unit of the linear stopping power is generally MeV cm^{-1} . The quantity divided by the material density, $-dE/(\rho dx)$, is called the mass stopping power, whose unit is $\text{MeV cm}^2 \text{g}^{-1}$. The values of the stopping power vary according to particle, energy, and medium.

EXAMPLE 8.1

Calculate the maximum energy that a 5 MeV proton can lose in a single electronic collision.

SOLUTION 8.1

Neglecting m compared with M , the maximum energy transfer can be approximated by

$$Q_{max} = \frac{4mE}{M} = \frac{4 \times 1 \times 5}{1836} = 1.09 \times 10^{-2} \text{ MeV} = 10.9 \text{ keV}$$

8.2 Collision Stopping Power

We call both an electron and a positron an electron because their stopping powers and ranges are almost identical. The stopping powers of electrons are different from those of charged particles for two reasons. The first is that an electron loses a great deal of energy by a single collision. The second is that it is impossible to identify either an incident or hit electron. On the energy loss, the higher-energy electron after collision is regarded as the incident electron. Therefore, the maximum energy transfer becomes $T/2$ for the negatively charged electron with the kinetic energy T .

The stopping power formula derived from the quantum mechanics is summarized in ICRU Report 37. The mass collision stopping power is given by

$$\frac{S_{\text{col}}^{\mp}}{\rho} = \frac{2\pi r_e^2 mc^2}{\beta^2} \frac{ZN_A}{A} \ln \frac{T}{I} + \ln \left(1 + \frac{\tau}{2}\right) + F^{\mp}(\tau) - \delta \quad (8.4)$$

$$F^{-}(\tau) = (1 - \beta^2) \left(1 + \frac{\tau^2}{8} - (2\tau + 1) \ln 2\right) \quad \text{for electrons} \quad (8.5)$$

$$F^{+}(\tau) = 2 \ln 2 - \frac{\beta^2}{12} \left(23 + \frac{14}{\tau + 2} + \frac{10}{(\tau + 2)^2} + \frac{4}{(\tau + 2)^3}\right) \quad \text{for positrons} \quad (8.6)$$

in which T = kinetic energy of electron, mc^2 = rest energy of electron, $\tau = T/mc^2$, $\beta = V/c$ = ratio of electron speed and light speed, $r_e = e^2/mc^2$ = classical electron radius, Z = atomic number of target atom, A = atomic mass of target atom, N_A = Avogadro number, and I = mean excitation energy of medium.

In liquid and solid mediums, the density effect appears, which decreases the energy loss because of the polarization of the medium affected by the electric field of the incident charged particle. The last term in Equation (8.4), δ , represents the density effect. S_{col} omitted ρ is called the linear collision stopping power. The subscript col is added to discriminate the radiative stopping power S_{rad}/ρ , described in the next section. The mean excitation energy I for various elements is obtained from the following approximations:

$$\begin{aligned} I &\approx 19.0 \text{ eV}, \quad Z = 1 \\ 11.2 + 11.7Z \text{ eV}, \quad 2 \leq Z \leq 13 \\ 52.8 + 8.71Z \text{ eV}, \quad Z > 13 \end{aligned} \quad (8.7)$$

The mass collision stopping power for compounds and mixtures can be approximated by the linear combination of the constituent atoms.

$$\frac{S_{\text{col}}}{\rho} = \sum_j w_j \frac{S_{\text{col}}}{\rho_j} \quad (8.8)$$

where w_j is the weight ratio of the j th atom. The corresponding mean excitation energy is given by

$$\ln I = \frac{\sum_j w_j (Z_j/A_j) \ln I_j}{\sum_j w_j (Z_j/A_j)} \quad (8.9)$$

Figure 8.1 shows the linear collision stopping powers of various matters for electrons. Table 8.1 shows the various data regarding the stopping power of water for electrons. Although electrons lose at most half of the energy in a collision, positrons have the possibility of losing all energy. Therefore, the collision stopping powers for positrons slightly differ from those of electrons. The collision stopping powers for positrons are ~98% those of electrons in the energy range greater than 500 keV. In opposition, those are larger than electron data by ~5% at 100 keV and 10 ~ 20% at 10 keV.

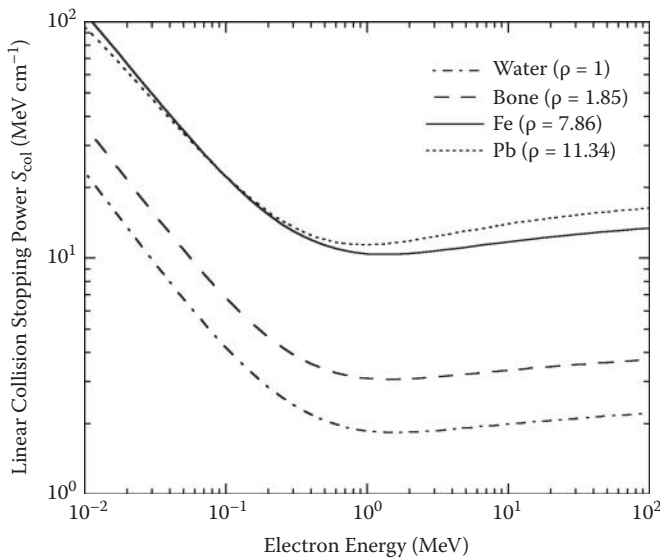


FIGURE 8.1

Linear collision stopping powers of various media for electrons.

TABLE 8.1
Mass Collision Stopping Powers, Mass Radiative Stopping Powers,
Radiation Yields, and Ranges of Water for Electrons

Kinetic Energy (MeV)	β^2	$\frac{S_{col}}{\rho}$	$\frac{S_{rad}}{\rho}$	$\frac{S_{tot}}{\rho}$	Radiation Yield	Range (g cm ⁻²)
		MeV cm ² g ⁻¹				
0.001	0.0039	126.		126.		5 × 10 ⁻⁶
0.002	0.00778	77.5		77.5		2 × 10 ⁻⁵
0.005	0.0193	42.6		42.6		8 × 10 ⁻⁵
0.010	0.0380	23.2		23.2	0.0001	0.0002
0.025	0.0911	11.4		11.4	0.0002	0.0012
0.050	0.170	6.75		6.75	0.0004	0.0042
0.075	0.239	5.08		5.08	0.0006	0.0086
0.1	0.301	4.20		4.20	0.0007	0.0140
0.2	0.483	2.84	0.006	2.85	0.0012	0.0440
0.5	0.745	2.06	0.010	2.07	0.0026	0.174
0.7	0.822	1.94	0.013	1.95	0.0036	0.275
1	0.886	1.87	0.017	1.89	0.0049	0.430
4	0.987	1.91	0.065	1.98	0.0168	2.00
7	0.991	1.93	0.084	2.02	0.0208	2.50
10	0.998	2.00	0.183	2.18	0.0416	4.88
100	0.999	2.20	2.40	4.60	0.317	32.5

EXAMPLE 8.2

Calculate the collisional stopping power of water ($I = 75$ eV) for 1 MeV electrons assuming $\delta = 0$.

SOLUTION 8.2

Using $\tau = \frac{1}{0.511} = 1.96$ and $\beta^2 = 1 - (\frac{0.511}{1+0.511})^2 = 0.886$,

$F^- = -0.22$

$r_e^2 = 7.94 \times 10^{-26}$, $N_A = 6.022 \times 10^{23}$, $Z = 10$, $A = 18.015$,

$\ln \frac{10^6}{75} = 18.996$, $\ln 1 + \frac{1.96}{2} = 0.683$

$\frac{S^-}{\rho} = \frac{2\pi \times 7.941 \times 10^{-26} \times 0.511}{0.886} \cdot \frac{10 \times 6.022 \times 10^{23}}{18.015} [18.996 + 0.683 - 0.22]$
 $= 1.87 \text{ MeV cm}^2 \text{ g}^{-1}$

EXAMPLE 8.3

Calculate the collisional stopping power of water ($I = 75$ eV) for 1 MeV positrons assuming $\delta = 0$.

SOLUTION 8.3

Using $F^+ = -0.625$,

$$\begin{aligned} \frac{S^+}{\rho} &= \frac{2\pi \times 7.941 \times 10^{-26} \times 0.511}{0.886} \cdot \frac{10 \times 6.022 \times 10^{23}}{18.015} [18.996 + 0.683 - 0.625] \\ &= 1.83 \text{ MeV cm}^2 \text{ g}^{-1} \end{aligned}$$

EXAMPLE 8.4

Calculate the mean excitation energy of SiO_2 .

SOLUTION 8.4

$$I_{\text{Si}} = 52.8 + 8.71 \times 14 = 174.7, \quad I_{\text{O}} = 11.2 + 11.7 \times 8 = 104.8$$

$$w_{\text{Si}} = \frac{28}{28 + 16 \times 2} = 0.467, \quad w_{\text{O}} = \frac{16 \times 2}{28 + 16 \times 2} = 0.533$$

$$\ln I = \frac{0.467 \times 0.5 \times \ln 174.7 + 0.533 \times 0.5 \times \ln 104.8}{0.467 \times 0.5 + 0.533 \times 0.5} = 4.891$$

$$\therefore I_{\text{SiO}_2} = 133 \text{ eV}$$

8.3 Radiative Stopping Power

Bremsstrahlung emitted from the collision of heavy charged particles with an atom can be ignored because particles are not accelerated. On the other hand, electrons receive strong acceleration and emit bremsstrahlung. The definition of mass radiative stopping power is given by

$$\frac{S_{\text{rad}}}{\rho} = \frac{N_A}{A} \int_0^T k \frac{d\sigma}{dk} dk \quad (8.10)$$

where $d\sigma/dk$ is the differential cross section that emits a photon energy k due to the electron interaction with the nuclear Coulomb field. It is possible to evaluate the radiative stopping powers if the cross section is known. However, it is difficult to represent $d\sigma/dk$ using a unique analytical formula.

Instead, numerical calculations are done dividing the regions into low, intermediate, and high energies.

We see that the bremsstrahlung efficiency is in proportion to Z^2 and linearly increases depending on electron energy. The collision stopping powers for high-energy electrons show the logarithmic increase. Bremsstrahlung becomes a dominant mechanism of energy loss at high energies. The next approximation provides the ratio between radiative loss and collision loss for the electron with the total energy E (MeV).

$$\frac{S_{\text{rad}}}{S_{\text{col}}} \cong \frac{ZE}{800} \quad (8.11)$$

For lead ($Z = 82$), the energy for which both stopping powers are identical is $E = 9.8$ MeV; $T = E - mc^2 = 9.3$ MeV is obtained. The total mass stopping power is the sum of two losses such as

$$\frac{S_{\text{tot}}}{\rho} = \frac{S_{\text{col}}}{\rho} + \frac{S_{\text{rad}}}{\rho} \quad (8.12)$$

Figure 8.2 shows the radiative and total stopping powers of water and Pb. The radiation yield Y represents a fraction of energy dissipated for bremsstrahlung emission until electrons completely stop. For 100 MeV electrons in

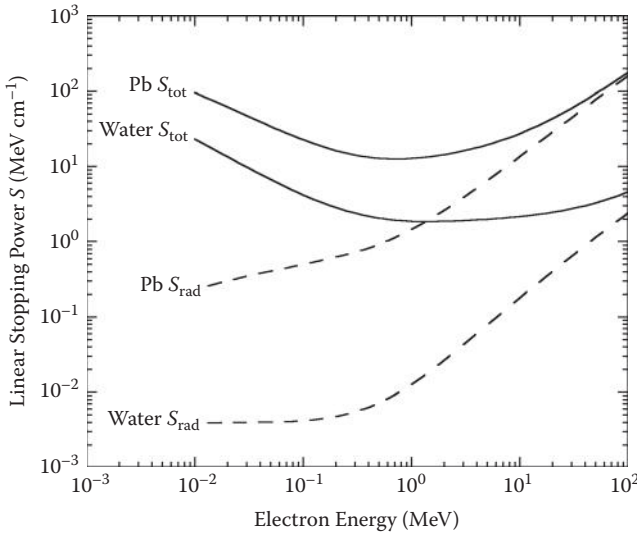


FIGURE 8.2

Linear radiative stopping powers and linear total stopping powers of water and Pb for electrons.

water, Y becomes 31.7%. If electrons of the initial kinetic energy T (MeV) stop in the absorber of the atomic number Z , Y is approximated by

$$Y \approx \frac{6 \times 10^{-4} Z T}{1 + 6 \times 10^{-4} Z T} \quad (8.13)$$

Bremsstrahlung for positrons is almost the same as for electrons at high energies, but becomes smaller at low energies.

EXAMPLE 8.5

Calculate the energy for which both stopping powers are identical for water.

SOLUTION 8.5

Using $Z = 10$ for water, $E = 80$ MeV and $T = 79.5$ MeV.

EXAMPLE 8.6

Calculate the radiation yield for 10 MeV electrons in Pb.

SOLUTION 8.6

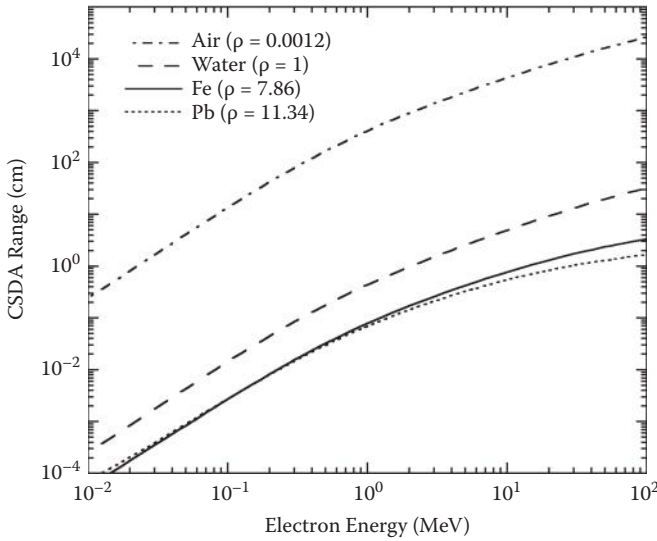
$$Y = \frac{6 \times 10^{-4} \times 82 \times 10}{1 + 6 \times 10^{-4} \times 82 \times 10} \times 100 = 33\%$$

8.4 Ranges

The distance that charged particles advance until stop is called the range. It is assumed that charged particles continuously slow down until the initial energy is completely lost. This is called the continuous slowing down approximation (CSDA) range. This approximation is not realistic for electrons because they lose a considerable fraction of the energy by a single collision. In addition, the electron path is tortuous, unlike heavy particles. However, the term *electron range* means the CSDA range defined by the next equation. That defines the mean path length extended from the start to the end of penetration. This is distinguished from the distance covered along the path of the electron through the absorber. The CSDA range $R(T)$ is written by

$$R(T) = \int_0^T [S_{\text{col}}(T) + S_{\text{rad}}(T)]^{-1} dT \quad (8.14)$$

in which the unit is cm. If multiplying ρ , then the unit changes to g cm^{-2} . Figure 8.3 shows the CSDA range in cm units for electrons in various matters.

**FIGURE 8.3**

CSDA ranges of electrons in various matter.

The collision stopping powers of the material with large Z are smaller than those of water. Therefore, the range below 20 MeV for lead is larger in comparison with that for water. At the high-energy region, the range for lead shortens because of the increase of bremsstrahlung loss.

The empirical formula for the electron range for small Z materials is available.

$$\begin{aligned}
 R &= 0.412T^{1.27-0.0954\ln T} \quad \text{for } 0.01 \leq T \leq 2.5 \text{ MeV} \\
 &= 0.530T - 0.106 \quad \text{for } T > 2.5 \text{ MeV}
 \end{aligned} \tag{8.15}$$

in which the range is in g cm^{-2} unit and the kinetic energy in MeV. In the measurement, the practical range R_p is obtained from the absorption curve for the material. For high-energy electron beams used for radiation therapy, the practical range in water is measured under the condition of the fields $10 \times 10 \text{ cm}^2$, or 10 cm diameter. The relationship is obtained as

$$R_p = 0.52T - 0.30 \tag{8.16}$$

EXAMPLE 8.7

Calculate the range of a 2 MeV electron in water.

SOLUTION 8.7

$$R = 0.412 \times 2^{1.27-0.0954\ln 2} = 0.95 \text{ cm}$$

8.5 Multiple Scattering

The reasons of nonlinearity of the electron path are: (1) a large scattering angle at the inelastic scattering with an orbital electron, and (2) a large deflection by the elastic scattering with a nucleus. If the kinetic energy T of the incident electron degrades T' by an inelastic scattering, the scattering angle θ is determined from the kinematical relationship,

$$\cos \theta = \sqrt{\frac{T(T + 2mc^2)}{T(T + 2mc^2)}} \quad (8.17)$$

EXAMPLE 8.8

Calculate the scattering angle (in degrees) when the incident electron energy of 1 MeV degrades to 0.99 MeV by an inelastic scattering.

SOLUTION 8.8

$$\cos \theta = \sqrt{\frac{0.99 \times (1 + 1.022)}{0.99 + 1.022}} = 0.99746 \quad \therefore \theta = 4.1^\circ$$

On the other hand, electron cross sections scattered by a nucleus taking into account the screening effect of orbital electrons is represented by Moliere's formula. The detailed expressions will be given in Section 13.3. This formula is for a single scattering. If the material layer is thick, a large number of scattering is repeated. This is called the multiple scattering. The cause of back scattering for electrons is the multiple scattering. This theory treats the averaged angular distributions overlapping a large number of elastic scattering in the material with finite thickness. The relative scattering intensity at the θ direction is written by

$$I(\theta) \sim \sqrt{\theta \sin \theta} \times f^{(0)} + \frac{f^{(1)}}{B} + \frac{f^{(2)}}{B^2} \quad (8.18)$$

in which $f^{(0)}, f^{(1)}, f^{(2)}$ are functions of the reduced angle Θ . Table 8.2 shows the numerical values for them given by Bethe. The parameters Θ and B are calculated using the electron radius r_e , the Avogadro constant N_A , the density of material ρ , and the thickness of layer t . For the i th atom in compound materials or mixtures, the atomic number, the atomic mass, and the number of atoms in a mole are Z_i, A_i , and p_i , respectively.

$$\Theta = \frac{\theta}{\chi_c \sqrt{B}} \quad (8.19)$$

$$\chi_c^2 = \frac{4\pi r_e^2 N_A \rho t Z_s (1 - \beta^2)}{A \beta^4} \quad (8.20)$$

TABLE 8.2
Reduced Angles and Parameters for Electron Multiple Scattering

Θ	$f^{(0)}$	$f^{(1)}$	$f^{(2)}$
0	2	0.8456	2.4929
0.2	1.9216	0.7038	2.0694
0.4	1.7214	0.3437	1.0488
0.6	1.4094	-0.0777	-0.0044
0.8	1.0546	-0.3981	-0.6068
1	0.7338	-0.5285	-0.6359
1.2	0.4738	-0.4770	-0.3086
1.4	0.2817	-0.3183	0.0525
1.6	0.1546	-0.1396	0.2423
1.8	0.0783	-0.0006	0.2386
2	0.0366	0.0782	0.1316
2.2	0.01581	0.1054	0.0196
2.4	0.00630	0.1008	-0.0467
2.6	0.00232	0.08262	-0.0649
2.8	0.00079	0.06247	-0.0546
3	0.00025	0.0455	-0.03568
3.2	7.3×10^{-5}	0.03288	-0.01923
3.4	1.9×10^{-5}	0.02402	-0.00847
3.6	4.7×10^{-6}	0.01791	-0.00264
3.8	1.1×10^{-6}	0.01366	0.00005
4	2.3×10^{-7}	0.010638	0.001074
4.5	3×10^{-9}	6.14×10^{-3}	0.001229
5	0	3.831×10^{-3}	8.326×10^{-4}
5.5	0	2.527×10^{-3}	5.368×10^{-4}
6	0	1.739×10^{-3}	3.495×10^{-4}
7	0	9.080×10^{-4}	1.584×10^{-4}
8	0	5.211×10^{-4}	7.830×10^{-5}
9	0	3.208×10^{-4}	4.170×10^{-5}
10	0	2.084×10^{-4}	2.370×10^{-5}

and

$$B - \ln B = \ln \quad_0 \quad (8.21)$$

$$\quad_0 = 6702.33 \frac{Z_S e^{Z_E/Z_S} \rho t}{e^{Z_X/Z_S} A \beta^2} \quad (8.22)$$

where

$$\begin{aligned} A &= \sum p_i A_i \\ Z_S &= \sum p_i Z_i (Z_i + 1) \\ Z_E &= \sum p_i Z_i (Z_i + 1) \ln Z_i^{-2/3} \\ Z_X &= \sum p_i Z_i (Z_i + 1) \ln 1 + 3.34 \frac{Z_i}{137\beta} \end{aligned} \quad (8.23)$$

B is obtained solving Equation (8.22) numerically. Moliere's theory holds for electrons of > 10 keV and for the thickness in which elastic scattering occurs more than 20 times. Figure 8.4 shows the angular distributions of electron multiple scattering in Al for various energies.

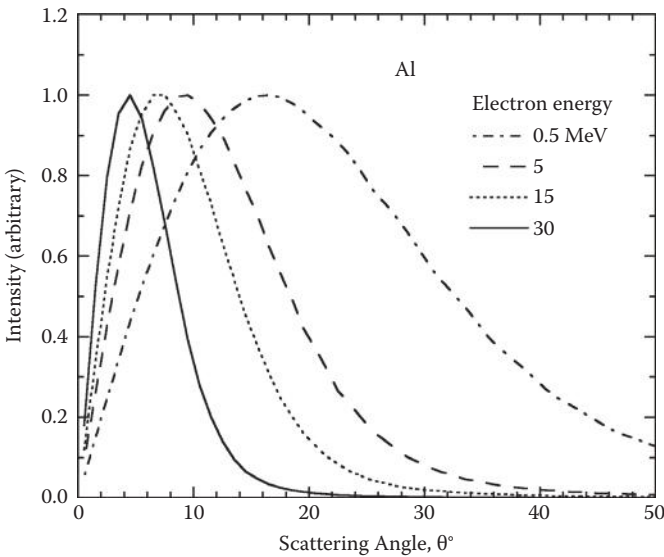


FIGURE 8.4

Angular distributions of electron multiple scattering in Al for various energies.

EXAMPLE 8.9

Calculate the angular distribution of multiple scattering, $I(\theta)$, for 1 MeV electrons in Al ($\rho = 2.69 \text{ g cm}^{-3}$) setting the step size = 2% and the cutoff 10 keV for both electrons and photons.

SOLUTION 8.9

Using $\beta = 0.94108$, $A = 26.98$, $Z_s = 182$, $Z_E = -311.2$, and $Z_X = 6.078$ are obtained from Equation (8.23).

The thickness of layer, t , can be calculated by $t = \Delta E/S$, in which $\Delta E = 1,000 \times 0.02 = 20 \text{ keV}$ and the restricted stopping power $S = 3,097 \text{ keV/cm}$. Therefore, $t = 6.458 \times 10^{-3} \text{ cm}$. From Equations (8.20) and (8.22), $\chi_c = 0.1662$ and $\Omega_0 = 155.15$ are obtained. From Equation (8.21), $B = 6.988$ is obtained. Using Equation (8.19) and Table 8.2, the angular distribution is calculated as a function of θ . A part of the results is shown in the following table.

θ°	Θ	$f^{(0)}$	$f^{(1)}/B$	$f^{(2)}/B^2$	$I(\theta)$
1	0.0397	1.9844	0.1170	0.0493	0.0375
3	0.1192	1.9533	0.1089	0.0459	0.1104
5	0.1986	1.9221	0.1009	0.0424	0.1801
7	0.2781	1.8435	0.0806	0.0342	0.2389
9	0.3575	1.7639	0.0601	0.0259	0.2900
11	0.4370	1.6637	0.0380	0.0175	0.3291
13	0.5164	1.5398	0.0141	0.0089	0.3531
15	0.5959	1.4159	-0.0099	0.00036	0.3661
17	0.6753	1.2758	-0.0284	-0.0047	0.3660
19	0.7548	1.1349	-0.0466	-0.0096	0.3544
21	0.8342	0.9997	-0.0602	-0.0125	0.3360
23	0.9137	0.8723	-0.0676	-0.0128	0.3136
25	0.9931	0.7449	-0.0750	-0.0130	0.2821

8.6 Cerenkov Radiation

When a charged particle passes through an insulator at a constant speed greater than the speed of light in that medium, a visible blue glow is emitted. This phenomenon is called Cerenkov radiation, which is analogous to a shock wave of a supersonic aircraft. As the charged particle travels, it disrupts the local electromagnetic field in the medium. Atomic electrons of the medium will be displaced, and the atoms become polarized by the passing

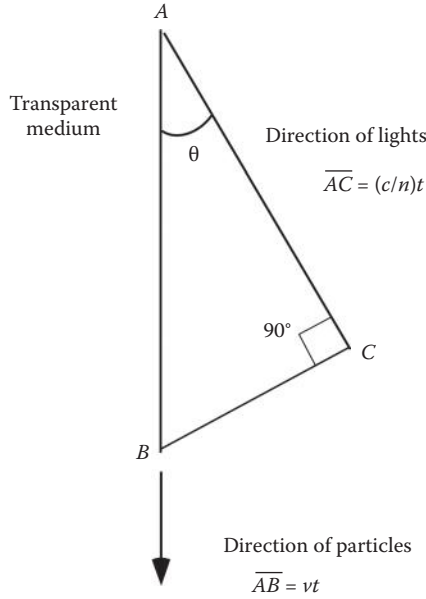


FIGURE 8.5
Principle of Cerenkov radiation.

electromagnetic field of a charged particle. Photons are emitted as an insulator's electrons restore themselves to equilibrium after the disruption has passed. Assuming the speed of light in vacuum, c , the velocity of a charged particle, $v = \beta c$, and the refractive index of the medium, n , the speed of light becomes c/n . If $v > c/n$, then Cerenkov radiation is emitted. In Figure 8.5 a particle travels the direction from point A to point B. The distance is vt . The electromagnetic wave emitted from A reaches C within the time t . Namely, \overline{AC} becomes $(c/n)t$. Therefore, the light wave is emitted with the conical pattern having the polar angle θ satisfying

$$\cos \theta = \frac{\overline{AC}}{\overline{AB}} = \frac{(c/n)t}{vt} = \frac{1}{\beta n} < 1 \quad (8.24)$$

The threshold kinetic energy that enables emitting of Cerenkov light for the particle with the rest mass m is derived using the condition $\beta n > 1$ and

$$\beta = \sqrt{1 - [mc^2/(T + mc^2)]^2}$$

$$T = mc^2 \left(\frac{n}{\sqrt{n^2 - 1}} - 1 \right) \quad (8.25)$$

This is called the critical energy. For electrons in water or lucite, those are 257 and 175 keV, respectively. The contribution of Cerenkov radiation to the electron stopping power can be neglected.

8.7 Summary

1. A charged particle moving in matter affects the electromagnetic force on the atomic electron. The particle loses energy by ionizing and exciting the atom.
2. The mean energy loss of charged particles per a unit length in medium is called the stopping power of the medium for the particles.
3. The total mass stopping power for electrons is the sum of the mass collision stopping power and mass radiative stopping power.
4. The electron path is significantly bent by the collision with the atomic electron and the multiple scattering with the nucleus. Electrons do not move straight forward. However, the range is defined by the continuous slowing down approximation.
5. The threshold energy of Cerenkov radiation for electrons in water is 257 keV.

QUESTIONS

1. Calculate the I value of water from those of H and O ($I_H = 19.2$ eV and $I_O = 95$ eV) and comment on the validity of the method.
2. Estimate how many interactions occur along a $1\text{ }\mu\text{m}$ track of a 1 MeV proton in liquid water, given that the mass stopping power for a 1 MeV proton in liquid water is $260.6\text{ MeV cm}^2\text{ g}^{-1}$ (NIST). How large is the electronic cross section from this estimation?
3. For a 1 cGy dose deposited in a cell layer of $1\text{ }\mu\text{m}$ thick, how many electrons of energy 1 MeV need to traverse the cell layer, assuming the cell is a water-equivalent cube?
4. How is the collisional stopping power of aluminum compared to the corresponding value of lead for 50 MeV electrons?
5. Calculate the thickness of an aluminum shield for a $^{90}\text{Sr}/^{90}\text{Y}$ β source.
6. β -Electrons with unknown maximum energy are emitted. If at least 1 cm plastic with the density of 1.3 g cm^{-3} is required to stop the electrons, calculate the maximum energy.

7. A 550 keV electron pencil beam travels from the top angle of a plastic cone, along the axis of the cone. The cone opening angle is 40° . Calculate the refractive index of the plastic, if the Cerenkov radiation passes through the bottom of the cone parallel to the cone axis.
-

For Further Reading

Bethe HA. 1953. Moliere's theory of multiple scattering. *Phys. Rev.* 89: 1256–1266.
Turner JE. 1995. *Atoms, Radiation, and Radiation Protection*, 2nd ed. New York: John Wiley & Sons.

9

Interaction of Heavy Charged Particles with Matter

9.1 Collision Stopping Powers

The mass collision stopping power formula for heavy charged particles was derived by H.A. Bethe using relativistic quantum mechanics.

$$\frac{S_{\text{col}}}{\rho} = -\frac{dE}{\rho dx} = \frac{4\pi r_e^2 mc^2 z^2 Z N_A}{\beta^2 A} \ln \frac{2mc^2 \beta^2}{I(1-\beta^2)} - \beta^2 \quad (9.1)$$

where $\beta = V/c$ is the ratio of particle velocity to the velocity of light. This is represented, if the mass of particle, M , and the kinetic energy, T , are used, as

$$\beta = \sqrt{1 - \frac{Mc^2}{T + Mc^2}^2} \quad (9.2)$$

and mc^2 = rest energy of an electron, $r_e = e^2/mc^2$ = classical electron radius, z = charge of heavy charged particle, Z = atomic number of the target atom, A = atomic mass of the target atom, N_A = Avogadro constant, and I = mean excitation energy of medium.

The reliability of Bethe's formula was confirmed in comparison with the experimental data. However, that cannot reproduce the experimental data in the low-energy region below a few hundred keV. When fast ions slow down around the Bragg peak ($\sim 0.3 \text{ MeV u}^{-1}$), interactions involving electron capture and loss by the moving ions become an increasingly important component of the energy loss process. The effect of charge exchanges is corrected introducing a parameter called the effective charge. ICRU Report 49 recommends the formula adding various correction terms.

$$\frac{S_{\text{col}}}{\rho} = \frac{4\pi r_e^2 mc^2 z^2 Z N_A}{\beta^2 A} L(\beta) \quad (9.3)$$

$$L(\beta) = L_0(\beta) + zL_1(\beta) + z^2L_2(\beta) \quad (9.4)$$

L is called the stopping number. The first term is

$$L_0(\beta) = \frac{1}{2} \ln \frac{2mc^2\beta^2 Q_{\max}}{1-\beta^2} - \beta^2 - \ln I - \frac{C}{Z} - \frac{\delta}{2} \quad (9.5)$$

where C and δ represent the shell correction and the density effect, respectively. Q_{\max} is the maximum energy loss at a collision with a free electron.

$$Q_{\max} = \frac{2mc^2\beta^2}{1-\beta^2} \frac{1}{1 + \frac{2m}{M\sqrt{1-\beta^2}} + \frac{m}{M}^2} \quad (9.6)$$

This quantity becomes $Q_{\max} = 4mT/M$ at the nonrelativistic limit. The second and third terms of Equation (9.4) are called the Barkas correction and Bloch correction, respectively. Figure 9.1 shows the linear collision stopping powers of various materials for protons. Figure 9.2 shows those for α -particles. In the low-energy region the term in front of the bracket increases for $\beta \rightarrow 0$, while the logarithmic term decreases. Consequently, the maximum stopping powers called the Bragg peak appear at around 100 keV for protons and 600 keV for α -particles.

A relationship between S and z holds for a velocity V regardless of the particle type.

$$S/z^2 = \text{constant} \quad (9.7)$$

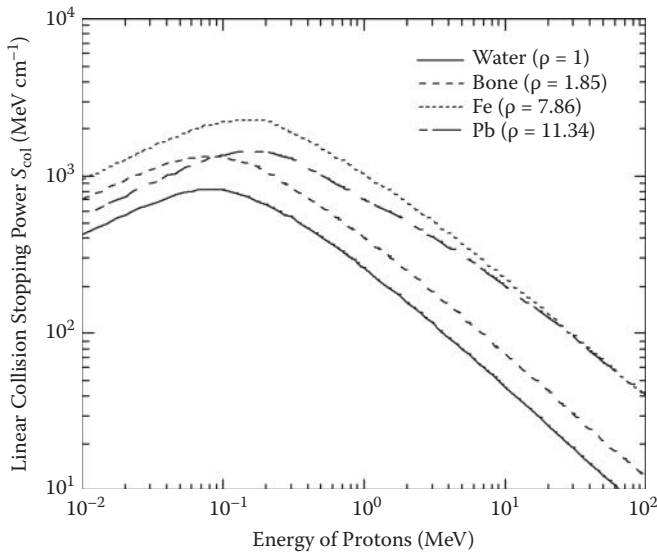
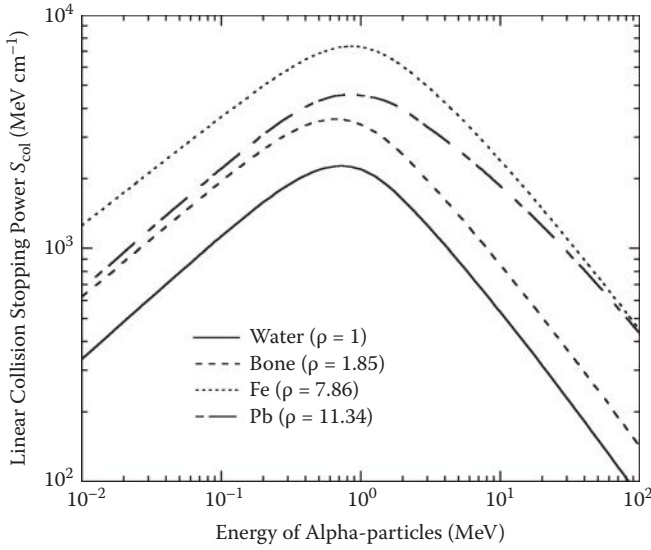


FIGURE 9.1

Linear collision stopping powers of various matters for protons.

**FIGURE 9.2**

Linear collision stopping powers of various matters for α -particles.

If the stopping power of a particle is known, it is possible to estimate the stopping power of a different particle with the same velocity. For instance, it is assumed protons and heavy particles are moving with the same velocity V . The kinetic energies are given by

$$T_p = \frac{1}{2} m_p V^2, \quad T_{HI} = \frac{1}{2} m_{HI} V^2 \quad (9.8)$$

Then,

$$T_{HI} = T_p \frac{m_{HI}}{m_p} \quad (9.9)$$

is obtained. If $HI = \alpha$ -particles, the velocity of 4 MeV α -particles is equal to that of 1 MeV protons. From Equation (9.7), S_α is represented using S_p .

$$S_\alpha = S_p \frac{z_\alpha^2}{z_p^2} = 4S_p \quad (9.10)$$

Therefore, the collision stopping power of 4 MeV α -particles is equal to four times that of 1 MeV protons. This scaling law is effective for the high-energy region in which the charge exchange processes can be neglected. The collision stopping powers for particles other than α -particles are calculable from the scaling law, as shown in Table 9.1.

TABLE 9.1
Scaling Law for Mass Collision Stopping Powers for Heavy Charged Particles

Proton		Deuteron		³ He ²⁺		α		¹² C ⁶⁺	
<i>T_p</i>	<i>S_p</i>	<i>T</i>	<i>S</i>	<i>T</i>	<i>S</i>	<i>T</i>	<i>S</i>	<i>T</i>	<i>S</i>
<i>T_p</i>	<i>S_p</i>	<i>T_p</i> × 2	<i>S_p</i> × 1	<i>T_p</i> × 3	<i>S_p</i> × 4	<i>T_p</i> × 4	<i>S_p</i> × 4	<i>T_p</i> × 12	<i>S_p</i> × 36
1	260.6	2	260.6	3	1,042	4	1,042	12	9,382
2	158.5	4	158.5	6	634.0	8	634.0	24	5,706
3	117.1	6	117.1	9	468.4	12	468.4	36	4,216
4	94.0	8	94.0	12	376.0	16	376.0	48	3,384
5	79.1	10	79.1	15	316.4	20	316.4	60	2,848
10	45.6	20	45.6	30	182.4	40	182.4	120	1,642

Note: *T* = energy (MeV), *S* = mass collision stopping power for liquid water (MeVcm²g⁻¹).

EXAMPLE 9.1

Calculate Pb collision stopping power for 1 GeV α-particles (assume *I* = 823 eV).

SOLUTION 9.1

$$\begin{aligned} \gamma &= \frac{T + mc^2}{mc^2} = \frac{1 + 3.727}{3.727} = 1.268 \\ \beta^2 &= 1 - \gamma^{-2} = 1 - 1.268^{-2} = 0.3783 \\ S_{\text{col}} &= \frac{4\pi r_e^2 mc^2 z^2 Z \rho N_A}{\beta^2 A} \ln \frac{2mc^2 \beta^2}{I(1 - \beta^2)} - \beta^2 \\ &= \frac{4\pi \times (2.82 \text{ fm})^2 \times 0.511 \text{ MeV} \times 2^2 \times 82 \times 11.34 \text{ g/cm}^3 \times 6.022 \times 10^{23}}{0.3783 \times 207 \text{ g/mol}} \\ &\quad \times (10^6 \text{ cm}^3/\text{m}^3) \ln \frac{2 \times 1 \times 10^9 \times 0.3783}{823 \text{ eV}(1 - 0.3783)} - 0.3783 \\ &= 20.7 \text{ GeV/m} \end{aligned}$$

EXAMPLE 9.2

Calculate the maximum energy loss at a collision with a free electron for 1 GeV α-particles.

SOLUTION 9.2

$$\begin{aligned}
 Q_{\max} &= \frac{2mc^2\beta^2}{1-\beta^2} \frac{1}{1 + \frac{2m}{M\sqrt{1-\beta^2}} + \frac{m}{M}} \\
 &= \frac{2 \times 0.511 \text{ MeV} \times 0.3783}{1 - 0.3783} \frac{1}{1 + \frac{2 \times 0.511 \text{ MeV}}{3727 \text{ MeV} \sqrt{1 - 0.3783}} + \frac{0.511 \text{ MeV}}{3727 \text{ MeV}}} \\
 &= 0.622 \text{ MeV}
 \end{aligned}$$

9.2 Nuclear Stopping Powers

Energy loss due to the elastic scattering of heavy charged particles with a nucleus in the energy range lower than 10 keV cannot be ignored. This is called nuclear stopping powers, which means the recoil energy of the target nucleus derived from the kinematical relationship. Putting the differential cross section for elastic scattering as $d\sigma_{\text{el}}/d\Omega$, the mass nuclear stopping power S_{nuc}/ρ is represented by

$$\frac{S_{\text{nuc}}}{\rho} = \frac{2\pi N_A}{A} \int_0^\pi \frac{d\sigma_{\text{el}}}{d} W(\theta, T) \sin\theta d\theta \quad (9.11)$$

where $W(\theta, T)$ is the recoil energy, which depends on the scattering angle, θ , and the kinetic energy of the charged particle, T . Using the mass of the particle, M , and the mass of the target atom, M_t , $W(\theta, T)$ is given by

$$W(\theta, T) = 4T \frac{M_t M}{(M_t + M)^2} \sin^2 \frac{\theta}{2} \quad (9.12)$$

The elastic scattering cross section for a high-energy region above a few MeV is described by the Rutherford cross section:

$$\frac{d\sigma_{\text{el}}}{d} = \frac{N_A Z^2 z^2 r_e^2}{4A} \frac{mc}{p\beta} \frac{1}{\sin^4 \frac{\theta}{2}} \quad (9.13)$$

in which the momentum of the heavy charged particle, p , is given by

$$p = \frac{1}{c} \sqrt{(T + Mc^2)^2 - (Mc^2)^2} \quad (9.14)$$

Since the radiative stopping power can be neglected for heavy charged particles, the total stopping power is the sum of collision loss and nuclear loss.

$$\frac{S_{\text{tot}}}{\rho} = \frac{S_{\text{col}}}{\rho} + \frac{S_{\text{nuc}}}{\rho} \quad (9.15)$$

The contribution of nuclear stopping power to the total stopping power is negligible for the energy region greater than 10 keV; however, it increases as the energy is lowered. That amounts to about 30% at 1 keV.

EXAMPLE 9.3

1. What is the probability of carbon ions scattering through 45° , given that the density of lead is 11.3 g/cm^3 ?
2. What is the counting rate of carbon ions scattered through this angle, given that the flux, Ψ , of incident ions is 10^{11} per second on the foil? The lead target is 0.5 mm thick and a detector of detecting area, Δa , 1 cm^2 is placed 150 cm away from the collision center.
3. What is the energy loss of the incident ions in such a collision?

SOLUTION 9.3

1. The probability per unit thickness of the target is

$$P(\theta) = 2\pi \sin \theta \cdot \frac{\rho N_A}{A} \cdot \frac{d\sigma_{\text{el}}}{d} \text{ (unit sr}^{-1} \text{ cm}^{-1}\text{)}$$

The differential cross section is calculated from

$$\begin{aligned} \frac{d\sigma_{\text{el}}(45^\circ)}{d} &= \frac{6^2 \cdot 82^2 \cdot (2.818 \cdot 10^{-17} \text{ cm})^2}{4} \cdot \frac{0.511 \text{ MeV}}{pc\beta} \cdot \frac{1}{\sin^4 \frac{45^\circ}{2}} \\ &= \frac{5.851 \cdot 10^{-28}}{(pc\beta)^2} \text{ MeV}^2 \text{ cm}^{-1} \text{ sr}^{-1} \end{aligned}$$

from Equation (9.14) the relative velocity can be calculated:

$$\beta = \sqrt{1 - \frac{M_C c^2}{T + M_C c^2}} = \sqrt{1 - \frac{12 \cdot 931.494 \text{ MeV}}{1 \text{ MeV} + 12 \cdot 931.494 \text{ MeV}}} = 0.013$$

where the momentum of the carbon ion is given by

$$\begin{aligned} pc &= \sqrt{(T + M_C c^2)^2 - (M_C c^2)^2} \\ &= \sqrt{(1 \text{ MeV} + 12 \cdot 931.494 \text{ MeV})^2 - (12 \cdot 931.494 \text{ MeV})^2} \\ &= 149.52 \text{ MeV} \end{aligned}$$

therefore,

$$\begin{aligned}
 P(45^\circ) &= 2\pi \sin 45^\circ \cdot \frac{(11.3 \text{ g/cm}^3) \cdot (6.022 \cdot 10^{23} \text{ mol}^{-1})}{207.2 \text{ g/mol}} \\
 &\quad \cdot \frac{5.851 \cdot 10^{-28} \text{ MeV}^2 \text{ cm}^{-1}}{(0.013 \cdot 149.52 \text{ MeV})^2} \\
 &= 2.26 \cdot 10^{-5} \text{ cm}^{-1} \text{ sr}^{-1}
 \end{aligned}$$

2. From the relationship $\frac{dN}{d\Omega} = 2\pi \sin \theta \cdot \frac{a}{r^2}$, the rate of scattered ions are calculated from

$$\begin{aligned}
 R(45^\circ) &= \Psi \cdot P(45^\circ) \cdot \theta \cdot t = \frac{P(45^\circ)}{2\pi \sin \theta} \cdot \frac{a}{r^2} \cdot t \\
 &= 10^{11} \text{ s}^{-1} \cdot \frac{2.26 \cdot 10^{-5} \text{ cm}^{-1} \text{ sr}^{-1}}{2\pi \sin 45^\circ} \cdot \frac{1}{(150)^2} \text{ sr} \cdot (0.05 \text{ cm}) \\
 &= 1.13 \text{ s}^{-1}
 \end{aligned}$$

where t is the lead's thickness and $R(45^\circ)$ is the counting rate at 45° .

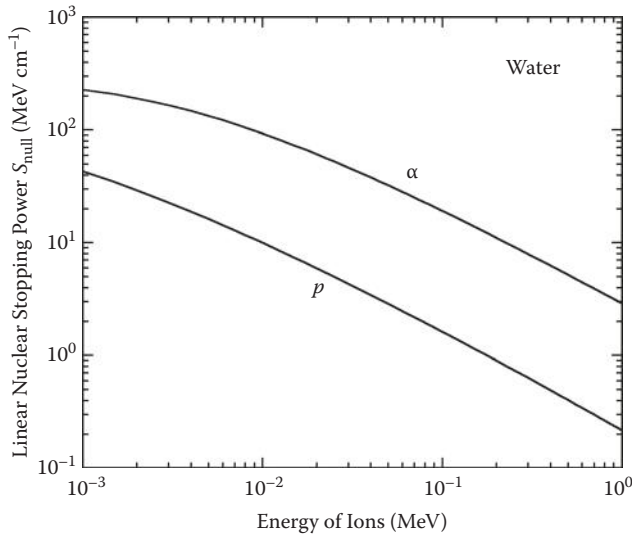
$$\begin{aligned}
 3. \quad W &= 4T \frac{M_C M_{Pb}}{(M_C + M_{Pb})^2} \cdot \sin^2 \frac{\theta}{2} \\
 &= 4 \cdot 1 \text{ MeV} \frac{12 \cdot 207.2}{(12 + 207.2)^2} \cdot \sin^2 \frac{45}{2} = 0.2 \text{ MeV} \cdot 0.146 = 0.029 \text{ MeV}
 \end{aligned}$$

2.9% of the incident energy.

In the low-energy region below 100 keV, Equation (9.13) cannot be used because of the increase of the screening effect due to the orbital electrons of an atom. A calculation method taking into account the screening effect is needed. In that case, the interaction of the incident particle with the target is represented by the screened Coulomb potential such as

$$V(r) = \frac{zZe^2}{r} F_s(r/r_s) \quad (9.16)$$

in which $F_s(r/r_s)$ is a function taking into account the screening, and r_s is a parameter representing the degree of screening. The differential cross section is obtained using the classical mechanics trajectory calculation.

**FIGURE 9.3**

Linear nuclear stopping powers of water for protons and α -particles.

The solution is obtainable not analytically but numerically. Figure 9.3 shows the nuclear stopping powers of water for protons and α -particles.

9.3 Ranges

For heavy charged particles, unlike electrons, the effect of multiple scattering is not considered. It is approximated those continuously slow down nearly on a straight line. Originally, the continuous slowing down approximation (CSDA) was defined for heavy particles. The CSDA range $R(T)$ is obtained by

$$R(T) = \int_0^T [S_{\text{col}}(T) + S_{\text{nuc}}(T)]^{-1} dT \quad (9.17)$$

Figure 9.4 shows the ranges, in cm, of protons in various materials. Figure 9.5 shows the ranges of α -particles in air ($\rho = 1.205 \times 10^{-3} \text{ g cm}^{-3}$) under the standard condition. If the range of a kind of particle is known, the range of another kind of particle can be obtained. A relationship between

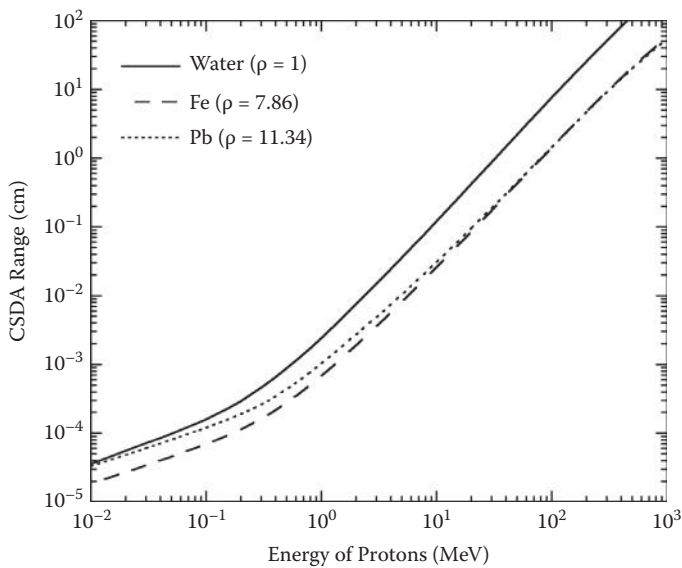


FIGURE 9.4
CSDA ranges of protons for various matters.

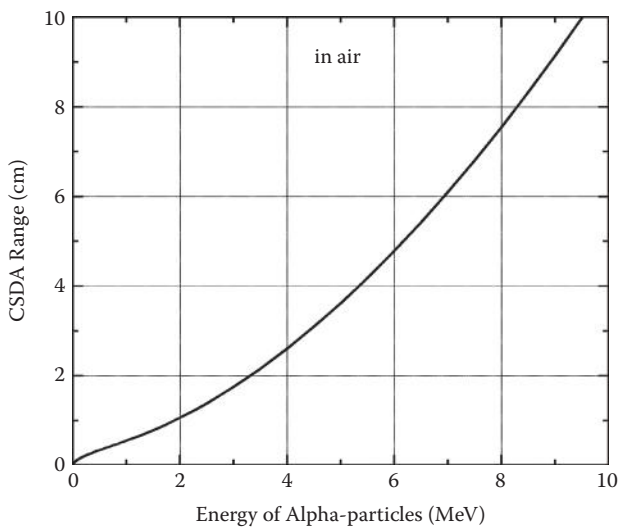


FIGURE 9.5
CSDA ranges of α -particles in air.

the ranges of different types of two particles with the same initial velocity is represented by

$$\frac{R_1(\beta)}{R_2(\beta)} = \frac{z_2^2 M_1}{z_1^2 M_2} \quad (9.18)$$

Assuming the range of the proton as particle 2 is known, the range R of the other particle becomes

$$R(\beta) = \frac{M}{z^2} R_p(\beta) \quad (9.19)$$

EXAMPLE 9.4

Estimate the range of an 8 MeV α -particle in water using Figure 9.4 for the proton range.

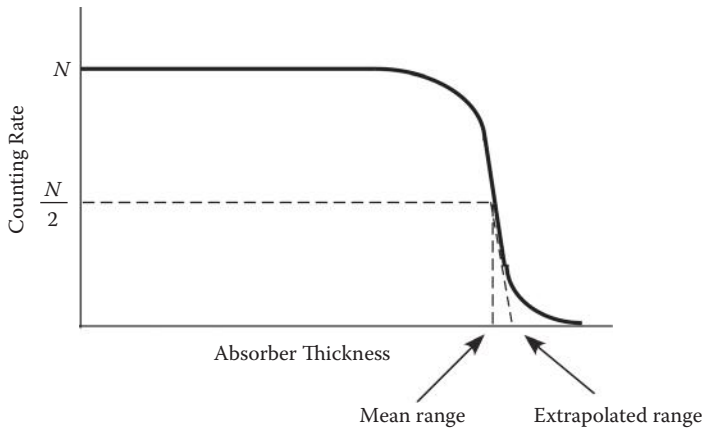
SOLUTION 9.4

The kinetic energy of a proton with the same speed as an 8 MeV α -particle is 2 MeV from Equation (9.9). Therefore, $R_\alpha = \frac{4}{2^2} R_p = R_p$. Using Figure 9.4, $R_\alpha = 7.5 \times 10^{-3}$ cm is obtained.

9.4 Straggling of Energy Loss and Range

When charged particles pass through the material, statistical fluctuation in the number of collision and the energy loss arises. Consequently, many particles started under the same condition show fluctuation in (1) the energy after traveling a given depth and (2) the pass length until stopping. The former phenomenon is called the energy loss straggling and the latter the range straggling. The distribution of the energy straggling becomes a Gaussian shape for the case of a large number of collisions between the charged particles and the absorber atoms. In this case, the whole energy loss is much greater than the maximum energy loss in a single collision. On the contrary, the distribution becomes asymmetrical for the case of a small number of collisions; in other words, for a short track segment.

The range straggling for heavy charged particles can be measured using the absorber and the counter. A monochromatic energy beam hits the absorber consisting of a variable thickness. Figure 9.6 shows the counting rate as a function of the absorber thickness. At a thin thickness, the number of particles is kept constant until the particle range increase leads to energy degradation. Then, the count number decreases abruptly. The reason for the shape is due to the range straggling. The thickness of the absorber at half of the total count is defined as the mean range. The extrapolated range

**FIGURE 9.6**

Measurement of heavy particle range (Uehara 2002).

is determined by the point of intersection of the extrapolated line with the abscissa. The range straggling is not large; for example, for 100 MeV protons in biological material it is $\sim 1\%$. The ionization current is measured using an ionization chamber. The variation of the current per unit thickness as a function of the absorber depth is called the Bragg curve. The energy deposition near the end of the range enhances and forms the sharp peak called the Bragg peak, which is characteristic of heavy charged particles. Heavy ion cancer therapy utilizes this feature of heavy charged particles.

9.5 Summary

1. All particles with $26 \geq Z \geq 1$ are called heavy particles.
2. A heavy charged particle moving in matter affects the electromagnetic force on the atomic electron. The particle loses energy by ionizing and exciting the atom.
3. Collision stopping powers for heavy charged particles are evaluated using Bethe's formula. Nuclear stopping powers are evaluated using the classical mechanics trajectory calculations.
4. Total mass stopping power for heavy charged particles is the sum of mass collision stopping power and mass nuclear stopping power.
5. Heavy charged particles travel almost straightforward in matter. Ranges are obtained by the continuous slowing down approximation.
6. The energy deposition of heavy charged particles enhances just before stopping in matter. This phenomenon, called the Bragg peak, is utilized in the heavy ion cancer therapy.

QUESTIONS

1. What is the difference between the terms *CSDA range* and *penetration distance*?
 2. On average, what percentages of the energy lost by a heavy ion track are by primary particle and δ electrons?
 3. Approximately, in a proton therapy beam, how much of the energy lost is in the Bragg peak area?
 4. What is the difference between the terms *linear stopping power* and *linear energy transfer*?
 5. What is the current definition of the term *LET*?
-

References

ICRU. 1993. *Stopping Powers and Ranges for Protons and Alpha Particles*. ICRU Report 37.
Uehara S. 2002. *Radiation Physics*, 4th ed. Tokyo: Nanzando Publishing (in Japanese).

For Further Reading

Turner JE. 1995. *Atoms, Radiation, and Radiation Protection*, 2nd ed. New York: John Wiley & Sons.

10

δ -Ray, Restricted Stopping Power, and LET

10.1 δ -Ray

Electrons and heavy charged particles moving in materials often cause emission of secondary electrons having enough energy to separate from the path of the initial particle. These electrons, called the δ -rays, make distinct track branches themselves. Figure 10.1 shows the projected tracks of a 10 MeV proton in water generated by Monte Carlo simulation. Some δ -rays emitted from the path of a proton are seen. In the figure, almost all secondary electrons are ejected vertically in the direction from the path of the heavy particles. This is explained from the kinematical relationship of the collision between a heavy particle and a free electron. The emission angle is given by

$$\cos \theta = \sqrt{\frac{m_{\text{HI}} \varepsilon}{4m_e T}} \quad (10.1)$$

EXAMPLE 10.1

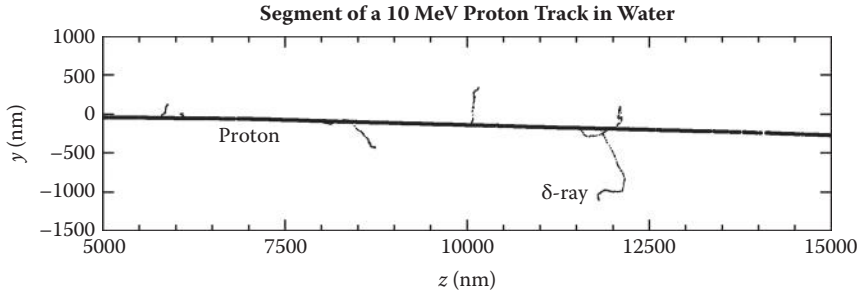
What is the energy of electrons emitted from a 12 MeV carbon ion path through an angle 45° relative to the projectile's path?

SOLUTION 10.1

From Equation (10.1):

$$\varepsilon = \frac{4m_e T}{m_{\text{HI}}} \cos^2 \theta = \frac{4 \cdot 5.486 \cdot 10^{-4} \text{ u} \cdot 12 \text{ MeV}}{12 \text{ u}} \cos^2 45^\circ = 1.097 \text{ keV}$$

in which m_{HI} and T are the mass and kinetic energy for a heavy particle, and m_e and ε for an electron, respectively. For 1 MeV protons, the average energy of secondary electrons is ~ 60 eV. Therefore, $\theta \sim 80^\circ$ is obtained. This is understood by the momentum conservation law. The momentum of heavy particles does not change largely before and after the collision; therefore, the momentum component along the particle path for secondary electrons becomes nearly zero. There is not an accurate criterion to classify δ -rays.

**FIGURE 10.1**

δ -Rays generated by a 10 MeV proton in water. Dots represent the energy deposition points.

The absorbed dose of radiation is defined as the energy absorbed per unit mass of irradiated material. The stopping power means the energy lost by charged particles in the material. This quantity is not necessarily equal to the absorbed energy by the target. Above all, a problem occurs for the target smaller than the range of secondary electrons. Such a microscopic concept in dosimetry, called microdosimetry, plays an important role to understand the radiation effect on cells ($\sim\mu\text{m}$ range) or DNA (at $\sim\text{nm}$ range).

10.2 Restricted Stopping Power

The concept of restricted stopping power was introduced to relate the energy loss in the target with that actually absorbed energy in the target. The restricted collision stopping power, $-(dE/dx)$, is defined as the energy loss just by a collision in which the energy transfer does not exceed a value Δ , which is called the cutoff. Replacing Q_{\max} in Equation (7.3) by Δ ,

$$-\frac{dE}{dx} = \int_{Q_{\min}} QW(Q)dQ \quad (10.2)$$

is obtained. The explicit formula of mass restricted collision stopping power for heavy charged particles is given by

$$-\frac{dE}{\rho dx} = \frac{2\pi r_e^2 mc^2 z^2 Z N_A}{\beta^2 A} \ln \frac{2mc^2 \beta^2}{I^2 (1 - \beta^2)} - \frac{(1 - \beta^2)}{2mc^2} - \beta^2 - 2\frac{C}{Z} - \delta \quad (10.3)$$

For electrons,

$$-\frac{dE}{\rho dx} = \frac{2\pi r_e^2 mc^2 z^2 Z N_A}{\beta^2 A} \ln \frac{T^2}{I^2} + \ln \left(1 + \frac{\tau}{2}\right) + G - \delta \quad (10.4)$$

TABLE 10.1
Restricted Mass Stopping Powers of Water for Protons
(MeV cm² g⁻¹)

Energy (MeV)	$-\frac{dE}{\rho dx}$ 100eV	$-\frac{dE}{\rho dx}$ 1keV	$-\frac{dE}{\rho dx}$ 10keV	$-\frac{dE}{\rho dx}$ ∞
0.05	910.0	910.0	910.0	910.0
0.10	711.0	910.0	910.0	910.0
0.50	249.0	424.0	428.0	428.0
1.0	146.0	238.0	270.0	270.0
10.0	24.8	33.5	42.2	45.9
100.0	3.92	4.94	5.97	7.28

where $\tau = T/mc^2$, $\eta = \Delta/T$, and G is a function of τ and η as follows:

$$G = -1 - \beta^2 + \ln[4\eta(1 - \eta)] + \frac{1}{1 - \eta} + (1 - \beta^2) \frac{\tau^2 \eta^2}{2} + (2\tau + 1)\ln(1 - \eta)$$

(10.5)

Table 10.1 shows the mass restricted collision stopping powers of water for various Δ for protons. Unrestricted stopping power is represented by ∞ . For protons below 0.05 MeV, collision transfer energy greater than 100 eV does not contribute to the stopping power. In fact, Q_{max} is 109 eV at 0.05 MeV protons. For 0.1 MeV protons, the restricted stopping power at $\Delta = 1$ keV is much greater than that at $\Delta = 100$ eV because $Q_{\text{max}} = 220$ eV. It is found that the energy transfer greater than 10 keV is scarce at 1 MeV. For 10 MeV protons, about 8% of the stopping power comes from the transfers greater than 10 keV. Table 10.2 shows the mass restricted collision stopping powers of water for electrons.

The value of Δ is chosen in accordance with the objective of the subject. We refer Monte Carlo simulation of electron transport as an example. If $-(dE/dx)_{\text{1eV}}$ is assumed, the secondary electron having an energy greater than 1 keV is treated as independent electron tracks or δ -rays. The secondary electrons having smaller energies than 1 keV are lumped in the restricted collision stopping powers. The restricted radiative stopping power is treated in the same manner. Bremsstrahlung photon energy less than Δ is included in the restricted radiative stopping power. On the other hand, photons having energies higher than Δ are traced as individual photons.

EXAMPLE 10.2

Estimate the dose deposited by a plane-parallel monoenergetic electron beam of 1 MeV in a water target that has a cylindrical shape with the length and radius equal to the range of 10 keV electrons. The cylindrical axis is centered on the particle’s path and the electron fluence is 10^{10} cm⁻².

TABLE 10.2
Restricted Mass Stopping Powers of Water for Electrons (MeV cm² g⁻¹)

Energy (MeV)	$-\frac{dE}{\rho dx}_{100\text{eV}}$	$-\frac{dE}{\rho dx}_{1\text{keV}}$	$-\frac{dE}{\rho dx}_{10\text{keV}}$	$-\frac{dE}{\rho dx}_{100\text{keV}}$	$-\frac{dE}{\rho dx}_{\infty}$
0.01	15.3	20.2	23.2	23.2	23.2
0.02	8.63	11.2	13.5	13.5	13.5
0.03	6.22	8.02	9.62	9.88	9.88
0.05	4.18	5.32	6.38	6.75	6.75
0.07	3.25	4.12	4.94	5.31	5.31
0.1	2.54	3.19	3.82	4.20	4.20
0.2	1.69	2.09	2.49	2.84	2.84
0.3	1.41	1.73	2.05	2.35	2.39
0.5	1.19	1.46	1.72	1.97	2.06
0.7	1.11	1.34	1.58	1.81	1.94
1.0	1.05	1.27	1.49	1.71	1.86
2.0	1.02	1.22	1.42	1.63	1.84
3.0	1.02	1.22	1.42	1.62	1.87
5.0	1.03	1.22	1.42	1.62	1.92
7.0	1.03	1.23	1.43	1.63	1.95
10.0	1.04	1.24	1.44	1.63	1.99
20.0	1.05	1.25	1.44	1.64	2.06
30.0	1.05	1.25	1.45	1.64	2.10
50.0	1.05	1.25	1.45	1.64	2.14

SOLUTION 10.2

Dose can be estimated from

$$D \approx \phi \cdot -\frac{dE}{\rho dx}_{1\text{keV}} = \frac{10^{10}}{\text{cm}^2} \cdot \frac{1.49 \cdot 10^6 \cdot 1.6 \cdot 10^{-19} \text{ J cm}^2}{10^{-3} \text{ kg}} = 2.38 \text{ Gy}$$

EXAMPLE 10.3

What should be the cutoff energy for the dose calculation for a cylindrical water target of radius 2.5 μm?

SOLUTION 10.3

2.5 μm is about the range of 10 keV electrons in liquid water. Therefore, the restricted stopping power with cutoff energy Δ ≥ 10 keV should be used for the dose calculation.

10.3 LET

LET stands for linear energy transfer. The concept of LET is defined by ICRU Report 16 (1970). It is denoted by L_{Δ} , which is the same as the restricted stopping power for the energy transfer less than Δ .

$$L = \frac{dE}{dl} \quad (10.6)$$

in which dl is the path length of the particle, and dE is the mean energy loss less than the cutoff energy Δ . The L_{∞} means the ordinary stopping power. L without ∞ means L_{∞} . Although not included in the present definition, another LET, L_r , other than L_{Δ} has been considered that restricts the position of energy deposition. This quantity is defined as the energy deposited in a cylinder with the radius r and the length dl centered on the particle path.

$$L_r = \frac{dE}{dl}_r \quad (10.7)$$

It is easy to evaluate L_{Δ} using the analytical equations ((10.3) and (10.4)); however, it is difficult to measure it directly. Figure 10.2 shows the ratio of

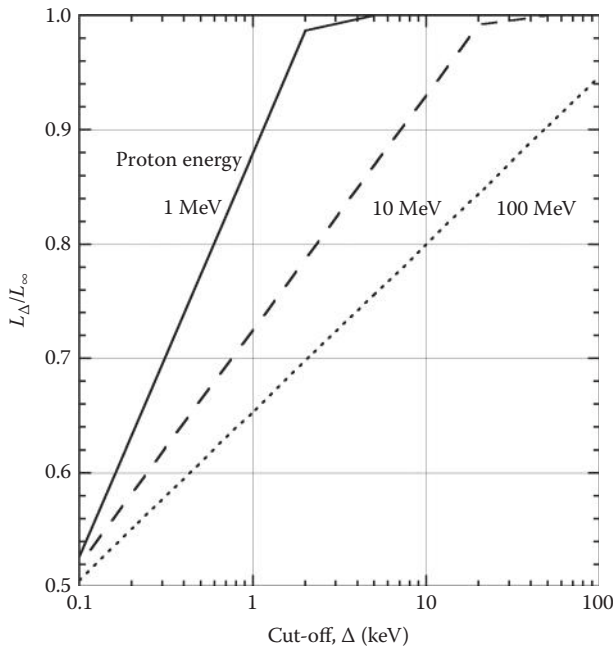


FIGURE 10.2

Ratio of energy restricted stopping power L_{Δ} to unrestricted stopping power L_{∞} for the proton energies 1, 10, and 100 MeV as a function of cutoff energy Δ .

L_{Δ} to L_{∞} as a function of Δ for various energies of protons. Analytical calculations are difficult for L_{ν} but the measurement is basically possible by putting the cylindrical gas ionization chamber in place. Further analyses are given in Section 18.5.

10.4 Summary

1. Some of the secondary electrons generated by ionization are energetic. Those called δ -rays form an independent track of the primary electron.
2. The concept of macroscopic and averaged stopping powers cannot be applied to the absorbed dose in the target the size of μm or nm .
3. Restricted collision stopping powers are defined as the energy transfer caused collision not exceeding the cutoff Δ .
4. Linear energy transfer (LET) is the same as the restricted stopping power. The notation is L_{Δ} .

QUESTIONS

1. What is the condition for normal ejection of secondary electrons from a high-energy ion's path?
 2. Explain why the restricted stopping powers for a 50 keV proton are the same for the cutoff energy $\Delta = 100 \text{ eV}$, 1 keV, 10 keV, and ∞ . Why does the difference become larger when the proton energy increases?
 3. What is the condition of using $\left(\frac{dE}{\rho dx}\right)$ for dose calculations in a target volume?
 4. Give reasons why absorbed dose calculated using the approach given in Question 3 deviates from the measured value.
-

References

- ICRU. 1970. *Linear Energy Transfer*. ICRU Report 16.
ICRU. 1983. *Microdosimetry*. ICRU Report 36.
ICRU. 1984. *Stopping Powers for Electrons and Positrons*. ICRU Report 37.